A STUDY OF BOILING PARAMETERS UNDER CONDITIONS OF LAMINAR NON-NEWTONIAN FLOW WITH PARTICULAR REFERENCE TO MASSECUITE BOILING

by

ERNEST EDOUARD ANDRE ROUILLARD M.Sc. (Chem.Eng.)

A thesis submitted in partial fulfilment of the requirements for the degree of Doctor of Philosophy in the Department of Chemical Engineering, University of Natal.

Durban.

October, 1985.

The work described in this thesis was carried out in the Department of Chemical Engineering, University of Natal between November, 1980 and February, 1982 and is my original and independent work except where specifically acknowledged in the text.

E.E.A. ROUILLARD

SUMMARY

Crystallization is done in the sugar industry using natural circulation vacuum evaporative crystallizers known as vacuum pans. the fluid which is known as massecuite consists of a suspension of crystals in concentrated molasses. It is highly viscous and slightly non-Newtonian, and laminar conditions prevail in the apparatus.

Research on forced convection boiling heat transfer, pressure drop and vapour holdup has been done mostly in turbulent flow under pressures higher than atmospheric, but no studies have been made when boiling viscous fluids under vacuum.

This thesis describes a series of experiments which were undertaken with the following objectives:

(a) to determine the influence of the pertinent variables on heat transfer, friction losses and vapour holdup while boiling under laminar conditions

(b) to produce a method for the calculation of the evaporation and circulation rates in vacuum pans, as this would make possible the optimization of this type of equipment.

The apparatus used consisted of a single tube steam heated forced circulation evaporator. The void fraction, pressure and centerline temperature were measured along the tube. The fluids used were syrup, molasses and massecuite covering a thousandfold change in viscosity. The tests were conducted under different conditions of vacuum and steam pressures with varying tube inlet velocities.

The experimental results show that the boiling heat transfer coefficient can be correlated as a function of the two phase Reynolds number and dimensionless density ratio and that it is inversely proportional to the tube length to the power of one third. The pressure drop can be estimated using the equation of Oliver and Wright (1964) for bubbly flow. Equations are proposed for calculating the void fraction in the highly subcooled region and point of bubble departure. These equations form the basis of a computer program which by a stepwise and iterative method simulates the boiling process along the tube.

Measurements taken on a natural circulation pan with tubes of different length show that this method predicts the effect of the tube length with reasonable accuracy. The limitations of this study are that the experiments were done with a single diameter tube so that the effect of diameter has not been established with certainty. Only sugar products were used in the experiments, and caution is necessary if this method is applied to other fluids.

ACKNOWLEDGEMENTS

This project was undertaken while in the service of the Sugar Milling Research Institute, and my thanks are due to the Chairman and Members of the Board of Control who made it possible.

I express also my gratitude to Dr. M. Matic, former director of the Institute, for his encouragements during the early stages.

I was privileged to have Prof. E.T. Woodburn and afterwards Prof. M. R. Judd of the University of Natal as supervisors, and thank them for their interest and advice.

The help and cooperation of Neville Allan who helped in the design of the experiment pan and of the late Derek Grady who erected the apparatus, and of members of the Analytical Division of the Institute, is greatly appreciated.

I am also indebted to Mrs. J. Vreugdenhil for typing this thesis.

Finally, I wish to thank my wife, Linda, for her understanding and encouragement.

CONTENTS

LIST OF FIGURES

Fig.

CHAPTER I

INTRODUCTION

In the earliest days of the sugar industry evaporation was done at atmospheric pressure in direct fired pans until crystallisation began. In consequence sugar losses and darkening of the products occurred because of the thermal degradation. These problems were overcome by the invention of the vacuum evaporative crystallizer or vacuum pan by Howard in 1813 (Deer 1950). In the original vacuum pan heating was done by means of a steam jacketted bottom. The evolution of the method of heating which followed was first to use steam coils, then horizontal tubular elements and finally in 1852 vertical tubes or calandria which up to now is the type generally used.

Over the years the trend has been towards larger pans so as to reduce capital costs and labour requirements. The oldest pans were spherical in shape, and often their capacity was increased by inserting a cylindrical section between the two hemispheres forming the pan. Thus the ratio of the height to the diameter which originally was 1:1 became much greater.

The mixture of concentrated molasses and sugar crystals boiled in vacuum pans is called massecuite. Its rheological properties are complex. It is highly viscous and slightly non-Newtonian, and boiling takes place under laminar conditions.

Two types of pans are used, batch and continuous. In batch pans a sufficient amount of massecuite composed of fine crystals is introduced in the apparatus so as to immerse fully the heating surface. The crystals are grown by feeding syrup or molasses to the pan while evaporation takes place. As crystallization proceeds the volume of massecuite

increases until the maximum operating level is reached. At this point the pan is emptied, and a new cycle is started. However, if the crystal size desired has not been obtained, part of the contents of the pan are stored in another vessel while the remainder of the massecuite is crystallized further. Thus batch pans start the cycle with relatively low viscosity material and low hydrostatic head, and finish with high viscosity and high head. In these pans the initial massecuite volume must represent as small a fraction of the final volume as possible so as to allow maximum growth of the crystals during each cycle, and the level reached at the end must be as low as possible, because high hydrostatic head adversely affects circulation. A typical batch pan is shown in Figure 1:1.

The principal objective of pan design has been to increase the circulation. This is because low crystallization rates and poor sugar quality such as conglomerates and colour formation result from insufficient circulation. The changes in design done to improve batch pan performance have been to increase the diameter of the downtake, shorten the length of the boiling tubes and decrease the depth of fluid above the tubes. These changes were the results of trial and error, because, although research work on the factors affecting the boiling characteristics of vacuum pans has been going for at least fifty years, to date no satisfactory method has been proposed for optimizing pan design and operation. The lack of progress arises from the large number of experimental variables which are present.

Continuous pans have come into use during the past ten years. Generally they are made up of a number of cells in series. Massecuite with small crystals is pumped continuously into the first compartment, and the product is withdrawn from the last. Flow occurs due to the difference in level between the first and last cells. Evaporation and addition of syrup or molasses take place in each compartment. These pans operate with a relatively low and uniform

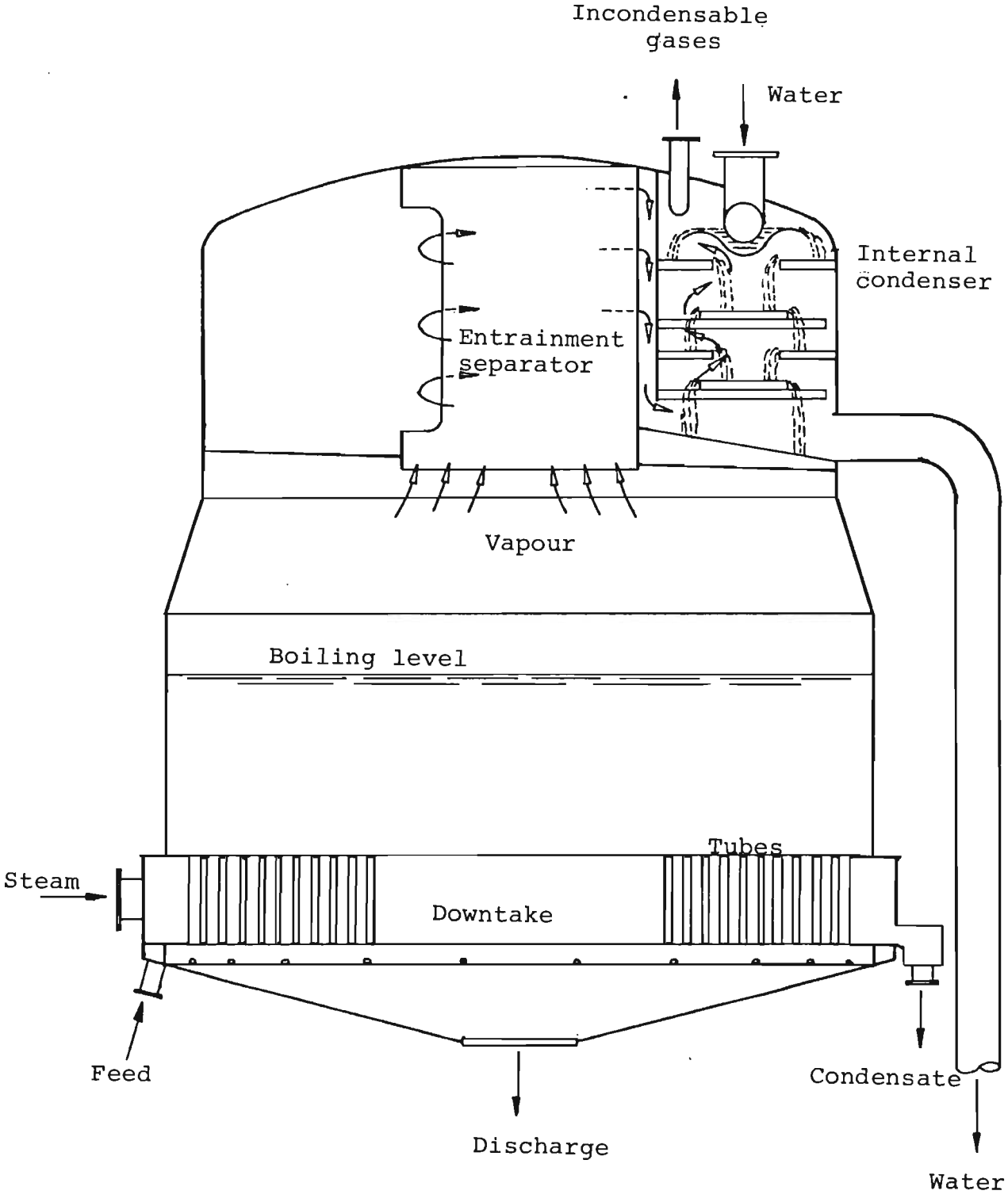

Figure 1.1. Typical C-massecuite batch pan.

hydrostatic head, but the massecuite in the pan becomes progressively more viscous between the inlet and outlet. To date no effort has been made to optimize the design of the individual cells. This and the different concepts of the pans in service are an indication of the inadequacy of optimizing techniques. Two types of continuous pans are shown in Figure 1.2.

In pans with natural circulation the movement of massecuite up the boiling tubes and down the downtake is caused by the difference in hydrostatic head between the two-phase mixture of massecuite and vapour in the tubes and single phase massecuite in the downtake. It is affected by the hydraulic resistance of the channel through which flow takes place and by the physical properties of the fluid and amount of vapour formed.

In order to optimize the design and operation of vacuum pans it is necessary to formulate a method for the calculation of the boiling process which takes into account the heat transfer, vapour holdup and hydraulic friction losses under different boiling regimes and changing fluid properties. The principal objective of this study was to produce such a method, and to achieve this it was necessary

(a) to obtain a clear understanding of the mechanism of circulation

(b) to determine the influence of the pertinent variables on heat transfer, friction losses and vapour holdup while boiling under laminar conditions.

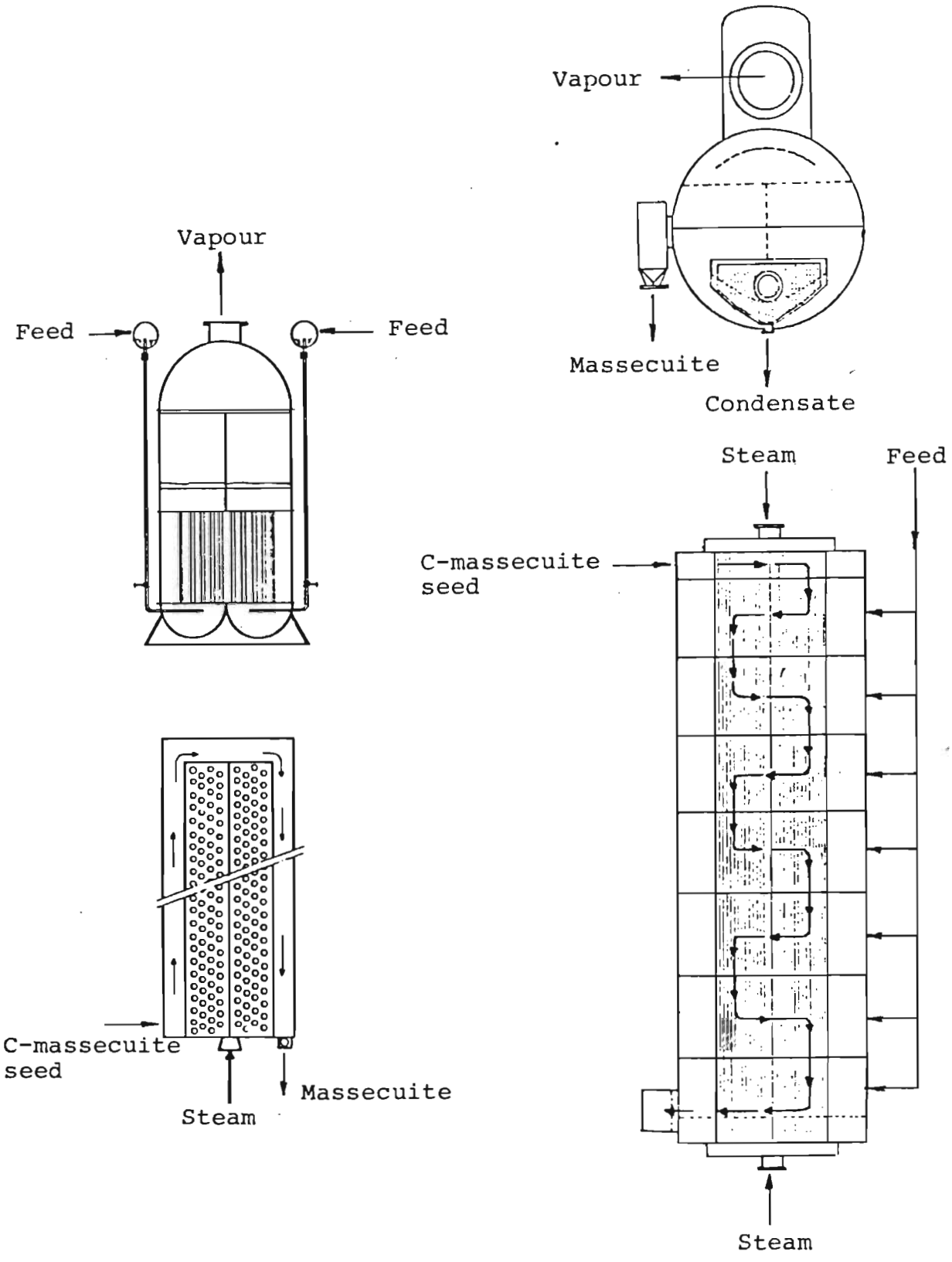

Figure 1.2. Two types of continuous pans. (Langreney, 1977)(left) and (Graham and Radford, 1977)(right).

CHAPTER 2

REVIEW OF PREVIOUS WORK

In boiling, the heat transfer and hydrodynamic processes are interdependent. The addition of heat causes changes in the amount and distribution of the phases which in turn produce variations in the heat transfer rate. When boiling occurs in a vertical tube under vacuum the problem is made more complex because of the pressure gradient along the tube which itself is a function of the void fraction.

Studies of the boiling process have been done primarily for the development of water-cooled nuclear reactors where performance and safety of operation are of paramount importance. They were done mostly with single-component systems under turbulent flow and pressure above atmospheric.

Research on massecuite boiling under vacuum presents additional difficulties, for it is a multi-component system whose physical properties are not well defined. For this reason studies have been generally of a qualitative nature and concerned almost exclusively with the pattern and velocity of circulation.

2.1. PROPERTIES OF MASSECUITE

Massecuite is a multicomponent system which consists of sugar crystals in a saturated aqueous solution of sugar and non-sugars. Its composition varies as a result of the process, and being of vegetable origin is affected by the plant from which it was obtained, that is whether sugar cane or sugar beet, the locality where the plant was grown and the climate.

Crystallization in vacuum pans is usually done in three stages. After each stage the massecuite is centrifuged, so as to separate the crystals, and the molasses obtained is

used to boil a new massecuite. These are known as the A, B and C-massecuites. The reasons for the three stage process are as follows:

(a) The first stage produces high purity crystals, and in South Africa this is the product which is sold as raw sugar.

(b) It is necessary to limit the crystal content of the massecuite, so as to maintain the fluidity at such a level that it will flow out of the pan, and be conveyed to the centrifuges.

(c) As sugar is removed from the molasses crystallization becomes more difficult, because of the increasing concentration of the non-sugars. Yet it is important to crystallize as much sugar as possible, for what remains in the final molasses is lost from the process. This loss represents between 8 and 13 percent of the material entering the factory, and is the most important loss in sugar manufacture.

The main constituents of the non-sucrose emanating from sugar-cane are glucose and fructose, while these substance are practically absent in sugar-beet products. Other important substances are inorganic salts and gums. The composition and concentration of non-sugars have a strong influence on the properties of massecuite, but because of their variability it has not been possible to establish these accurately.

The properties that may affect massecuite boiling are the density, viscosity, surface tension, thermal conductivity, specific heat and boiling point elevation.

2.1.1. Density

The density of pure sucrose solutions of different con-

centrations has been studied extensively over a period of many years. The most accurate density table available is considered to be that published in 1900 by the German Normal-Aichungs-Kommission based on the determinations of Plato et al. (1900). No study of the density of impure solutions has been made.

The percentage by weight of sucrose in a pure solution is called the degree Brix in the sugar industry. It is customary to consider the degree Brix as the percentage of solute although this is only true for pure sucrose solutions.

2.1.2. Rheological properties

Adkins (1951) showed that massecuites are pseudoplastic. For fluids of this type the ratio of shear stress to the shear rate falls progressively with shear rate and becomes constant only at very high rates of shear. An empirical relation called the power law originally proposed by Ostwald (1926) is generally used to characterize pseudoplastic fluids. It may be written as

$$\tau = K (du/dr)^n \qquad (2.1)$$

where τ is the shear stress, K is a measure of the consistency of the fluid, the higher it is more viscous the fluid, du/dr is the shear rate and n is the flow behaviour index. The smaller n is the more pronounced are the non-Newtonian properties of the fluid. One of the more recent papers by Awang and White (1976) states that the flow behaviour index of C-massecuite varies between 0,8 and 0,9, and that this value is not greatly affected by crystal content, crystal size and temperature. They have also developed an equation which relates the relative viscosity to the volumetric ratio crystal/molasses, the crystal size and the crystal size distribution. The relative viscosity is the ratio of the massecuite viscosity to that of the molasses

surronding the crystals. The viscosity of molasses itself is a function of the temperature and of the amount of sucrose, fructose plus glucose, gums and inorganic salts present as shown by Rouillard (1984). The same author gives the following range of viscosities for the three massecuites at 70°C.

Massecuite	Viscosity Pa.s
A	2 - 10
B	10 - 90
C	90 - 1000

Behne (1964) reported that massecuites also exhibit thixotropic properties, that is their consistency depends not only on the rate of shear but also on the time that this shear has been applied. In thixotropic fluids there is a progressive breakdown of structure with shearing, and the consistency decreases with time until equilibrium is reached. The equilibrium position depends upon the intensity of shear. It is a reversible process and during a period of rest the structure builds up again gradually.

2.1.3. Surface tension

The determination of surface tension in viscous fluids and in the presence of crystals is difficult. One of the few studies done on sugar and molasses is that of Vanhook and Biggins (1952). They state that the results obtained with viscous materials are at best approximate.

2.1.4. Thermal conductivity

The only data available on thermal conductivity result from a study done by Bosworth (1947) on pure sucrose solutions. Using these data, Baloh (1967) has obtained an equation which expresses the thermal conductivity as a function of the temperature and concentration. No information

is available for impure sucrose solutions.

2.1.5. Specific heat

The specific heat of impure sugar beet solution has been studied by Janovskii and Archangelskii (1928) who developed equations to calculate this parameter as a function of the concentration and purity.

Hugot (1950) recommends the following formula for cane products.

$$c_p = (1 - 0{,}007\ \text{Brix})\ 4186{,}8 \qquad (2.2)$$

2.1.6. Boiling point elevation

Measurements of the boiling point elevation have been done by Batterham and Norgate (1975) using impure cane sugar solutions. They have proposed equations that relate this property to the dry substance, purity and pressure.

The dry substance is the percentage of dissolved material in a molasses determined as the percent weight remaining after drying.

The purity is the percentage by weight of the dissolved material that is sucrose.

2.1.7. Discussion

Since massecuite is of vegetable origin, its composition is variable and its physical properties are not well established. Most of the data available are based on pure sucrose solutions. Because of the strong influence exerted by the impurities the properties of impure solutions may be significantly different.

2.2. CIRCULATION

The study of the factors affecting circulation has retained the interest of sugar technologists for many years.

Webre (1932) measured the temperatures at various depths in a boiling pan and compared these to the temperature at which boiling should have taken place under equivalent pressures. From these results he drew the erroneous conclusion that practically no ebullition takes place in the tubes except when the level is close to the upper tube sheet, and even then only in the upper part of the tubes. This conclusion was to have an adverse influence on the understanding of pan circulation for a long time.

He also measured temperatures by doing a traverse across the top of a vacuum pan tube as close to the tube sheet as practicable (Webre 1934), and found that at the end of the cycle the temperature at the centre of the tube approached that observed using the pan thermometer, but that the temperature close to the tube wall was higher by as much as 30°C.

Claasen (1938) concluded that circulation is caused by vapour formation on the heating surface in the tubes, and that, because of the low thermal conductivity, the bubbles formed do not condense in the surrounding massecuite although it is at a lower temperature.

One of the first to express doubts about the circulation theory of Webre was Allan (1962). He considered that the forces involved were of a much greater magnitude than those that would result from the difference in massecuite density caused by temperature.

An indication that ebullition occurs in the tubes was obtained by Troino and Vaisman (1964) who measured temperatures along the axis of the tubes. They found that the

maximum temperature was recorded at 30% of the tube length at the beginning of the cycle and that this point rose progressively, and was close to the top of the tube at the end of the cycle.

The proof that ebullition takes place in the tubes was given by Skyring and Beale (1967) who mounted a boiling tube fitted with sight glasses on the side of a conventional pan. They were able to observe the formation of bubbles at depths as low as 0,3 m from the tube inlet.

The formation of a vapour-massecuite zone over the heating surfaces was measured by Austmeyer (1980) by means of conductivity probes. His experiments showed that sub-cooled boiling takes place in the lower part of the tube.

2.2.1. Design factors affecting circulation

The main design parameters that are considered to affect circulation in pans are as follows:

(a) The depth of massecuite over the tubes.
(b) The tube length.
(c) The tube diameter.
(d) The ratio of the sectional area of the downtake to that of the tubes.
(e) The ratio of the heating surface to the volume of massecuite.

In batch pans the depth of massecuite increases gradually from the beginning to the end of the cycle with a corresponding decrease in the speed of circulation. The early pans boiled at depths of up to 2,5 m above the tubes (Smith, 1935). The importance of reducing the hydrostatic head above the tubes was stressed by Venton (1950) who recommended that the depth should be limited to 2 m. Perk (1952) advised 1,5 m while Beardmore et al. (1969) considered that it should be even lower at 1,2 m.

The 'low head' vacuum pan (Hamill, 1956) was introduced so as to reduce the depth while maintaining the same massecuite volume. This was done by enlarging the body of the pan above the calandria.

In continuous pans the depth of massecuite over the tubes is relatively constant, and is less than in batch pans, normal operating values being between 0,3 and 1 m.

The early batch pans had tubes over one metre in length. Webre (1926) mentions tubes of between 1,2 and 1,4 m. Claasen (1938) considered that the length should not exceed one metre so as to minimize the hydraulic resistance. From calculations based on single phase friction throughout the circulation path Jenkins (1958) recommended that the tubes should be as many and as short as possible, but Allan (1962) disagreed, and wrote that on the contrary circulation is promoted by long tubes. Beardmore et al. (1969) considered that maximum heat transfer is obtained with tubes of 1,2 m.

An unpublished survey done by the Sugar Milling Research Institute indicates that there has been a decrease in the length of the tubes of C-massecuite pans built after 1955, starting from an average value of 1,1 m for that year down to 0,6 m in 1975. No batch C-massecuite pans have been installed in South Africa after that date. This is illustrated in Figure 2.1.

The tendency has been to use comparatively long tubes in continuous pans. Broadfoot and Wright (1981) suggest a design with tubes between 1,2 and 2,0 m and McDougall and Wallace (1982) describe a pan having 1,2 m tubes.

Tube diameters have varied between 0,086 and 0,127 m. Webre (1926) mentions diameters of 0,102 to 0,114 but said it should not be less than 0,089 m. Claasen (1938) considered the optimum to be 0,089 to 0,102 m. French manufacturers have supplied pans with tubes as small as 0,086 m (Hugot, 1950). Hugot and Jenkins (1959) concluded from

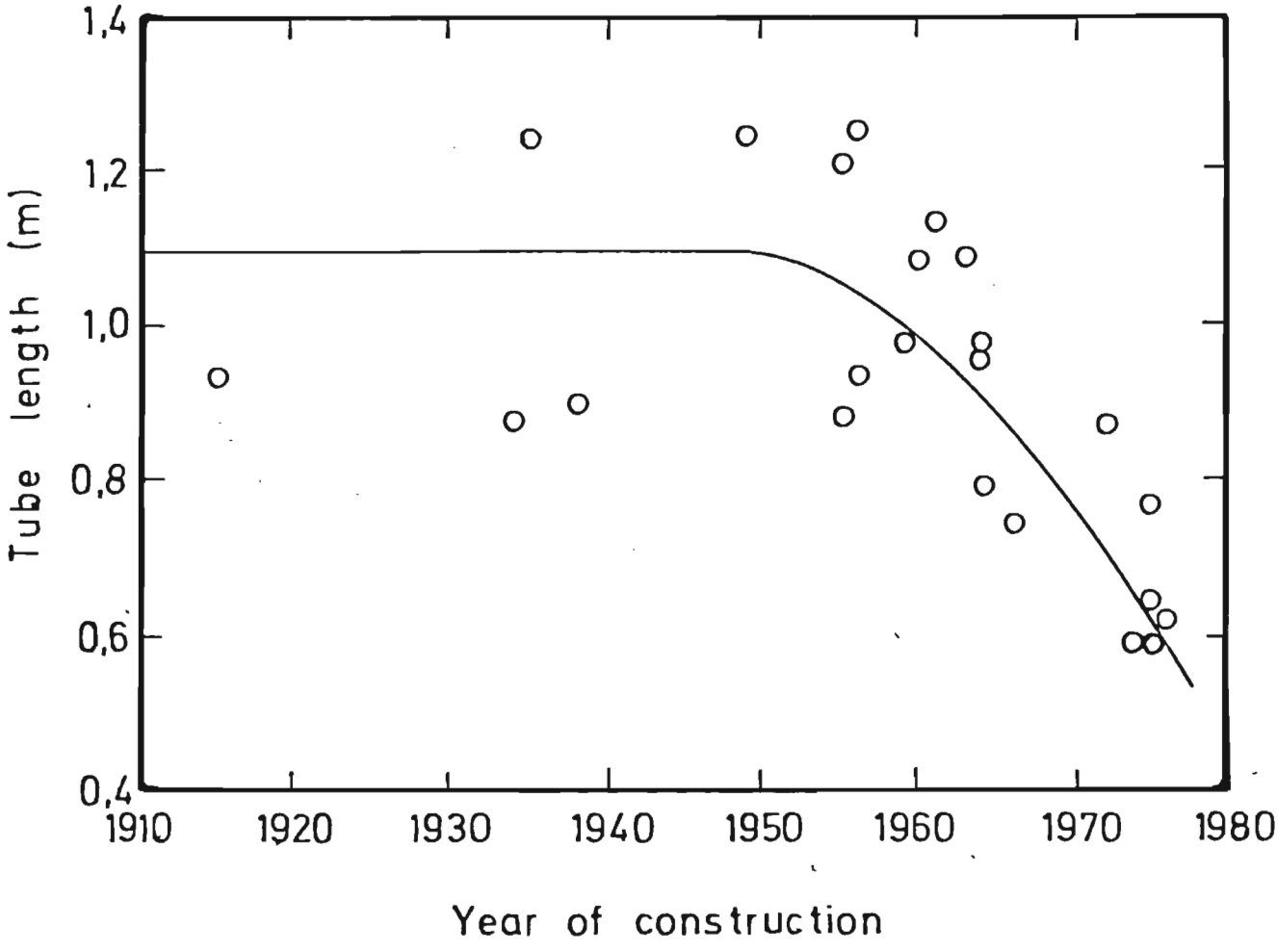

Figure 2.1. Change in tube length of C-massecuite batch pans.

calculations of the frictional losses in the circulation path that the tube diameters should be larger than those in use, but based on their experiments Beardmore et al. (1969) reported that 0,10 m tubes gave circulation velocities one and a half times greater than 0,127 m tubes. A study done by Behne et al. (1971) in an experimental pan fitted with plate heating elements, has shown that circulation was improved when the gap between the plates was reduced from 0,1 to 0,079 m. It was believed that the smaller gap produced a greater driving force because of the more concentrated heat input which more than compensated for the increased friction loss.

Unusual shapes of heating elements have been used in continuous pans. Graham and Radford (1977) describe a pan fitted with plate elements, Jullienne and Munsamy (1981) tell of a pan with horizontal 30 mm dia. steam tubes forming banks 50 mm. apart and McDougall and Wallace mention a unit with square tubes 0,127 x 0,127 m. The use of 0,127 circular tubes is also reported by Broadfoot and Wright (1981).

Webre (1926) recommended that the downtake should be large in relation to the pan diameter, while the concept of the 'circulation ratio', which is the ratio of the sectional area of the tubes to the sectional area of the downtake, was introduced by Smith (1938), who considered that a ratio of two was desirable for good circulation. The location of the downtake was discussed by Hugot (1950). He described pans with central annular and diametral downtakes. Following the publication of Webre's paper there was a sharp reduction of the circulation ratio from about 5 in 1925 to a value of just above 1 in 1940. Subsequently the circulation ratio was increased gradually up to 2,5 in 1975. This is illustrated in Figure 2.2. based on an unpublished survey of the C-massecuite batch pans in service in the South African sugar industry done by the Sugar Milling Research Institute.

The location of the downtake in continuous pans also

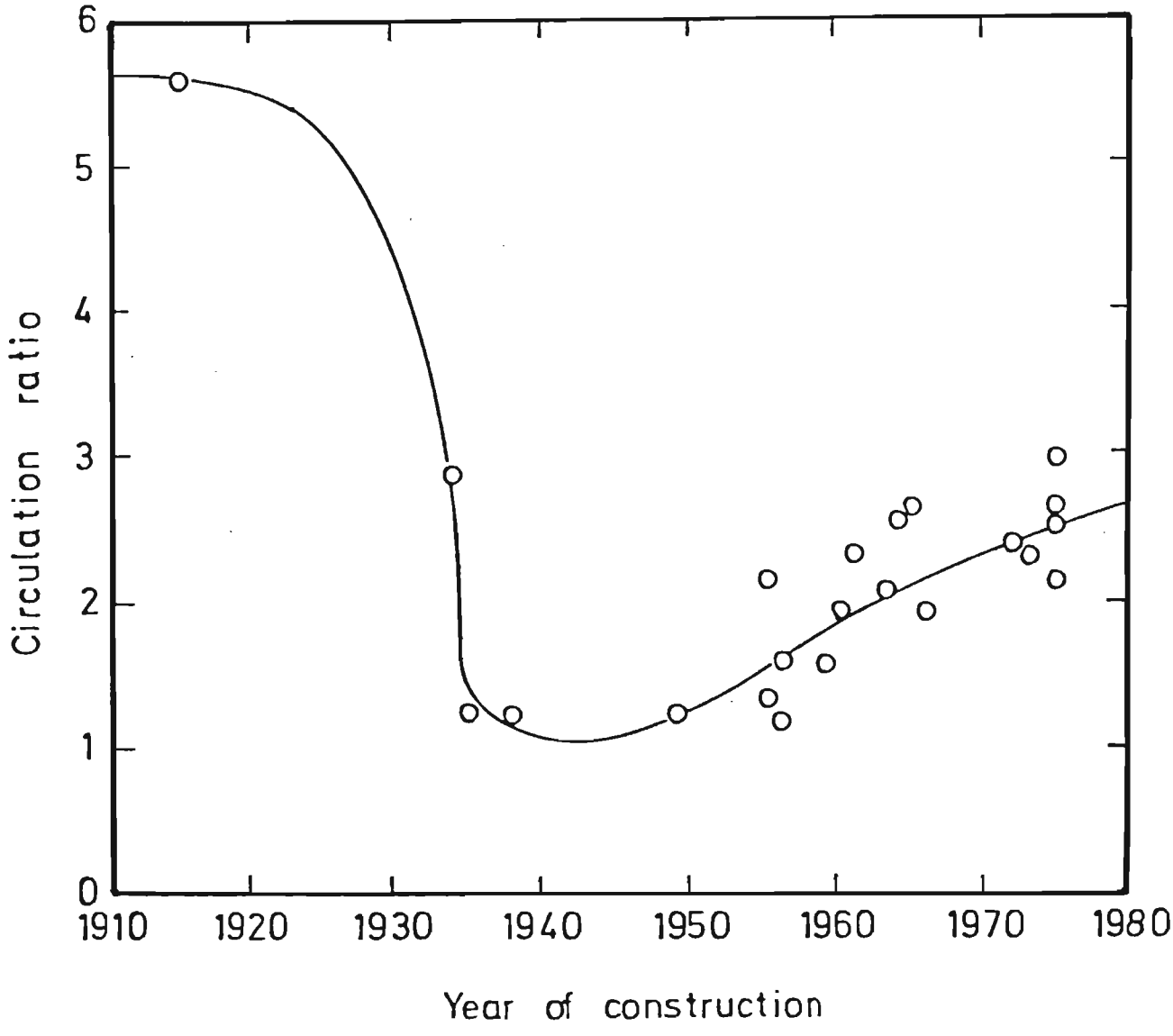

Figure 2.2. Change in circulation ratio of C-massecuite batch pans.

varies. It may be either two longitudinal downtakes located along the sides, Langreney (1977), Graham and Radford (1977), Broadfoot and Wright (1981), or one longitudinally along the central axis, McDougall and Wallace (1982).

The value of the ratio of the area of the heating surface to the volume of massecuite varies during the cycle of a batch pan. The optimum ratio at the end of the cycle was given by Webre (1926) as 7,4 to 8,2 m^{-1}. Hugot (1950) says that this ratio should be a function of the steam pressure and of the type of massecuite. He recommends a value of 5 to 8 when using a steam pressure of 40 to 60 kPa and 8 to 10 when using a pressure less than 40 kPa. According to him the present trend is toward an increase of the heating surface/volume ratio, and that new pans do not go below 6 m^{-1} even for low grade massecuite.

Van Hengel (1971) suggested pan characteristics as shown in Table 2.1. The depth above the tubes was given as 1,5 m, and the circulation ratio as 2,3 to 2,5.

TABLE 2.1.

Heating Surface and Tube Length Requirements as a Function of Massecuite Quality (Van Hengel, 1971)

Massecuite	Surface/Volume (m^{-1})	Tube Length (m)
Refinery	7	0,94
A	5,5	0,74
B	5	0,66
C	4	0,53

A pan recently completed in Australia for A-massecuite

had the dimensions shown in Table 2.2 (Nielson, 1974).

TABLE 2.2.

Dimensions of Pan for A-Massecuite (Nielson, 1974)

Tube diameter (m)	0,114
Tube length (m)	0,876
Depth above tubes (m)	1,6
Heating surface/volume (m^{-1})	5,18
Circulation ratio	2,21

Based on the data published by Allan (1983) the heating surface to volume ratio of the A, B and C pans in service in South Africa is 5,8; 5,7 and 5,6 respectively at the end of the cycle. The value at the start is approximately 14.

The continuous pans of Fives-Cail Babcock have a surface to volume ratio which is higher than that of batch pans at the end of the cycle being 9,8 to 10 m^{-1} (Jullienne and Munsamy, 1981). This is also the ratio suggested by Broadfoot and Wright (1981), while McDougall and Wallace (1982) describe a continuous pan with a ratio of 8,45 m^{-1}.

2.2.2. Flow pattern and velocity of circulation

One of the first attempts to define the flow pattern in vacuum pans was done by Werkspoor (1931) by means of tracer tests on a model pan fitted with observation windows. The massecuite in the pan was simulated by a mixture of glucose syrup and thick oil. Small holes were drilled in the tubes through which air was blown so as to simulate rising steam bubbles. The resulting flow pattern is shown in Figure 2.3.

Smith (1938) measured massecuite velocity in pans using two conductivity probes placed one above the other. The

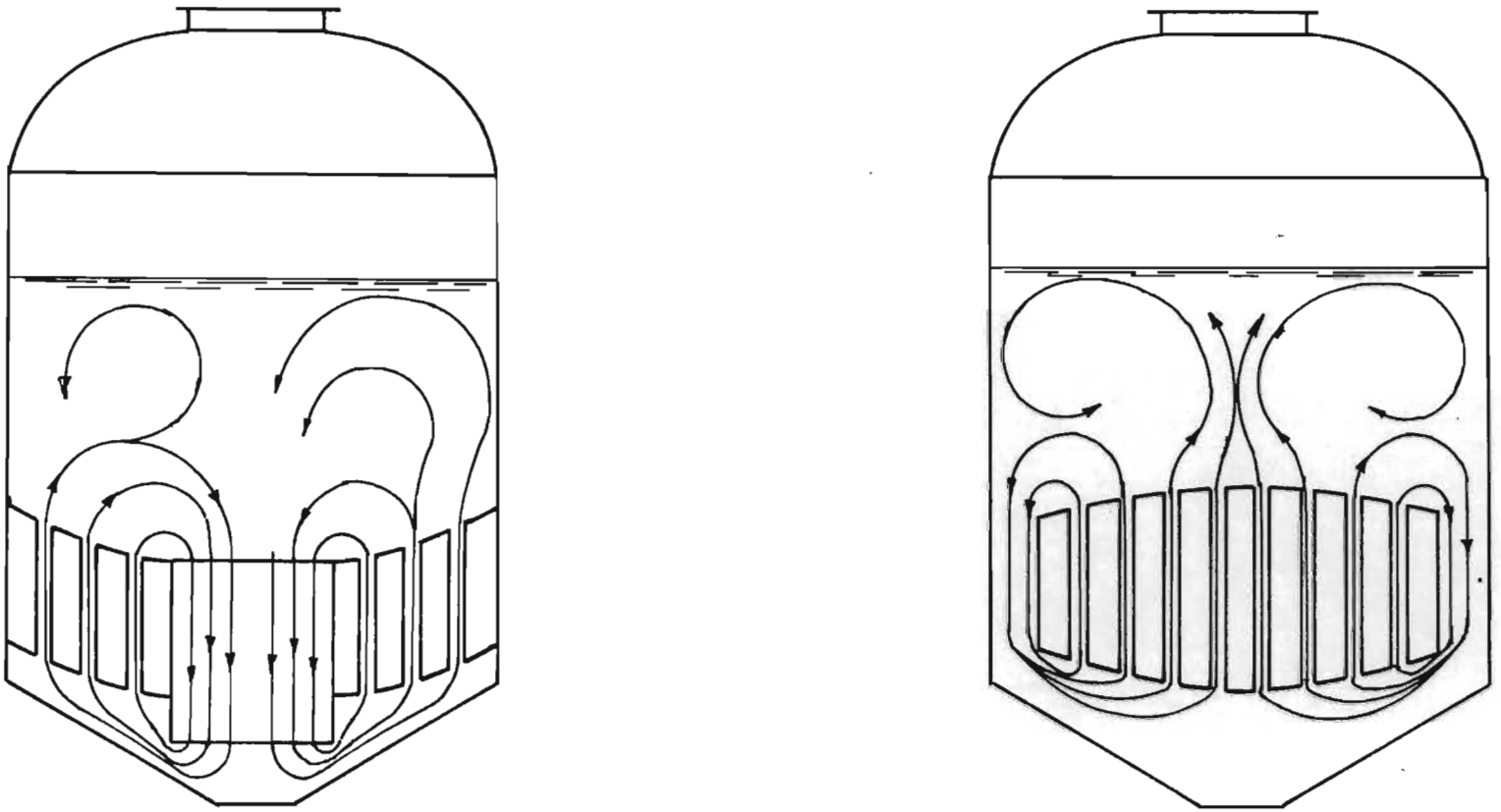

Figure 2.3. Circulation pattern observed in model batch pans (Werkspoor, 1931).

time difference for an impulse to register on the electrodes gave an indication of the velocity. The velocity ranged from 0,01 to 0,18 m s^{-1}.

Hot wire anemometers were used by Bosworth and Duloy (1950) to study the velocity by doing a traverse across different types of pans. The velocity observed varied between 0,02 and 0,16 m s^{-1}.

Massecuite temperatures were measured just above the top of the tubes, close to the surface and below the tubes (Anon. 1963). It was found that the temperature below the tubes was intermediate between those observed at the other two points.

The pattern and rate of circulation in pans were studied by the Sugar Research Institute (Anon., 1964, 1965) by monitoring the movement of a radioactive capsule using seven scintillation counters arranged around the pan. Typical flow patterns observed are shown in Figure 2.4. These tests indicated that intermittent ebullition is a factor which becomes increasingly important as the viscosity of the massecuite increases.

2.2.3. Calculation of circulation

Having concluded that only single phase convective heat transfer occurred in the tubes, Webre (1932) calculated the velocity of circulation by equating the heat from the condensate to the product of the mass flow rate, specific heat and temperature difference between the tube outlet and surface boiling temperature of the massecuite. He agreed, however, that this was only an approximation.

Tromp (1937) using the same principles calculated the velocity of the massecuite in the tubes and in the downtake for pans having different ratios of downtake to pan diameter.

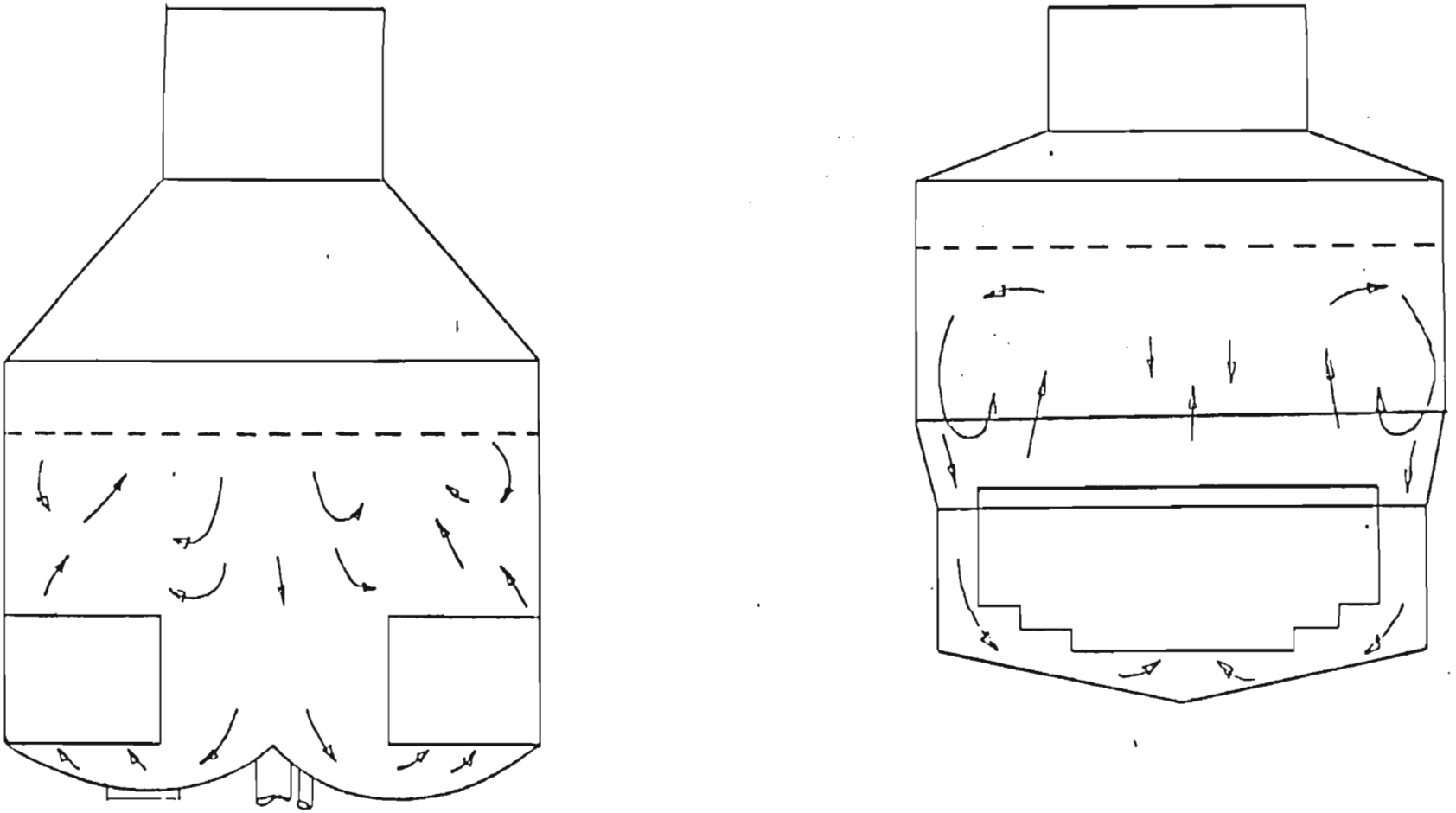

Figure 2.4. Circulation pattern observed in fullscale batch pans (Sugar Research Institute 1964, 1965).

A method for calculating the relative friction losses in the tubes and in the downtake was suggested by Jenkins (1958). His calculations again assumed that no ebullition took place in the tubes, and he showed that for a pan with a circulation ratio of two, which was said to have good circulation, the friction loss in the tubes was 80 times greater than in the downtake. Thus he recommended that the friction in the tubes should be 80 times greater than in the downtake.

Still assuming single phase convective heat transfer as the sole driving force Hugot and Jenkins (1959) tried to correlate heat transfer and resistance to flow in the tubes. They did not use the equations recommended for the estimation of the heat transfer coefficient in laminar flow, but instead assumed that the overall heat transfer coefficient is simply proportional to the massecuite velocity. From this they developed an expression for what they called the rapidity ratio; a function of the ratio of tube diameter to pan diameter, downtake diameter to pan diameter and cross sectional area of the tubes to area of the tube plate.

Troino (1968) was the first to attempt calculation of the circulation velocity assuming ebullition in the tubes. He used equations developed for two phase pressure drop in boiler tubes and produced an equation for the pressure head available for massecuite circulation. This work was continued by Garyazha et al. (1974) and Pavelko and Garyazha (1975) who devised equations for calculating the friction losses in the tubes and the length of tube under single phase convective heat transfer.

2.2.4. Discussion

The mechanism of circulation in pans has long been misunderstood, because it was believed that no ebullition took place in the tubes. It is only during the last twenty years that vapour formation was shown to occur on the

heating surfaces.

The main factor affecting circulation is believed to be the hydraulic resistance of the circulation path, and all improvements in pan design are interpreted in this light. The use of shorter tubes and of smaller circulation ratios is supposed to reduce the friction loss in the tubes and downtake respectively (Claasen 1938, Jenkins 1958).

Calculation of the circulation velocity has been attempted assuming single phase heat transfer and friction losses, with the heat transfer coefficient function only of the massecuite velocity (Hugot and Jenkins 1959). More recently another attempt was made at calculating the circulation velocity using equations developed for water tube boilers (Troino 1968).

These calculations are inaccurate because they are not based on a sound theoretical background.

2.3. THE BOILING PROCESS

The flow pattern and the liquid and tube surface temperature that occur over the length of a vertical evaporator tube are shown in diagrammatic form in Figure 2.5. The liquid that enters is generally subcooled, that is its temperature is below the saturation temperature corresponding to the pressure at that point. In region AB heat transfer is entirely by single phase forced convection. As heat is transferred to the liquid the temperature adjacent to the heating surface increases until at point B the boiling temperature is exceeded and vapour formation occurs, but the bulk of the liquid is still subcooled. Between B and D the vapour bubbles grow because of the additional heat input, and as a result of the decompression as the hydrostatic head decreases. At the same time heat penetrates towards the centre of the tube so that the liquid temperature increases.

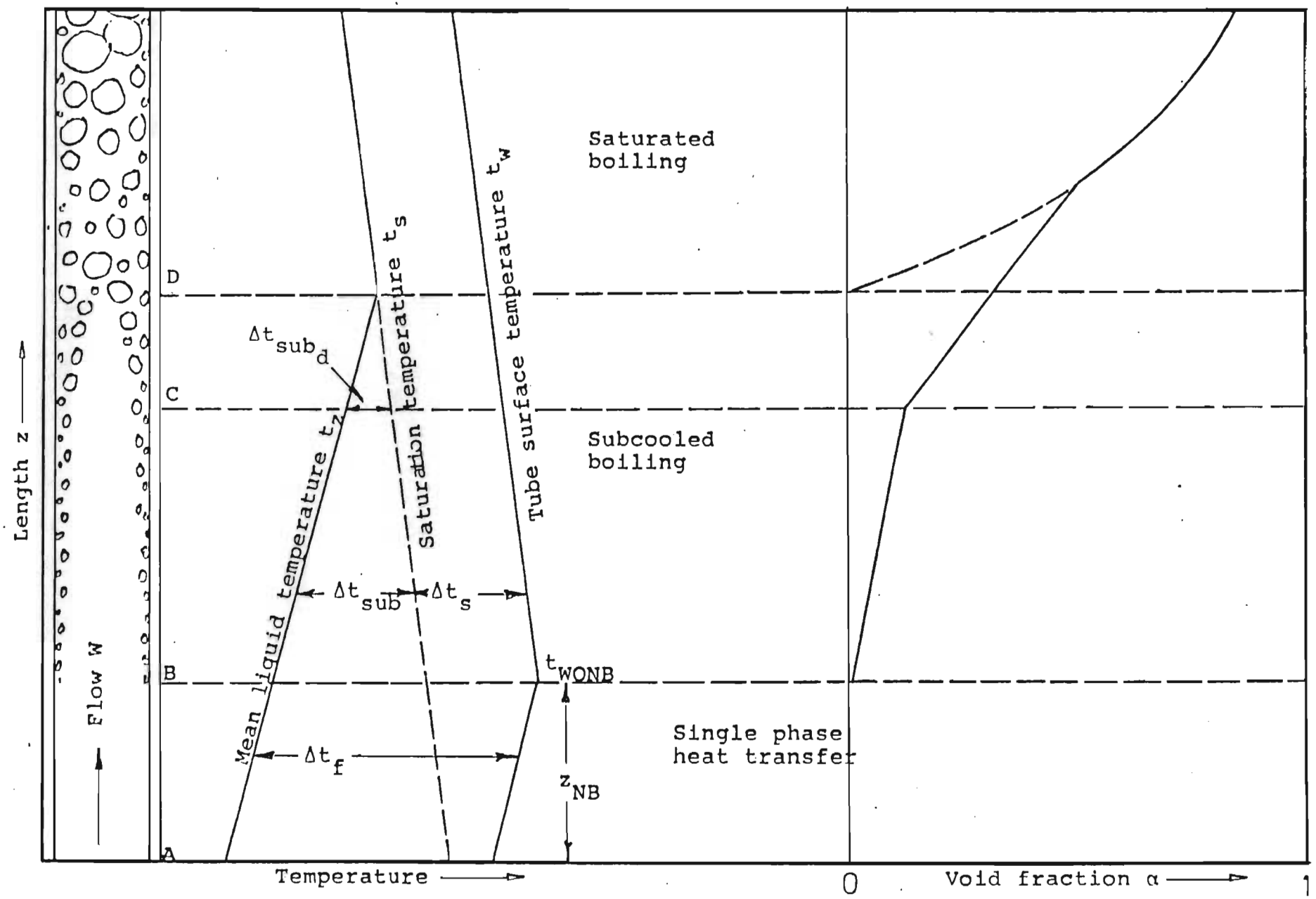

Figure 2.5. Diagram of temperatures and void fractions in subcooled boiling.

The heat transfer under these conditions is known as subcooled boiling. Transition to saturated boiling occurs when the average combined enthalpy of the liquid and vapour equals the saturation enthalpy of the liquid. This happens a short distance upstream of point D. At point D boiling extends across the entire sectional area of the tube, and from this point there is a gradual decrease of the fluid temperature because of the decompression effect. However, under certain conditions transition to saturated boiling does not occur and subcooled boiling extends to the tube outlet.

2.3.1. Single phase liquid heat transfer

Because massecuite is a viscous pseudoplastic fluid, the heat transfer coefficient in region AB can be calculated using the Seider and Tate equation as modified by Charm and Merrill (1959). This equation has been developed for determining the heat transfer coefficient of pseudoplastic fluids in straight tubes

$$\frac{h_f D}{k_f} = 2{,}0 \left[\frac{W c_p}{k_f z}\right]^{1/3} \left[\frac{K_b(3n+1)}{K_w 2(3n-1)}\right]^{0{,}14} \qquad (2.3)$$

where h_f is the film heat transfer coefficient, D the tube diameter, k_f the thermal conductivity, W the mass rate of flow, c_p the specific heat, z the distance from the tube inlet, K_b the fluid consistency index at bulk temperature, K_w the fluid consistency index at wall temperature and n is the flow behaviour index.

In this equation the Nusselt number is a function of the Graetz number that is the product of the Reynolds and Prandtl numbers and the dimensionless viscosity ratio.

Equation (2.3) predicts values of h_f with a mean absolute deviation of 10,8 percent with a maximum deviation of

+18 and -24 percent. (Skelland 1967).

2.3.2. The onset of subcooled boiling

Boiling starts when the tube surface temperature exceeds the saturation temperature by a value which is a function of the heat flux. The equation for estimating the value of $(\Delta t_s)_{ONB}$, the wall superheat necessary to cause nucleation, is based on a treatment originally proposed by Hsu (1962) for pool boiling. He postulated that the bubble nuclei on cavities in the tube surface will only grow if the bubble temperature furthest away from the wall exceeds t_g, the vapour temperature. An analytical solution of this postulate by Davis and Anderson (1966) yielded the following equation

$$\phi_{ONB} = \frac{k_f}{4B} (t_w - t_s)^2_{ONB} \qquad (2.4)$$

where ϕ_{ONB} is heat flux to cause boiling, t_w is the inside tube surface temperature, t_s the saturation temperature, and B is given by the equation

$$B = \frac{2 \sigma t_s v_{fg}}{i_{fg}} \qquad (2.5)$$

in which σ is the surface tension, i_{fg} is the latent heat of vaporisation and v_{fg} is the difference in specific volumes of saturated liquid and vapour.

2.3.3. Boiling Heat Transfer

Immediately after boiling has started the tube wall is not entirely covered by bubbles so that heat is still transferred partially by single phase forced convection. The area covered by bubbles increases along the tube until the

single phase component reduces to zero and fully developed subcooled boiling takes place. The mechanism of heat transfer at subcooled nucleate boiling has been discussed by Forster and Grief (1959). They concluded that heat is transferred by conduction, by latent heat transport, by vapour bubbles and by convection, but particularly by the transport of a quantity of hot liquid from the heating surface towards the axis of the tube during the growth of vapour bubbles.

Two fairly distinct methods have been proposed to estimate the boiling heat transfer coefficient in both the subcooled and saturated regions. In the first method which is more fundamental the heat flux, ϕ, is calculated by the superposition of the forced convective heat flux, ϕ_c, and the nucleate boiling heat flux, ϕ_n,

$$\phi = \phi_c + \phi_n \qquad (2.6)$$

whereas in the second method the combined heat flux is correlated using dimensionless groups.

The procedure proposed by Rohsenow (1953) follows the first approach. The single phase forced convection component is given by

$$\phi_c = h_{fo} (t_w - t_{(z)}) \qquad (2.7)$$

where h_{fo}, the heat transfer coefficient for the total flow assumed liquid, is calculated using the Dittus-Boelter equation, and $t_{(z)}$ is the bulk liquid temperature at axial position z.

The difference $(\phi - \phi_c)$ was sucessfully correlated by Rohsenow with an equation that he had previously suggested for pool boiling. This equation contains an arbitrary

constant C_{sf} which accounts for the different nucleation properties of various liquid - tube surface combinations and whose value varies between 0,0022 and 0,013.

$$Nu = \frac{1}{C_{sf}} Re_f^{0,33} Pr_f^{1,7} \qquad (2.8)$$

where Nu, Re and Pr are the Nusselt, Reynolds and Prandtl numbers. This equation has been rearranged to give

$$\left(\frac{c_p \Delta t_s}{i_{f_g}}\right) = C_{sf} \left[\frac{\phi_n}{\mu i_{f_g}} \left(\frac{\sigma}{g(\rho_f - \rho_g)}\right)^{\frac{1}{2}}\right]^{0,33} \left(\frac{c_p \mu}{k_f}\right)^{1,7} \qquad (2.9)$$

where Δt_s is the superheat necessary to cause nucleation, μ is the viscosity, σ is the surface tension and ρ_f and ρ_g are the densities of the liquid and vapour respectively.

Another correlation based on the same principle is that of Chen (1966). The boiling heat transfer coefficient h_{TP} is considered to be the sum of a forced convection component h_c and of a nucleate boiling component h_{NcB}.

$$h_{TP} = h_{NcB} + h_c \qquad (2.10)$$

For the forced convection Chen used a Dittus-Boelter type relationship for two phase flow. However, he argued that since the heat transfer takes place through a liquid film near the wall, and the values of the Prandtl number for vapour and liquid do not differ much, it was reasonable to assign liquid values to this modulus. He related the two phase Reynolds number to that of the liquid by the parameter

$$Re_f = F \left[\frac{G\ (1 - x) D}{\mu_f}\right]^{0,8} \qquad (2.11)$$

and showed that the factor F could be expressed as a function of the Martinelli parameter X_{tt}. The resulting expression for the forced convection heat transfer coefficient was

$$h_c = 0,023\left[\frac{G(1-x)D}{\mu}\right]^{0,8}\left[\frac{\mu c_p}{k}\right]_f^{0,4}\left(\frac{k}{D}\right)(F) \qquad (2.12)$$

where G is the mass velocity.

For the nucleate boiling component Chen adapted the correlation of Forster and Zuber (1955) for nucleate pool boiling. However, since the nucleate boiling component is less for convective boiling than it is for pool boiling at the same wall superheat, Chen incorporated a suppression factor defined as follows:

$$S = \left[\frac{\Delta t_e}{\Delta t_{sat}}\right]^{0,99} \qquad (2.13)$$

where Δt_e is the effective wall superheat into which the vapour bubbles grow. The equation for the nucleate boiling component is then

$$h_{NcB} = 0,00122\left[\frac{k^{0,79}c_p^{0,45}\rho_f^{0,49}}{\sigma^{0,5}\mu^{0,29}i_{fg}^{o,24}\rho_g^{o,24}}\right]\Delta t_{sat}^{0,24}\Delta p_{sat}^{0,75}(S) \qquad (2.14)$$

where Δp_{sat} is the saturated vapour pressure difference corresponding to Δt_{sat}.

Many equations have been proposed using the second method where the heat transfer data are expressed as a function of a number of dimensionless groups. Some of the equations based on this principle are of the form

$$\frac{h_{TP}}{h_{fo}} = a \left[\frac{1}{X_{tt}}\right]^{b} \qquad (2.15)$$

where h_{TP} is the boiling film heat transfer coefficient and X is the Lockhart and Martinelli (1949) parameter. The value of the constant a ranges from 2,2 to 7,6 and that of the exponent b from 0,3 to 0,75. Two correlations of this type are those of Dengler and Addoms (1956) and Schrock and Grossman (1959).

In the other equations using this method the ratio of the boiling to the single phase heat transfer coefficients are correlated with the Prandtl number, the boiling number ($\phi/i_{fg}G$), the Kutadelaze number ($i_{fg}/Cp\Delta t_s$) and the dimensionless density ratio (ρ_f/ρ_g). One such equation is that of Papell (1962)

$$\frac{h_{TP}}{h_f} = 90 \left[\frac{\phi}{i_{fg}G}\right]^{0,7} \left[\frac{i_{fg}}{c_p \Delta t_s}\right]^{0,84} \left[\frac{\rho_f}{\rho_g}\right]^{0,76} \qquad (2.16)$$

and another one is that of Moles and Shaw (1972)

$$\frac{h_{TP}}{h_f} = 78,5\,(Pr_f)^{0,46} \left[\frac{i_{fg}}{c_p \Delta t_{sub}}\right]_s^{0,5} \left[\frac{\phi}{i_{fg}\rho_g u}\right]_s^{0,67} \left[\frac{\rho_g}{\rho_f}\right]_s^{0,7} \qquad (2.17)$$

The importance of the boiling number ($\phi/i_{fg}G$) in these correlations has been pointed out by Davidson et al. (1943). This parameter is the ratio of the mass rate of vapour formation inside the tube to the total mass rate of flow of fluid in the tube. In effect it relates the single phase Reynolds number to that for two phase flow.

The significance of the dimensionless density ratio has

been discussed by McNelly (1953). This parameter accounts for the effect that the sudden change in volume that takes place at the moment of vapour formation has on the heat transfer coefficient.

Some studies on heat transfer to boiling massecuites have been done in Russia. Neduzhko (1964) proposed an empirical equation for first beet sugar massecuite and second refinery massecuite where the Nusselt number for the boiling fluid is a function of the liquid Prandtl number, the crystal content and the Tolubinskii number which is in fact a modified boiling number.

$$Nu = 16,4\ Pr_f^{-0,1}\left[\frac{100 - K_p}{K_p}\right]^2 \left[\frac{\phi}{i_{fg}\rho g u_o}\right]^{0,6} \qquad (2.18)$$

where K_p is the percent crystal content and u_o is the rate of bubble growth.

2.3.4. Discussion

The heat transfer coefficient in forced convection boiling has been studied mostly in the turbulent regime under pressures higher than atmospheric. Most studies have been done using steam-water systems, refrigerants and petroleum products. No reference has been found on boiling highly viscous non-Newtonian fluids in laminar flow under vacuum.

The equations proposed have been obtained by following two fairly distinct paths. In the first group which includes the work of Rohsenow (1953) and Chen (1966) a superposition or interpolation technique is used. The boiling heat flux is obtained from the addition of a single phase forced convection component and a correlation for a pool boiling component. The correlation of Chen is at present considered

one of the best for boiling heat transfer in the turbulent regime, but Moles and Shaw (1972) have shown that it gives incorrect results for the prediction of subcooled boiling heat transfer coefficient.

The second path involves data reduction by means of dimensionless groups, and in this category falls the majority of the boiling heat transfer equations proposed to date. The ratio of the two phase to the single phase heat transfer coefficient is usually correlated with the Prandtl number, boiling number and dimensionless density ratio, this last group accounting for the effect of pressure. Most of these equations apply only to the test liquid, for example the equation of Papell correlates only with water.

The average deviations of the correlations lies within the range +40 to -40 percent except for the correlation of Chen (1966) which ranges between +11 to -11 percent.

2.4. PRESSURE DROP IN EVAPORATOR TUBES

In the region just after the tube inlet the pressure drop consists of the friction loss for a single phase fluid plus the single phase hydrostatic head loss. Starting at point B in Figure 2.5. when boiling begins the pressure drop is made up of three contributions:

(i) The momentum effect which results from acceleration along the tube due to evaporation and expansion of the vapour phase.

(ii) The gravitational effect which results from the change in elevation along the tube.

(iii) The frictional effect due to shear forces acting on the two phase fluid.

2.4.1. Pressure drop in the single phase region

Virtually no work of an engineering nature has appeared in the literature on time-dependent thixotropic fluids. However, in an evaporative crystallizer the fluid is sheared continuously and can be considered to have become practically time-independent.

Metzner and Reed (1955) have developed a method for the calculation of friction losses in pipes for time-independent non-Newtonian fluids. Starting from the expression of Mooney (1931) for the shear stress at the pipe wall and Fannings equation for friction loss they obtained the generalized Reynolds number for pseudoplastic fluids

$$Re = \frac{D^n u^{2-n} \rho_f}{K_f} \cdot 8. \left[\frac{n}{6n+2}\right]^n \qquad (2.19)$$

Their derivation showed that all fluids which are not time-dependent obey the conventional Newtonian friction factor versus Reynolds number relationship when the flow is laminar provided that the generalized Reynolds number is used. The friction losses for isothermal conditions can then be calculated from Fannings equations

$$\Delta p_F = \frac{32 z u^2 \rho_f}{gDRe} \qquad (2.20)$$

where Δp_f is the pressure difference due to friction and g is the acceleration due to gravity.

However, in the evaporator tube, because the fluid is being heated it is non-isothermal. The value of the Fanning friction factor is sensibly decreased under these conditions. Sieder and Tate (1936) have suggested a factor to correct for the radial and axial viscosity gradients

resulting from non-isothermal flow.

$$\Delta p_{F_{noniso}} = \Delta p_{F_{iso}} \frac{1}{1,1} \left(\frac{\mu_w}{\mu_b}\right)^{0,25} \qquad (2.21)$$

where $\Delta p_{Fnoniso}$ and Δp_{Fiso} are the non-isothermal and isothermal friction losses and μ_w and μ_b are the viscosities at the wall and bulk temperatures respectively. This correction factor must be modified for application to non-Newtonian fluids. Charm and Merrill (1959) have shown that for pseudoplastic fluids the dimensionless viscosity ratio can be expressed as

$$\frac{\mu_w}{\mu_b} = \frac{K_w 2(3n+1)}{K_b(3n-1)} \qquad (2.22)$$

Thus the Sieder and Tate correction factor becomes

$$\Delta p_{F_{noniso}} = \Delta p_{F_{iso}} \frac{1}{1,1} \left[\frac{K_w 2(3n+1)}{K_b(3n-1)}\right]^{0,25} \qquad (2.23)$$

The elevation loss in the single phase region is given by the equation

$$\Delta p_z = z p_f g/g_c \qquad (2.24)$$

where g_c is a conversion factor.

2.4.2. Pressure drop in the two phase region

As stated previously pressure drop in the two phase boiling region consists of the elevation loss, acceleration loss and friction loss.

$$\frac{dp}{dz} = \frac{dp_z}{dz} + \frac{dp_A}{dz} + \frac{dp_F}{dz} \qquad (2.25)$$

For steady state flow the pressure loss can be expressed in terms of the momentum equation of which there are many versions. One of them is that suggested by Butterworth and Hewitt (1977)

$$-\frac{dp}{dz} = g\left[\alpha\rho_g + (1-\alpha)\rho_f\right] + G^2\frac{d}{dz}\left[\frac{x^2}{\alpha\rho_g} + \frac{(1-x)^2}{(1-\alpha)\rho_f}\right] + \frac{4\tau_w}{D} \qquad (2.26)$$

where τ_w is the wall shear stress, x is the mass vapour quality and α is the void fraction.

The elevation and acceleration losses can be calculated from the momentum equation if the mass vapour quality and void fraction are known. The frictional component must, however, be determined empirically.

For a finite length of pipe z, the gravitational pressure loss is expressed as

$$\Delta p_z = \frac{zg}{g_c}\left[\alpha\rho_g + (1-\alpha)\rho_f\right] \qquad (2.27)$$

and the acceleration loss as

$$\Delta p_A = \frac{G^2}{g}\left(\left[\frac{x^2}{\alpha\rho_g} + \frac{(1-x)^2}{(1-\alpha)\rho_f}\right]_2 - \left[\frac{x^2}{\alpha\rho_g} + \frac{(1-x)^2}{(1-\alpha)\rho_f}\right]_1\right) \qquad (2.28)$$

One of the earliest empirical methods for calculation of the friction loss was that proposed by Martinelli and Nelson (1948) and Lockhart and Martinelli (1949). Their method is based on the isothermal flow of an air-water system at close

to ambient conditions. They related the two-phase frictional pressure gradient to the frictional pressure gradient due to the gas and liquid flowing alone in the same pipe by means of the parameters ϕg, ϕf and X.

These parameters are defined as follows:

$$\phi_{g \text{ or } f} = \left[\frac{(dp_F/dz)_{TP}}{(dp_F/dz)_{g \text{ or } f}}\right]^{\frac{1}{2}} \qquad (2.29)$$

where $(dp_F/dz)_{TP}$ is the pressure gradient for two phase flow and $(dp_F/dz)_{g \text{ or } f}$ are the pressure gradients for the total flow of fluid having the vapour or liquid physical properties respectively, and

$$X = \left[\frac{(dp_F/dz)_f}{(dp_F/dz)_g}\right]^{\frac{1}{2}} \qquad (2.30)$$

The relation between ϕg and ϕf and X was expressed graphically by means of different curves depending on whether the liquid and vapour flow was laminar or turbulent.

A different method was that proposed by Griffith and Wallis (1961), and which was developed for the flow of oil-gas mixtures in oil wells in the bubble flow regime. They related the friction loss to a modified Fanning equation

$$\Delta p_F = \frac{2f_f \rho_f u_f^2 z}{gD(1-\alpha)^2} \qquad (2.31)$$

where f_f, the Fanning friction factor, is obtained from the conventional Reynolds number - Fanning friction factor plot using a velocity defined by

$$u_f = \frac{Q_f}{A(1-\alpha)} \qquad (2.32)$$

This method was used by Hsu and Dudukovic (1980) to calculate the friction loss in a gas-lift reactor. They observed that transition to turbulent flow took place at R_e = 1000.

This method was modified by Oliver and Wright (1964) for pseudoplastic non-Newtonian two-phase systems, and was based on isothermal slug flow regimes in horizontal tubes.

The liquid properties were considered to be dominant, the only parameter modified by the presence of gas was the liquid velocity which was obtained from the equation

$$u_{TP} = \frac{Q_f + Q_g}{A} \qquad (2.33)$$

Both the liquid and gas flow rates were measured during the experiment. The liquid friction factor was calculated using the relation 16/generalized Reynolds number. The two-phase generalized Reynolds number was calculated using the velocity given by equation (2.33). A plot of the product of the single phase friction factor and two phase Reynolds number against the liquid holdup R_f gave the following correlation for the two phase friction factor.

$$f = (R_f)^{0,73} \frac{16}{Re} \qquad (2.34)$$

Oliver and Young Hoon (1968) measured the pressure drop in two-phase isothermal flow of pseudoplastic fluids using

fluids having a flow behaviour index of about 0,5. They observed that the pressure gradient increased in the bubble flow regime, but decreased in the slug-flow regime. They found that the method of Lockhart and Martinelli (1949) predicted pressure drop values that were too high in the case of non-Newtonian systems. The decrease in pressure drop observed was also confirmed by Mahalingam and Valle (1972).

2.4.3. Discussion

The pressure drop in the evaporator tube is made up of the elevation, acceleration and friction losses. the elevation and acceleration losses can be calculated if the void fraction and amount of vapour formed are known. Collier (1972) expresses the opinion that the present state of knowledge relating to the friction loss in the subcooled boiling region is very unsatisfactory indeed.

The method proposed by Griffith and Wallis (1961) for the friction loss in the bubble flow regime assumes that the presence of the gas phase causes only an increase in the velocity of the two phase mixture, but that the liquid properties still remain dominant.

2.5. VOID FRACTION IN EVAPORATION

The change in void fraction that takes place in an evaporator tube is shown in Figure 2.5. At first the vapour formed consists of discrete bubbles attached to the tube surface, but at C they become detached to form bubbly flow. At point D boiling extends across the tube and from this point coalescence of the bubbles occurs fairly rapidly and transition to slug flow may take place.

The void fraction resulting is a function not only of the amount of vapour generated, but also of the rate at which it moves up the tube. The upward rate of flow of the vapour

depends upon the distribution of the vapour flow, that is whether it is flowing close to the tube centerline or close to the wall, and upon the bubble rise velocity.

The amount of vapour present in the boiling tubes must be known to permit calculation of the elevation and acceleration pressure losses. It also has an influence on both the friction losses and heat transfer coefficient. In the case of natural circulation evaporative crystallizers, the circulation results from the difference in hydrostatic head between the two phase mixture of massecuite and vapour in the tubes and single phase massecuite in the downtake. Knowledge of the volumetric fraction occupied by vapour is therefore necessary to calculate the circulation rate.

Because of the complex nature of the subcooled boiling process most of the attempts made to predict the void fraction in the subcooled region have been empirical.

2.5.1. Measurement of void fraction

A review of void fraction measurement techniques is given by Hewitt (1978). The main methods used are radioactive absorption and scattering, impedence and volume measurement.

The most widely used technique is the measurement of the attenuation of a beam of gamma rays by the flowing fluid. This technique has been used among others by Marchaterre (1956) and Isbin et al. (1957) and (1959).

Another method that has been used for void fraction determination is that involving the direct measurement of the volume of the liquid or vapour phase in the tube. This is achieved by the use of quick closing valves which isolate the test section so that the volume occupied by each phase can be measured. This technique has been used by Lockhart

(1945) and Oliver and Young Hoon (1968) among others.

A third method involves the measurement of conductance and capacitance since the electrical impedance of two phase flow depends on the concentration of the phases. The method has been used by Spight (1966) and Cimorelli and Evangelisti (1967).

Austmeyer (1980) measured the void fraction in boiling massecuite by means of a number of conductivity probes mounted along the tube, a different conductivity reading being obtained when the probe is in a vapour bubble.

2.5.2. Void fraction in subcooled boiling

In region BC small bubbles grow and collapse but remain attached to the tube surface. This is known as the highly subcooled region. A model has been developed by Griffith, Clark and Rohsenow (1958) to estimate the void fraction in this region.

This model assumes no net production of vapour so that the boiling component, ϕ_n, of total heat flux must equal the condensing heat flux, ϕ_c.

$$\phi_n = \phi_c = \text{Constant} \times h_{fo} \times \frac{A_c}{A} \times \Delta t_{sub} \qquad (2.35)$$

where A_c/A is the bubble-liquid interfacial area per unit heated surface area. The size of the bubbles is assumed to be proportional to the thickness of the hydrodynamic boundary layer which in turn depends on the thermal layer thickness k_f/h_{fo} and the liquid Prandtl number $(Pr)_f$. If the ratio A_c/A is expressed in terms of the hydrodynamic boundary layer thickness and the void fraction equation (2.28) becomes

$$\alpha = \frac{\phi_n . (Pr)_f}{B1 . (Nu)_f . h_{fo} . \Delta t_{sub}} \qquad (2.36)$$

where Bl is a constant and α is the void fraction.

At low pressures this relationship becomes incorrect since the diameter of the bubbles is then a function of the pressure as well as the hydrodynamic layer thickness. Under these conditions the voidage is overestimated.

At point C the vapour bubbles start to depart from the tube surface and there is a rapid increase in void fraction. Griffith et al. (1958) found that the subcooling at the point of bubble departure Δt_{sub_d} could be approximated by the relationship

$$\Delta t_{sub_d} = \frac{\phi}{5 h_{fo}} \qquad (2.37)$$

Equation (2.30) was modified by Bowring (1962) to give

$$\Delta t_{sub_d} = \eta \frac{\phi \rho_f}{G} \qquad (2.38)$$

For water the factor η was shown to increase slightly with pressure. Subsequent work by Levy (1967) indicated that the dependence on pressure increases as the flow is reduced and that at low pressure Δt_{sub_d} becomes smaller with increasing pressure.

In region CD, the low subcooling region, the void fraction increases rapidly, and an empirical model has been suggested by Levy (1967) for its estimation. He assumes that the true quality x' is related to the thermodynamic quality x by the relationship

$$x' = x - x_d \exp\left[\frac{x}{x_d} - 1\right] \qquad (2.39)$$

where x_d is the thermodynamic quality at the point of bubble departure given by

$$x_d = \frac{c_{p_f} (t_f - t_s)_d}{i_{fg}} \qquad (2.40)$$

The true quality, x', has a finite value between the point of bubble departure and the start of saturated boiling while the thermodynamic quality is negative and zero.

2.5.3. Correlations for vapour holdup

The relation between the vapour quality and the void fraction in the subcooled region and beyond depends on the relative velocity of the liquid and vapour phase which in turn is a function of the basic rising velocity and distribution of the vapour flow.

One of the earliest correlations to account for the distribution effect was that proposed by Armand (1946) for horizontal flow

$$\alpha = K\left[\frac{Q_g}{Q_g + Q_f}\right] \qquad (2.41)$$

where the factor K has a constant value equal to 0,833. This value of K is based on experiments performed at high mass flow rates, and thus in turbulent flow.

Bankoff (1960) observed that K was not constant but

varied between 0,6 and 1,0. He suggested that this variation was the result of the non-uniform distribution of gas across the cross section of the pipe. He was the first to recognize the reason for the distribution effect.

Nicklin et al. (1962) studying the vertical slug flow of air and water at a Reynolds number greater than 8 000 showed that the rising velocity of the gas is made up of two components, namely its basic rising velocity, V, in still liquid plus a contribution due to the non-uniform distribution of gas in the moving liquid.

$$\frac{Q_g}{\alpha A} = \frac{C_o\,(Q_g + Q_f)}{A} + V \qquad (2.42)$$

The first term of this equation is the same as that of equation (2.41) and represents the contribution due to the motion of the liquid. C_o, the flow distribution parameter, is equal to 1/K. Nicklin et al. (1962) also pointed out that the reciprocal of 1/0,833 is 1,2 which is close to the ratio of the maximum to the mean velocity for fully developed turbulent flow. Thus the gas velocity is close to the velocity of the liquid at the centre line of the tube plus the rising velocity in still liquid.

Griffith (1964) applied equation (2.42) to the experimental results obtained previously by other researchers when boiling water in vertical channels. He modified the equation so as to include three parameters C_o, C_1 and C_2.

$$\frac{Q_g}{\alpha A} = C_o\frac{(Q_g + Q_f)}{A} + C_1\,C_2\left[\frac{gD(\rho_f - \rho_g)}{\rho_f}\right]^{\frac{1}{2}} \qquad (2.43)$$

The value of C_1 is a function of gravity, inertia, surface tension, viscosity and tube diameter. The factor C_2 accounts for the increased bubble rise velocity which

occurs under boiling conditions where bubbles close enough to affect each other catch up and agglomerate. He found that it had a value of 1,6 and is independent of the heat flux. He stated that equation (2.43) only applied to the slug flow region, but mentioned the difficulty of determining the starting point of this region. Agreement with the data was good, but departures were observed at the lower experimental pressures (350 kPa absolute). The data for subcooled boiling were not considered.

Zuber and Findlay (1965) proposed a general expression which takes into account the effect of non-uniform flow and concentration profiles as well as the effect of the local relative velocity between the two phases. Their analysis was based on experimental data obtained in adiabatic vertical flows. They stated that the parameter C_o can have a value less than one in subcooled boiling because the vapour is then concentrated near the tube wall, and as the flow regime changes along the duct there will be a corresponding change in the value of C_o. They pointed out that the basic rising velocity in the slug flow regime can be calculated using a graph developed by White and Beardmore (1962). It gives the value of the parameter C_1 in terms of the Eotvos number Eo and the property number Y.

where

$$E_o = g D^2 \frac{(\rho_f - \rho_g)}{\sigma} \qquad (2.44)$$

and

$$Y = (g\mu^4 / \rho\sigma^3) \qquad (2.45)$$

For the bubbly flow regime they gave the following expression for the rising velocity

$$V = 1.53 \left[\frac{\sigma g (\rho_f - \rho_g)}{\rho_f^2}\right]^{1/4} \qquad (2.46)$$

They state that this equation is useful as it expresses the rising velocity, independently of the bubble diameter which is not known, but mention that the equation is approximate.

In a subsequent publication Kroeger and Zuber (1968) gave the mean rising velocity as

$$V = 1,41 \left[\frac{\sigma g (\rho_f - \rho_g)}{\rho_f^2}\right]^{1/4} \qquad (2.47)$$

They say that the value of the distribution parameter decreases with increasing pressure and tends to unity as the pressure increases.

Wallis (1969) has expressed the results of White and Beardmore (1962) by the following equation

$$C_1 = 0,345(1 - e^{-0,1N_f/0,345})(1 - e^{(3,37 - Eo)/m}) \qquad (2.48)$$

where N_f is the dimensionless inverse viscosity given by

$$N_f = \frac{(D^3 g (\rho_f - \rho_g) \rho_f)^{\frac{1}{2}}}{\mu_f} \qquad (2.49)$$

and m is a function of N_f

$$m = 69 N_f^{-0,35} \qquad (2.50)$$

for N_f between 18 and 250.

For vertical upflow of isolated small vapour bubbles Wallis (1969) suggested using a dispersion parameter $C_o = 1$ and proposed the following equation for the rising velocity

$$V = 1{,}53\,(1 - \alpha)^2 \left[\frac{\sigma g(\rho_f - \rho_g)}{\rho_f^2}\right]^{1/4} \qquad (2.51)$$

Rouhani and Axelsson (1970) found that an average value of 1,12 for C_o is adequate to correlate the data from a large variety of test geometries. However, for low velocities C_o was found to have a value as high as 1,54. They proposed a model for the calculation of vapour formation in the subcooled region. They assumed that heat is removed by vapour generation, heating the liquid that replaces the detached bubbles and in some parts single phase heat transfer.

An equation for the differential change in the true steam quality is obtained by considering the rate of vapour condensation in liquid.

The distribution parameter was expressed by Ahmad (1970) as a function of the Reynolds number and of the pressure by means of the following empirical equation applicable to pressures above 950 kPa absolute.

$$C_o = 1/\left[1 + (1 - \alpha)\,(Re^{0{,}016}/(\rho/\rho_g)^{0{,}203} - 1)\right] \qquad (2.52)$$

This model tends to underestimate the void at very low qualities for low pressure cases.

2.5.4. Discussion

The voidage in an evaporator tube may be characterized

by three distinct regions, namely the high subcooled, low subcooled and saturated boiling regions.

Griffith et al. (1958) has proposed an empirical equation for the estimation of the void fraction in the high subcooled region. He assumed that the size of the bubbles adhering to the heat transfer surface is proportional to the thickness of the boundary layer. At pressures below 2000 kPa the equation becomes incorrect since the bubble diameter then becomes a function of the pressure as well.

The transition point between the high and low subcooled regions is defined by the point of bubble departure. Griffith et al. (1958) found empirically that the subcooling at that point is proportional to the heat flux divided by five times the single phase heat transfer coefficient. Another empirical equation for the subcooling at the point of bubble departure is that proposed by Bowring (1962) for water at pressures between 11 and 139 bar. In this equation subcooling is a function of heat flux, velocity and pressure. The first of these equations does not take into account the effect of pressure while the second does not account for the effect of the physical properties of the liquid.

The low subcooled region which precedes the start of saturated boiling is characterized by a rapid increase in the void fraction. Levy (1967) has suggested a method for the estimation of the void fraction in this region. The basis of this method is an exponential function which satisfies the following boundary conditions.

(a) at point D $x' = 0$
(b) the change in quality at point D is zero
(c) the true local vapour mass fraction approaches the thermal equilibrium mass fraction downstream from the point of bubble departure.

The method of Levy is recommended by Collier (1972), as it is reasonably accurate and easy to use.

The relation between the vapour mass fraction and the quality is calculated using the correlation of Nicklin et al. (1962) which estimates the rising velocity of the vapour by adding the basic rising velocity in still liquid to the contribution due to the non-uniform distribution of the vapour phase in the rising liquid phase.

The main difficulty lies in the choice of the value of the flow distribution parameter Co, for there is reason to believe that it increases from zero at the onset of boiling to more than one in the saturated boiling region. However, there is no reliable method for its estimation, and it is recommended by Kroeger and Zuber (1968) that the value of Co for the saturated boiling region which lies between 1,12 and 1,13 should be used for the subcooled region as well.

CHAPTER 3

EXPERIMENTAL DETAILS

The first objective of this study being to obtain a better understanding of the boiling process in vacuum pans, the experimental plant was designed and operated so as to represent as closely as possible the industrial conditions in this type of equipment. Steam heating was used at a pressure between 100 and 175 kPa absolute, and the vacuum in the apparatus was adjusted in the range 10 to 28 kPa absolute which are the operating limits generally ecountered in industry.

As the second objective was to obtain correlations for the heat transfer, vapour holdup and friction loss, the apparatus was designed in such a way that the primary variables necessary to establish these equations could be measured along the length of the evaporator tube. These included the pressure, temperature and void fraction

3.1. EXPERIMENTAL PAN

A diagram of the experimental pan is shown in Figure 3.1 and a photograph in Figure 3.2. It consisted of a single steam jacketted Schedule 40 mild steel tube 0,1 m internal diameter and 1,3 m long. These dimensions were selected as this diameter is that generally used in industrial pans, while the length represents the maximum used in batch pans. Circulation was done by a positive displacement pump (Mono pump Type D60) fitted with a variable speed gearbox. Vacuum was provided by means of a water cooled surface condenser and a vacuum pump for removing the incondensible gases. The condensed vapour was returned continuously to the inlet of the circulating pump so as to maintain a constant concentration in the apparatus. The steam jacket was provided with an incondensible gas vent, pressure gauge and a steam

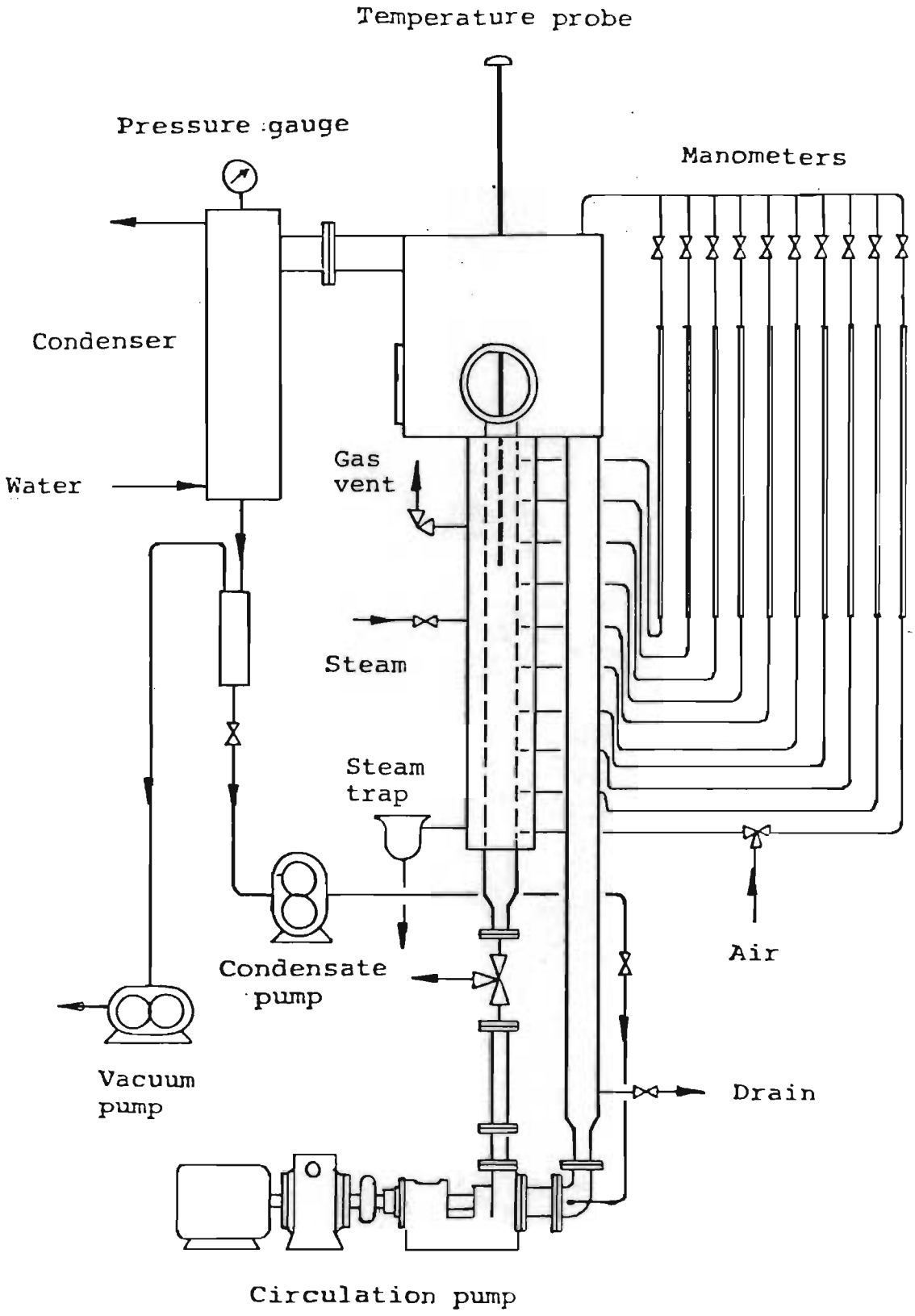

Figure 3.1. Diagram of experimental pan.

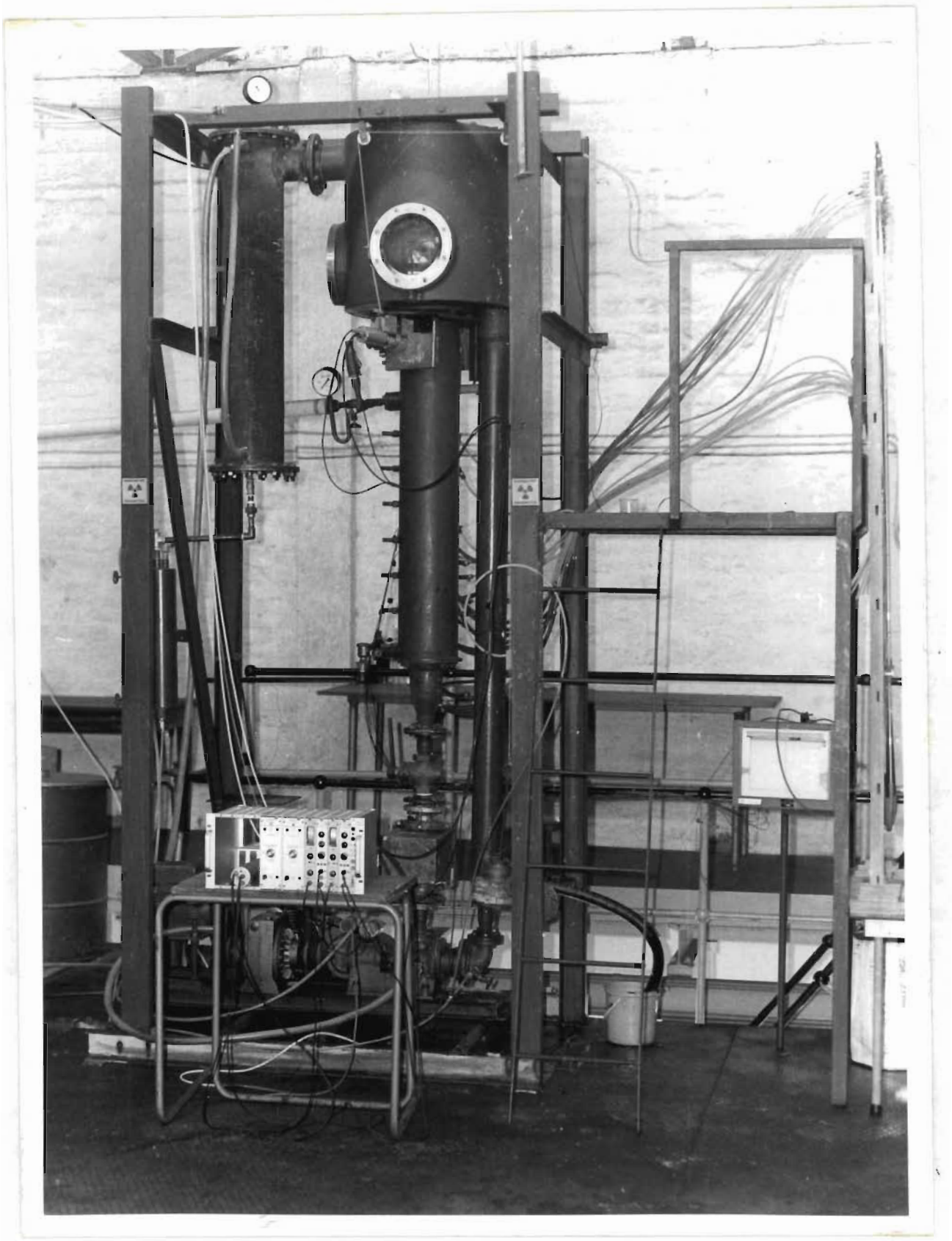

Figure 3.2. The Experimental Pan.

trap for the evacuation of the condensate.

The apparatus was put under vacuum by starting the vacuum pump, and the fluid to be boiled was sucked into the pan through a hose connected to the drain pipe. The amount of fluid introduced was such that the top of the boiling tube acted as a weir and maintained a constant level in the apparatus. Once the pan had been filled, condenser water and steam were turned on and the condensate recirculation pump was started. Fluid inlet velocity to the evaporator tube was set at the desired value by adjusting the speed of the circulation pump, and the vacuum required was maintained by bleeding air into the system. The following observations were made for each run.

(a) Pressure in vapour space.
(b) Pressure in steam jacket.
(c) Pressure along tube.
(d) Centerline temperatures along tube.
(e) Evaporation rate.
(f) Circulation rate.
(g) Void fraction along tube.
(h) A fluid sample was collected after each run for determination of density, dry substance, purity, brix, rheological properties and surface tension.

3.1.1. Measurement of pressure

Pressures in the vapour and steam spaces were measured using Bourdon type pressure gauges. Pressures along the boiling tube were obtained by means of liquid manometers.

Pressure transducers connected to a data acquisition system would have given more accurate readings, but could not be used because of the limited funds available for this study. The manometers were connected to ten equidistant

pressure tappings spaced at 0,125 m intervals. They were filled with Meriam fluid of specific gravity 1,75.

Precautions had to be taken to prevent entry of the boiling liquid into the manometers, and to prevent clogging of the pressure tappings to the evaporator tube. This was done by providing an air bleed through the system as shown in Figure 3.3. The rate of air ingress was observed by a bubble indicator and controlled by a needle valve.

Special care also had to be taken in operating the manometers to avoid loss of fluid. The procedure was as follows: with all the manometer taps closed, the taps connecting the top of the manometers to the vapour space were opened carefully and the fluid was allowed to rise just below the taps which were then closed. The taps connecting the manometers to the evaporator tube were then opened, and after the manometer fluid had moved down approximately to its operating level the taps to the vapour space were reopened. Air bleed through the system was then adjusted to a minimum value.

Partial blockage of the manometer tubing occurred occasionally at the point of access to the boiling tube; presumably because of crystallization of sugar. The method used to cope with this situation was to close all the taps of the faulty manometer, disconnect the tubing between the liquid trap and the tap connecting the manometer to the boiling tube and suck in some hot water through the blocked connection.

Pressure readings along the boiling tube were made by averaging visually the level in each manometer.

3.1.2. Measurement of temperature

The centerline temperatures were measured by means of a platinum resistance thermometer mounted on a probe intro-

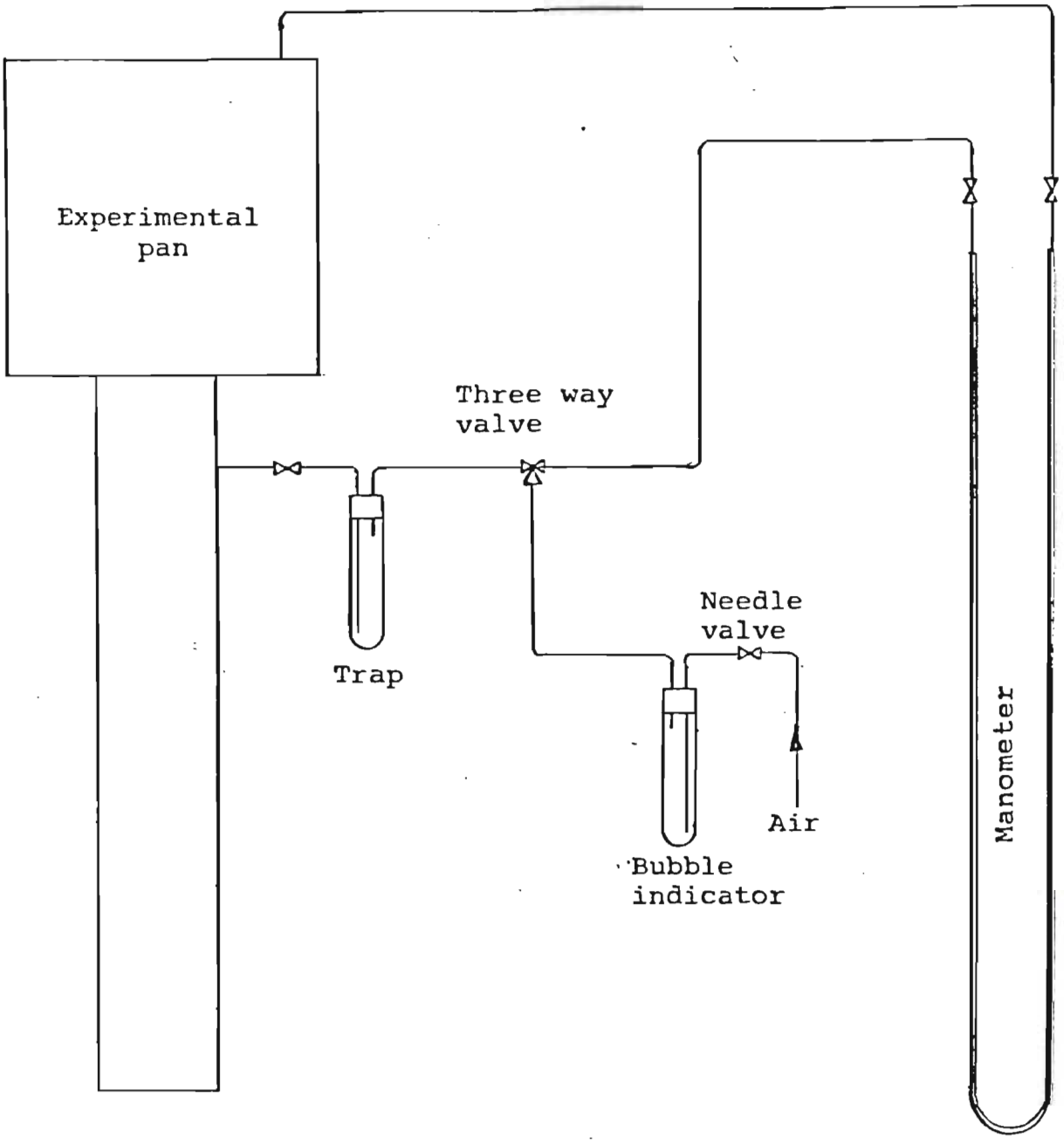

Figure 3.3. Detail of manometer arrangement.

duced through the top of the vapour space. This probe was kept centered in the tube by means of a spider attachment. The signal from the resistance thermometer was displayed with a 0,1°C resolution (Omega Model 199 P2). Using this probe observations were made at the centerline but close to the surface of the boiling fluid, at the level of the pressure tappings, that is at 10 equidistant points, and at the tube inlet. Traverses were made by moving the probe downwards and upwards and averaging the values obtained at each level.

3.1.3. Void fraction determination

Gamma ray absorption was chosen for the determination of the void fraction along the tube. Quick closing valves were not suitable for this study, because this method would not have given the distribution along the tube. The use of conductivity probes entails a large number of measurements and would not have given an accurate estimation of the void fraction.

The radioactive source was 11 mCi of Cesium - 137. The radiation was detected by a scintillation counter connected to an amplifier (Tennelec TC 213) and a ratemeter (Tennelec TC 590). Switches on the ratemeter made possible full scale deflections for counting ranges of 250, 500, 1 000 and 2 500 cps.

The source and detector were mounted on a traversing mechanism which allowed measurements to be made along the tube. The arrangement of the void fraction measuring equipment is shown in Figure 3.4.

The detector was calibrated in situ, as described by Hewitt (1978), by measuring the intensity of the radiation with the tube full of air I_g and full of the liquid phase I_f. The void fraction was then calculated from the two-

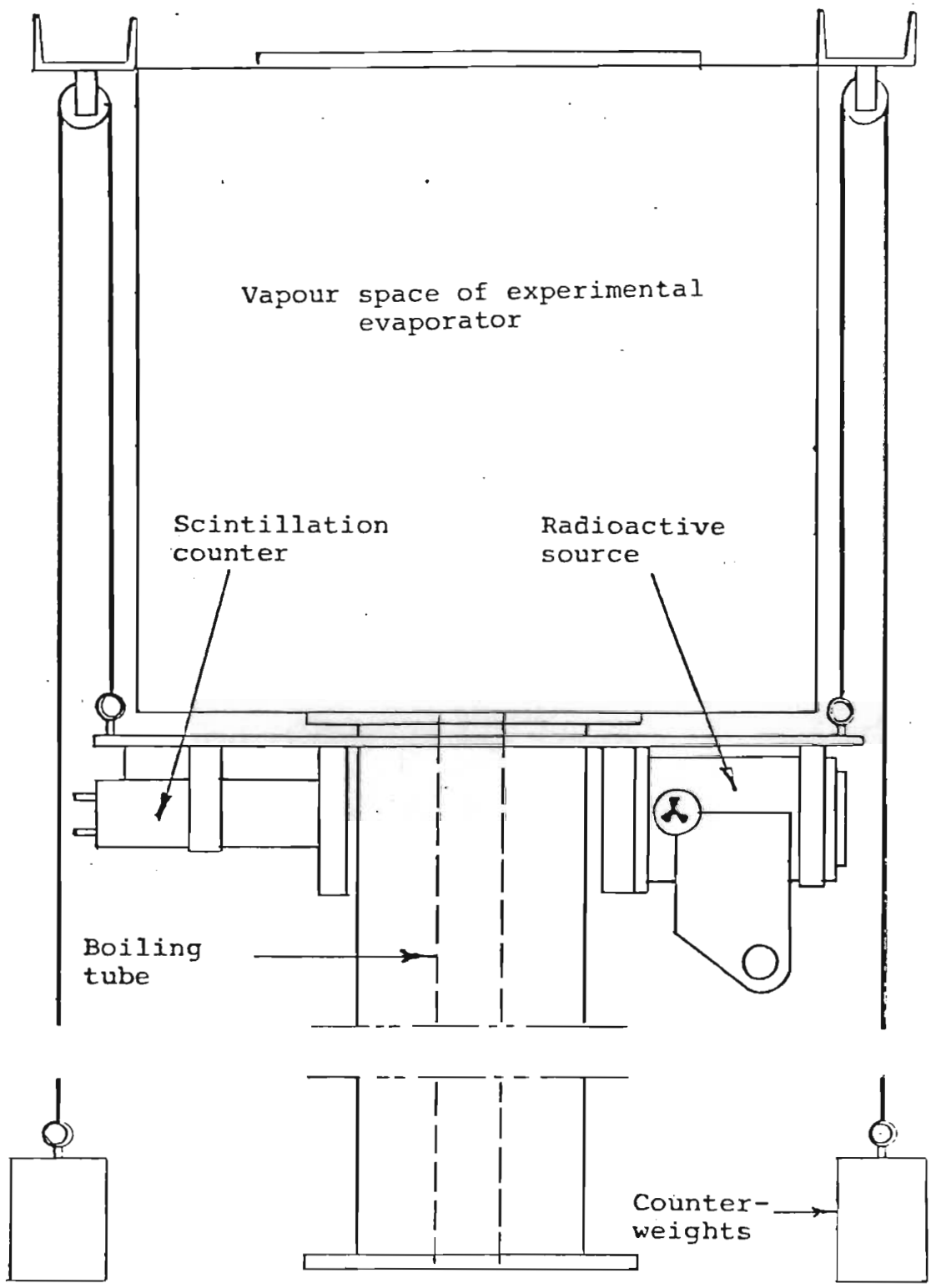

Figure 3.4. Details of void fraction detector

phase intensity I_{TP}, assuming an exponential absorption by means of the equation

$$\alpha = \frac{\ln I_{TP} - \ln I_f}{\ln I_g - \ln I_f} \qquad (3.1)$$

The instrument was recalibrated each time that a different liquid was used in the apparatus. The attenuation with two phase flow was determined at seventeen positions along the length of the tube; two between each pressure tapping starting from the bottom, and the last one halfway between the two topmost pressure points. Only one position was possible at the top because of interference with the travel of the traversing mechanism. The void fraction at the level of each pressure tapping and at the tube outlet was obtained by interpolation. Void measurements for Runs 1 to 38 were done with the air bleed of the manometers open. Because it was thought that this could have an effect on the observed void fraction, runs 39 to 57 were done with the air bleed closed.

No fluctuations of the ratemeter as caused by background noise were apparent when observing the intensity of radiation with the tube empty or full. Severe fluctuations did occur, however, due to the boiling process, particularly in the upper part of the tube. To control the magnitude of this fluctuation the standard deviation control on the ratemeter was set at the 10 per cent position, which refers to the relative standard deviation of the distribution at full scale. When recording the intensity of radiation of the boiling fluid, the reading on the ratemeter was averaged visually.

3.1.4. Velocity at tube inlet

The superficial fluid velocity at the tube inlet was obtained from a calibration of the circulation pump volu-

metric flowrate against the pump setting, that is the pump speed. The calibration was done using water with a viscosity of 0,001 Pas and syrup with a viscosity of 0,05 Pas No difference in calibration could be observed between these two fluids although the viscosity increased by fifty times. As the pump used was of the positive displacement type, and the discharge head and rotative speed were low slippage past the pump must have been negligible. Under these conditions it can be assumed that the calibration was maintained with a more viscous liquid such as C-massecuite seed. The calibration curve is shown in Figure 3.5.

3.1.5. Experimental fluids

The experiments were done using syrup molasses and C-massecuite seed. These fluids were used because as a result of the range of viscosity, it was possible to study both subcooled and saturated boiling under laminar conditions. The range of the operating variables are given in Table 3.1.

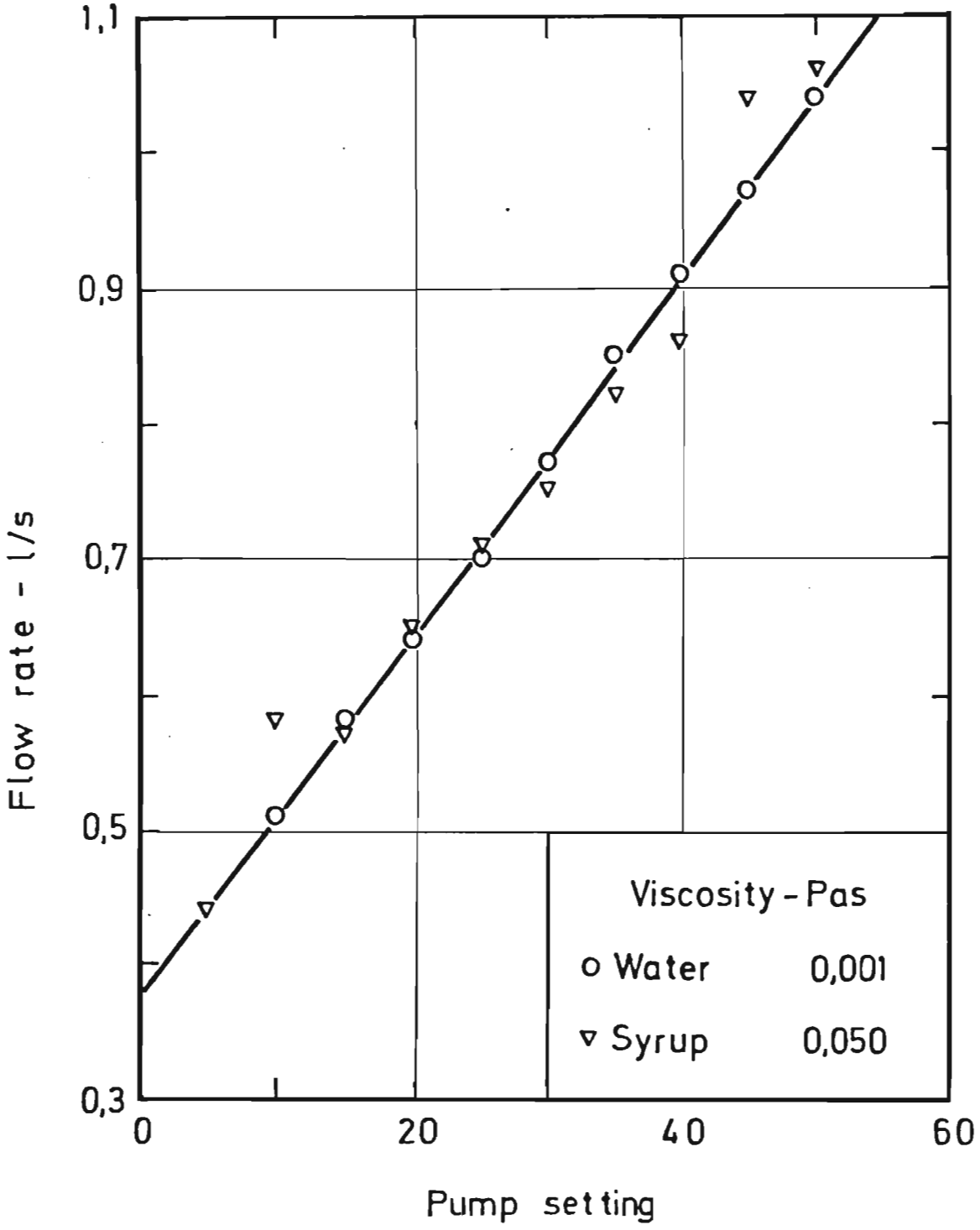

Figure 3.5. Calibration curve for circulation pump.

TABLE 3.1.

Range of Operating Variabes

Fluid	Brix	Purity	Tube inlet conditions			Flow behaviour index	Reynolds number	Abs. pressure	
			Velocity (m/s)	Density (kg/m^3)	Viscosity (Pas)			Vapour (kPa)	Steam (kPa)
Syrup	72	100	0,0379	1328	0,0296	1,000	357,000	12,5	100
			0,0792	1347	0,0791	1,000	85,400	27,0	122
Molasses	75	37	0,0462	1378	0,2050	1,000	60,300	11,5	113
			0,1210	1400	3,8900	0,932	1,820	27,5	136
C-massecuite seed	87	56	0,0462	1397	1,1300	0,980	13,200	9,4	140
			0,1210	1445	12,9000	0,904	0,551	26,5	173

CHAPTER 4

RESULTS

The experiments were done using syrup, molasses and C-massecuite seed. These fluids cover a thousandfold change in viscosity and allowed a study of both subcooled and saturated boiling regimes under laminar conditions. Fifty-seven runs were done, and the experimental data obtained are given in Appendix A.

4.1. Measurement of the main variables

The difficulty of obtaining reliable data when boiling a highly viscous fluid in a vertical tube is one of the main factors which has retarded the study of vacuum pans. An estimate of the accuracy of the data obtained in this study is discussed and the boiling process observed in these experiments is described.

4.1.1. Pressures

The pressure readings along the boiling tube were obtained by averaging visually the level in each manometer. Pressure pulsations caused by boiling which were particularly strong at the lower part of the tube made this difficult, and random errors occurred. Random errors were also experienced occasionally when the pressure tappings became obstructed, possibly due to crystallization of sugar. A systematic error may have been caused by the air bleed used in the system, as this may have produced a slight increase in pressure on the manometers.

In order to obtain an estimate of the magnitude of the random errors a third degree polynomial curve was fitted to the readings of pressure versus distance along the tube for each run. The average error noted was equivalent to four percent of the pressure difference between the bottom

and the top of the tube, but represented 29 percent of the friction loss observed. Maximum errors were twice this value.

The vacuum in the apparatus was measured by means of a Bourdon type pressure gauge which had been calibrated using a mercury manometer. The average fluctuation of the atmospheric pressure in Durban is about twenty millibars that is 0,2 kPa, and it is estimated that the maximum error in reading the vaccuum was about 0,5 kPa. However, since the vacuum was controlled manually by bleeding air into the system, fluctuations did occur. It is estimated that these amounted to an additional 0,5 kPa. The vacuum was thus accurate to plus or minus one kPa.

This error in the system pressure has an effect on the saturation temperature, which at 22 kPa, for example, amounts to $\pm$ 1°C.

4.1.2. Temperatures

Temperature measurements along the tube axis were done by traversing with a resistance thermometer. Traverses were done in both a downward and an upward direction, and the readings obtained were averaged. The thermometer had a slow response, and several minutes were required for obtaining a steady reading at each position. The average difference between the downward and upward values was 0,5°C with a standard error of 0,5. These differences were the result both of the slow response of the thermometer and of changes in temperature resulting from changes in the system pressure.

The inner tube surface temperature was obtained by calculation. Film type condensation was assumed, and the condensate film heat transfer coefficient h_c was estimated from the following equation (McAdams, 1942).

$$h_c = 1,47\left[\frac{\pi D\mu_f}{4W}\right]^{1/3}\left[\frac{k_f^3\rho_f^2 g}{\mu_f^2}\right]^{1/3} \qquad (4.1)$$

The temperature of the inner surface was calculated by iteration using h_c together with the tube wall resistance and the overall heat transfer coefficient and overall temperature difference. This approach ignores the resistance of any scale or oily film that may have been present on the heat transfer surfaces.

4.1.3. Void fraction

The reading on the ratemeter with the tube empty was about 1 750 cps with a standard error of 40 cps. Values for the tube full of fluid varied between 150 and 250 cps, depending on the fluid, with an error of 10 cps. Measurement of the two phase mixture in the saturated boiling region presented the same difficulties as pressure measurements because of the pulsating flow, and here also the readings had to be averaged visually. The fluctuations represented approximately 15% of the two phase signal.

However, as mentioned by Hewitt (1978), when fluctuations occur in two-phase flow the average signal does not represent the mean void fraction because the absorption is exponential.

It is estimated that the combined effects of the errors in reading the intensity of the radiation with the tube full of gas and full of liquid plus the error due to pulsation when reading the two phase radiation intensity amounted to a maximum of $\pm$ 5 percent of the calculated void fraction.

Another source of error mentioned by Hewitt is that resulting from the varying thickness of metal through which the radiation beam passes when making measurements in a

tube. The curvature of the tube wall causes a stronger weighing for the centre of the tube where the beam path length through the metal is shorter. In the experiments described in this thesis the boiling tube was relatively thin and the error is small.

4.1.4. Rheological properties

Measurements of the rheological properties of the fluids were made after each set of runs as described in Appendix B. Values of the consistency index, K, were obtained for four or five different temperatures, and an exponential equation was fitted to the data expressing the Consistency index as a function of the absolute temperature. The accuracy of the fit is shown in Figure 4.1. It can be seen that most of the measurements fall within a range of $\pm$ 10%, confirming the applicability of the power law model to these fluids.

4.1.5. Surface tension

After each set of runs the surface tension was measured on a sample of the liquid at 65°C using the ring method of du Nouy as described in Appendix B.5. As it had been determined previously by Vanhook and Biggins (1952) the accuracy of the measurements was poor, consecutive readings done on the same sample differed by an average value of 33 percent. This is attributed to the presence of crystals and also because of the impossibility of maintaining the upper surface of the sample at a constant temperature.

4.1.6. Heat flux

The rate of heat transfer in this study is based on the amount of condensate collected in a given time, and in calculating the heat content it was assumed that the steam was dry and saturated.

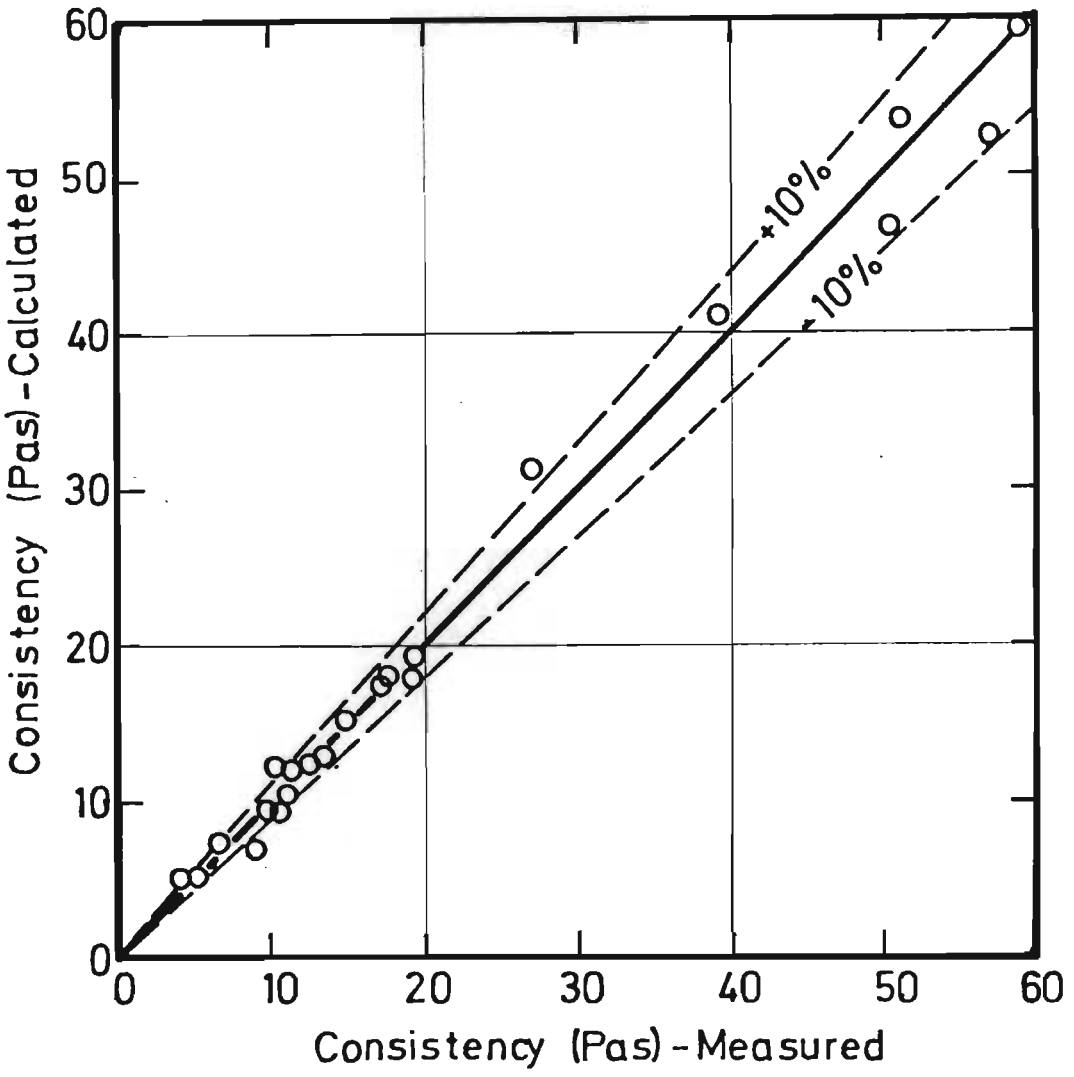

Figure 4.1. Errors observed between the measured and calculated consistency index of the test fluids.

4.1.7. Discussion

Measurement of the void fraction showed that initially there is a gradual increase in the vapour fraction characteristic of subcooled boiling, with a sudden increase taking place at the point where change to saturated boiling occurs. This point also coincides with the maximum axial temperature. One of the factors which affects the length of the subcooled region is the heat flux. This is shown in Figure 4.2. where the distance from the tube inlet at which the maximum temperature was observed is plotted against the heat flux. At heat fluxes below about 7 000 W/m^2 the subcooled region extended all the way to the tube outlet. Under these conditions, little change was observed in the axial temperature along the tube as can be seen from the data for Runs 19 and 20 in Appendix A.

The uniform axial temperature associated with subcooled boiling at low heat fluxes explains why when Webre (1932) measured the temperature of boiling massecuites at various depths he concluded that no ebullition took place in the tubes. Subcooled boiling also explains why when Webre (1934) did a traverse across the top of a vacuum pan tube he found that the temperature at the centre was close to that in the rest of the pan, while the temperature close to the tube wall was higher by as much as 30°C.

4.2. Calculation of results

Data reduction and regression analyses were done using a Hewlett-Packard-86 desktop computer.

4.2.1. Saturation temperature

The saturation temperature was obtained by the method of Batterham and Norgate (1975) which is given in Appendix B.4. These authors reported that their measurements agreed

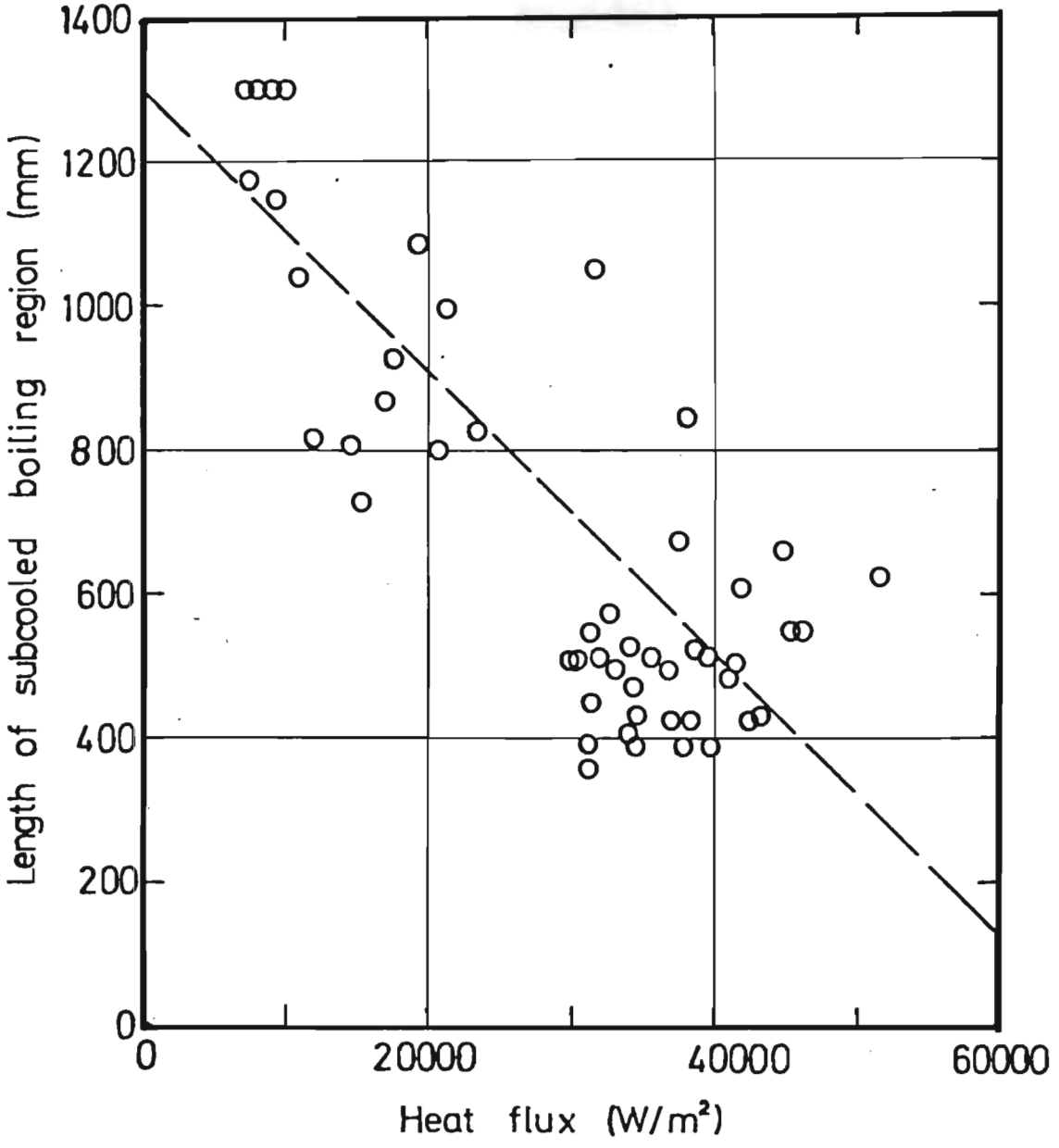

Figure 4.2. Effect of heat flux on length of subcooled region.

with the equations that they proposed with a standard error of 0,251°C. The most significant errors being at low purities and dry solids of 80 and higher.

In the runs where saturated boiling occurs, the axial temperature of the liquid phase close to the tube outlet should equal the saturation temperature corresponding to the pressure at the point provided that (a) thermal equilibrium exists between the liquid and the vapour and (b) the saturation temperature predicted is accurate. If thermal equilibrium does not exist the liquid will be hotter than the calculated saturation temperature, because flashing will have been imcomplete. In Figure 4.3. is given a graph of the axial temperature measured at the outlet against the calculated saturation temperature. As can be seen for temperatures below 65°C the measured axial temperatures are lower than the calculated values. The average difference observed for all the points shown was as follows:

Syrup	- 0,4°C
Molasses	+ 0,4°C
C-seed	- 2,1°C

Although the difference is not great, it is significant when compared to the axial temperature rise which occurs when saturated boiling takes place and which was observed in these experiments. These differences may have been caused by errors in measuring the system pressure and errors in determining the purity and dry substance of the liquids used in the experiments.

Accurate prediction of the saturation temperature is important because as we shall see the extent of subcooling affects the point of bubble departure, the quality in the low subcooled region and the transition point to saturated boiling.

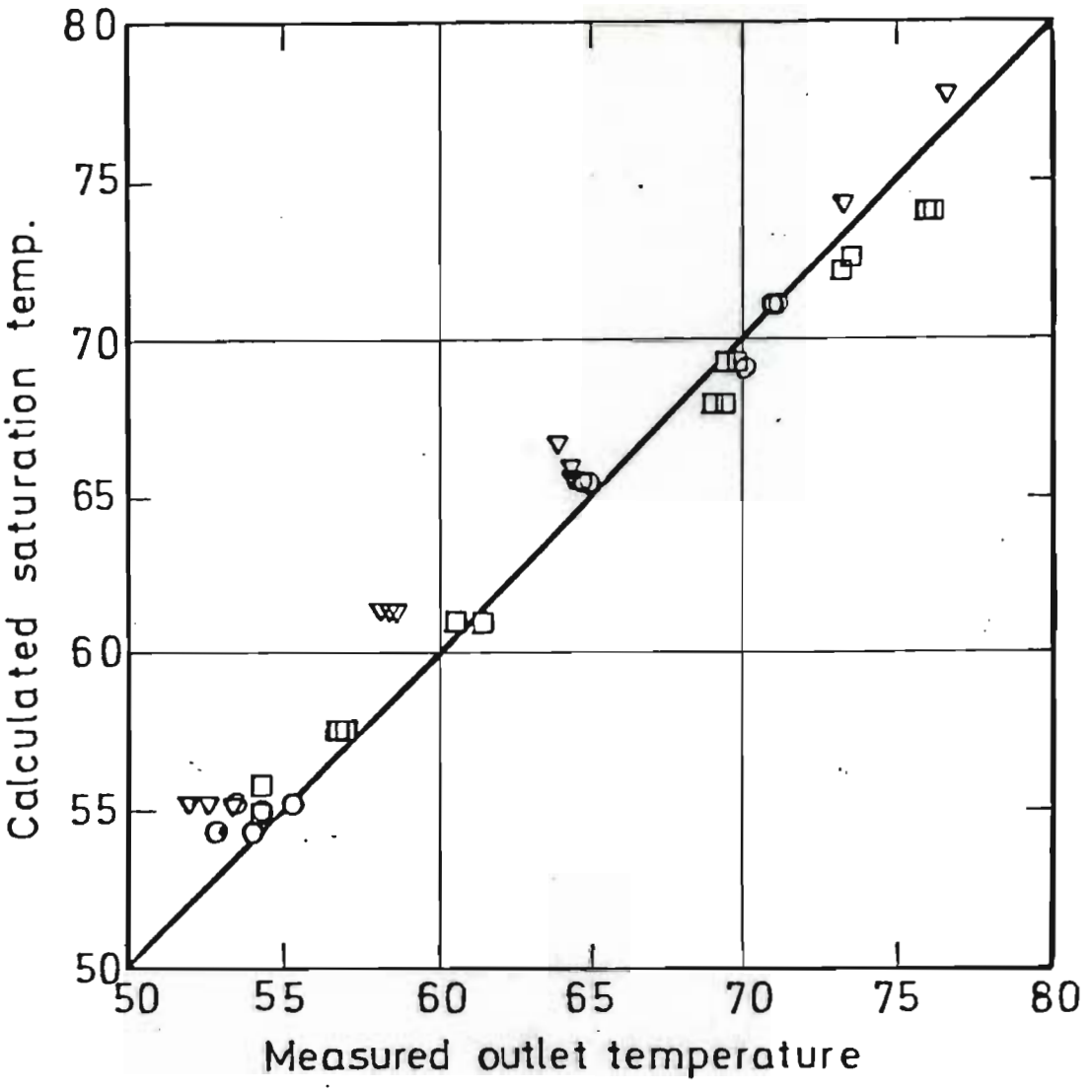

Figure 4.3. Relation between measured outlet temperature and calculated saturation temperature for saturated boiling (O syrup, □ molasses, △ C-seed).

4.2.2. Boiling heat transfer coefficients

In evaluating the boiling heat transfer coefficients it was decided to use the method where the total heat flow is correlated using dimensionless groups in preference to the superposition or interpolation technique as described in Section 2.3.3. The reason for this choice is that this method is simpler and more direct.

The physical properties chosen for inclusion in the dimensionless groups were those that have been shown previously by Papell (1962), Moles and Shaw (1972) and others to correlate boiling heat transfer. These include the thermal conductivity k, the specific heat c_p, the viscosity μ, the density of the liquid phase ρ_f and that of the vapour phase ρ_g. Also included was the tube diameter D, the tube length L and the two phase velocity u_{TP} which affect the thickness of the boundary layer. Although it has been shown by Rohsenow (1953) and Chen (1966) that the surface tension σ has an influence on boiling heat transfer due to its effect on bubble formation it was not included because of the difficulty in obtaining accurate values for this property. The heat flux ϕ which was used by other workers was also not included because it is believed that it is dependent on the boiling heat transfer coefficient h_{TP}. Dimensional analysis was used to obtain the groups corresponding to these variables. Details of the procedure are given in Appendix E.

The form of the correlation was found to be:

$$\frac{h_{TP}D}{k_f} = f\left\{\left[\frac{Du_{TP}\rho_f}{\mu_f}\right]^b \left[\frac{c_p\mu_f}{k_f}\right]^c \left[\frac{\rho_f}{\rho_g}\right]^d \left[\frac{L}{D}\right]^h\right\} \qquad (4.2)$$

Since the liquid phase is non-Newtonian it was necessary to use the generalized Reynolds number proposed by Metzner and Reed (1955).

$$Re = \frac{D^n u^{2-n} \rho_f}{K_f} \cdot 8. \left[\frac{n}{6n+2}\right]^n \qquad (2.19)$$

and the generalized Prandtl number (Skelland, 1967).

$$Pr = \frac{c_p K}{8k} \left[\frac{u}{D}\right]^{n-1} \left[\frac{6n+2}{n}\right]^n \qquad (4.3)$$

which both apply to pseudoplastic fluids. In these two dimensionless groups the increased velocity of the two-phase mixture is accounted for by dividing the volumetric rate of flow of the liquid phase by the sectional area of the tube and the volumetric fraction occupied by the liquid.

$$u_f = \frac{Q_f}{A(1-\alpha)} \qquad (2.32)$$

The specific heat was calculated using the equations of Janovskii and Archangelskii (1918) which are given in Appendix B.6. The average percentage error between the measured and calculated values used in establishing these equations was 0,53 with a maximum of 1,9 percent. The measurements were made on beet sugar factory products, but it is believed that the equations also apply to cane sugar factory products (Erlee, 1931).

The thermal conductivity was calculated using the equations of Baloh (1967) which are based on the data of Bosworth (1947). These are given in Appendix B.7. The measurements of Bosworth were done on pure sucrose solutions, and do not account for the effect that non-sucrose may have. The average percentage error between the measured

and calculated values was 0,35 with a maximum of 8,9 percent.

Both the Reynolds and Prandtl numbers were evaluated at the film temperature, that is the arithmetic average between the centerline and inside tube wall temperatures. This is preferable to the bulk temperature because in boiling the formation of vapour bubbles and particularly the transport of hot liquid from the heating surface towards the axis of the tube during bubble growth are affected by the film properties.

The density of the vapour phase was calculated at the saturation temperature of the liquid phase.

Since the pressure, temperature and void fraction do not vary linearly along the length of the tube, the dimensionless groups in equation (4.2) were calculated for the conditions prevailing at the level of each of the ten pressure measuring points and averaged arithmetically.

Because the experiments were done with a tube of only a single length, it was not possible to determine experimentally the effect of this variable. However, because the void fraction is relatively small when boiling a highly viscous liquid, it was felt that the effect would be similar to that for single phase heat transfer in laminar flow and a value of $-1/3$ was assigned quite arbitrarily to exponent h in equation (4.2). Subsequent experiments carried out on a full scale unit at Maidstone sugar factory where different tube lengths were employed have confirmed the validity of this assumption. These experiments are described in Chapter 6.

The values of exponents b, c and d in equation (4.2) were calculated from the data given in Appendix A using stepwise multilinear regression analysis. The equation obtained is

$$(Nu)_f = 4,48\ (Re_{TP})_f^{0,386}\ (\rho_f/\rho_g)^{0,202}\ (D/L)^{1/3} \qquad (4.4)$$

with a correlation coefficient of 0,963. The exponent for the Prandtl number was -0,026 and therefore this parameter is not statistically significant. This is because of the strong interaction between the Prandtl and Reynolds numbers as shown by the correlation matrix given in Table 4.1.

TABLE 4.1.

Correlation Matrix for Boiling Heat Transfer Coefficient

	(ρ_f/ρ_g)	$(Re_{TP})_f$	$(Pr)_f$	$(Nu)_f$
(ρ_f/ρ_g)	1,0000	- 0,0124	0,0708	0,0540
$(Re_{TP})_f$		1,0000	- 0,9832	0,9606
$(Pr)_f$			1,0000	- 0,9422
$(Nu)_f$				1,0000

This strong interaction results from the dominant effect of the viscosity. As it appears in both the Reynolds and Prandtl numbers only one of these dimensionless groups can have a significant effect on the Nusselt number. It is possible that the interaction between the Nusselt and Prandtl numbers could have been reduced had tubes of different diameters been used in the experiment because this variable has a greater effect on the Reynolds number. This was not done, however, due to the large scale of the apparatus and to the limited funds available. The effect of the diameter will be investigated in experiments to be carried out shortly on a full scale unit at Maidstone sugar factory.

As the Prandtl number is excluded from the correlation and the effect of tube diameter was not investigated, caution must be exercised when applying equation (4.4) to fluids other than sugar products. Use of this equation with different tube sizes must also be done with caution. It must also be pointed out that these experiments were done using mild steel tubes. As shown by Rohsenow (1953) other liquid-tube surface combinations may have different nucleation properties and thus different heat transfer coefficients.

The correlation is shown graphically in Figure 4.4. The average error is ± 18 percent with a maximum of 52 percent. Comparison with heat transfer to massecuite without change of phase as measured by Rouillard (1975) is shown in Figure 4.5. The effect of the Reynolds number with change of phase is similar to that without phase change. This lends support to the choice of the empirical equation for boiling heat transfer.

4.2.3. Flow distribution parameter at tube outlet

The retention of the vapour in the two phase mixture flowing up the tube is a function of its basic rising velocity plus a contribution due to the non-uniform distribution of vapour in the moving liquid which is characterized by the distribution parameter C_o.

The flow distribution parameter at the tube outlet was calculated using the equation of Nicklin et al. (1962) which accounts for both these effects

$$\frac{Q_g}{\alpha A} = \frac{C_o\,(Q_g + Q_f)}{A} + V \qquad (2.42)$$

in which

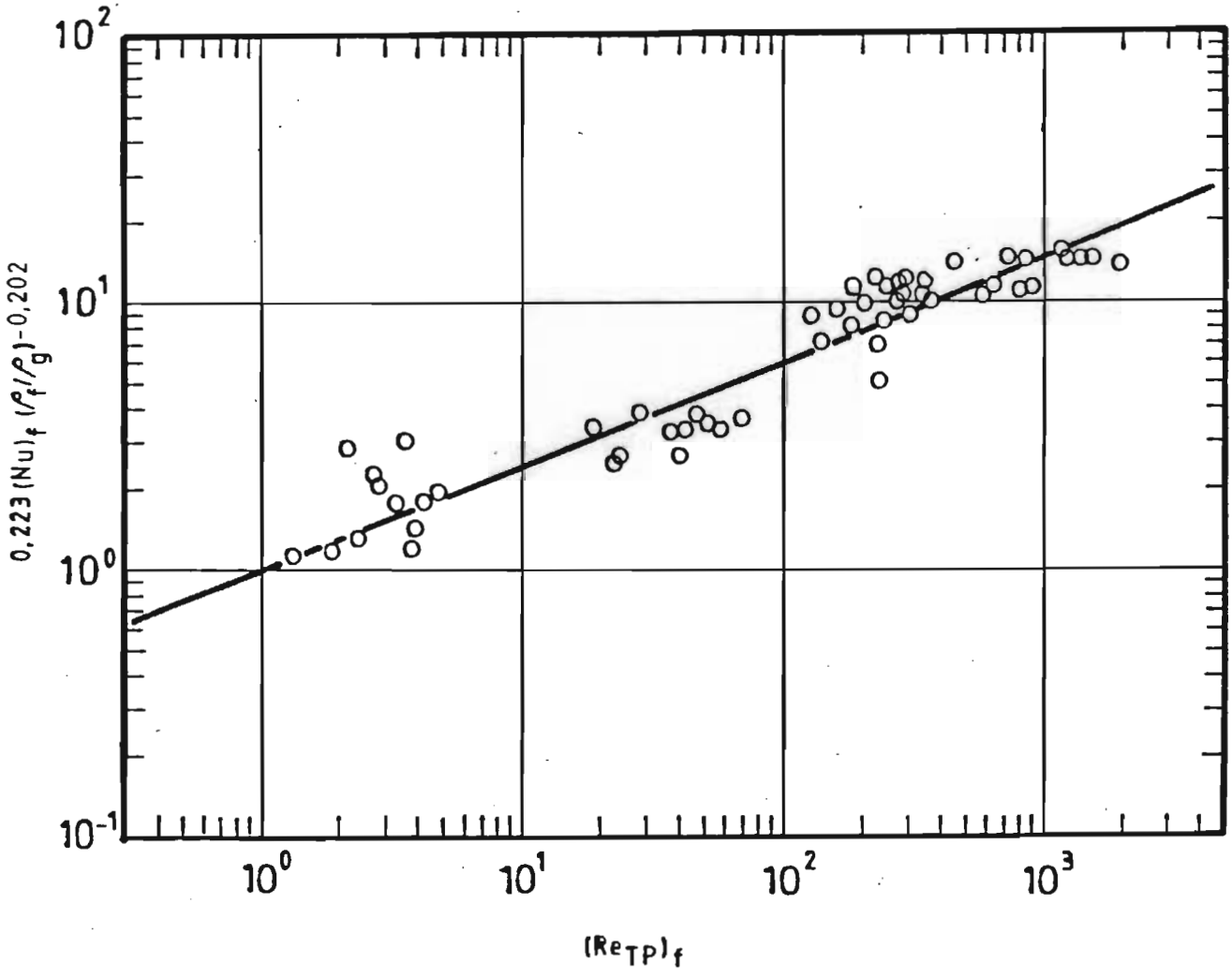

Figure 4.4. Boiling heat transfer coefficient

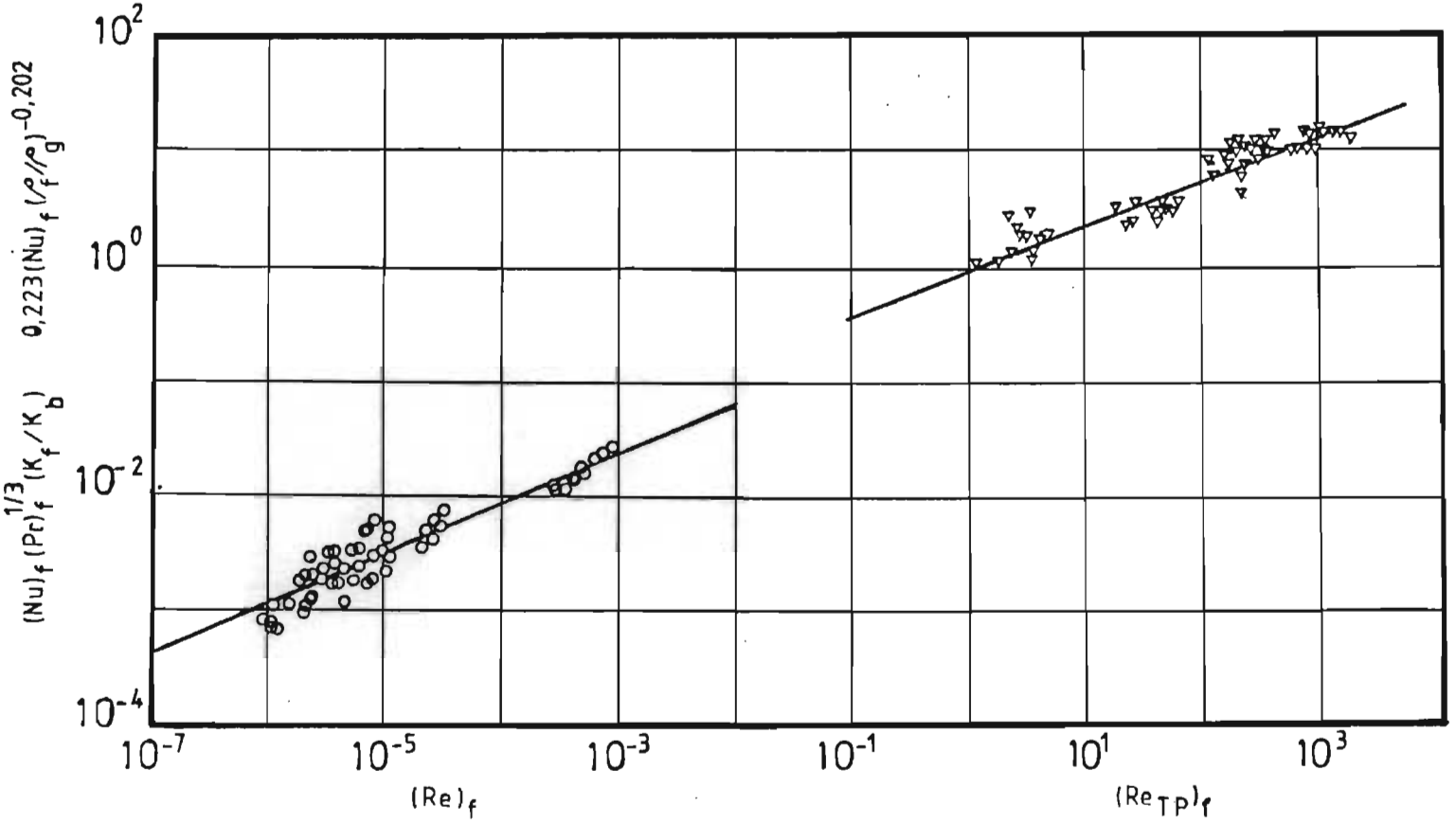

Figure 4.5. Heat transfer to single phase and boiling massecuite.

$$Q_f = \frac{\pi D^2 G (1 - x)}{4 \rho_f} \qquad (4.5)$$

and

$$Q_g = \frac{\pi D^2 G x}{4 \rho_g} \qquad (4.6)$$

The measured evaporation rates were used to calculate the mass vapour quality, x, at the tube outlet, and thus obtain the volumetric flowrate of the liquid and vapour phase Q_f and Q_g.

Because subcooled boiling occurred along the greater part of the tube, the rising velocity V was calculated using the equation of Zuber and Findlay (1965) for upflow of small vapour bubbles.

$$V = 1,53 \left[\frac{\sigma g (\rho_f - \rho_g)}{\rho_f^2}\right]^{1/4} \qquad (2.46)$$

A sample calculation is given in Appendix D.1.

The average value of C_o was found to be 1,13 for all the runs where saturated boiling took place. This is close to 1,12 that Rouhani and Axelsson (1970) found applies to most conditions.

4.2.4. Local mass vapour quality

The equation of Nicklin et al.(1962) was also used to predict the local mass vapour quality x by substituting equations (4.5), (4.6) and (2.46) into equation (2.42) and rearranging

$$x = \frac{GC_o}{\rho_f} + 1{,}53 \left[\frac{\sigma g (\rho_f - \rho_g)}{\rho_f^2}\right]^{1/4} \Big/ G\left[\frac{1}{\alpha \rho_g} - \frac{C_o}{\rho_g} + \frac{C_o}{\rho_f}\right] \qquad (4.7)$$

As evaporation takes place along the tube, the concentration and flow profile of the vapour phase change. Consequently , it can be expected that in equation (4.7) the value of the flow distribution parameter will change starting from $C_o = 0$ when there is no vapour present to $C_o > 1$ for the saturated boiling region. However, developing flow correlations are not available for predicting the value of C_o. The method generally accepted, and which was used in these calculations, is to assume that the flow distribution parameter has a constant value for the entire subcooled region corresponding to that for the saturated boiling region. This method has been used previously by Levy (1967), Kroeger and Zuber (1968) and Rouhani and Axelsson (1970).

In this way the progressive increase in mass vapour quality along the tube was obtained. A sample calculation is given in Appendix D.2.

4.2.5. Void fraction

The void fractions measured in this study are given in Appendix A. They clearly show the low voidage associated with the highly subcooled region, and the sudden increase that takes place at the point of bubble detachment.

The model of Griffith, Clark and Rohsenow (1958) which was developed for high pressure boiling of water

$$\alpha = \frac{\phi_n . (Pr)_f}{B1 . (Nu)_f . h_{fo} . \Delta t_{sub}} \qquad (2.36)$$

could not be used for the estimation of the void fraction in the highly subcooled region, because it is known (Collier, 1972) to give incorrect values at low pressures similar to those used in this study, when the void fraction also becomes a function of the pressure.

It was postulated that the void volume per unit surface area, a, would be proportional to the ratio of the boiling heat transfer coefficient h_{TP} to the single phase heat transfer coefficient h_{fo}, times a proportionality constant B_o, which would be a function of the pressure and of the hydrodynamic boundary layer thickness which is, in turn, related to the thickness of the thermal boundary layer (k_f/h_{fo}).

$$a = B_o \frac{h_{TP}}{h_{fo}} \tag{4.8}$$

where

$$B_o = f(Pr, k_f/h_{fo}, \rho_f/\rho_g) \tag{4.9}$$

For a circular pipe the void volume per unit heated surface area can be related to the average local void fraction by the equation

$$a = \alpha \frac{\P D^2}{4\P D} = \alpha \frac{D}{4} \tag{4.10}$$

Substituting into equation (4.8) gave the equation

$$\alpha = B. \frac{h_{TP}.k_f}{h_{fo}^2.D} (Pr)^a (\rho_f/\rho_g)^b \tag{4.11}$$

The value of the constant B and of the exponents a and b were determined by doing a multilinear regression of

$$\frac{\alpha \; D \; h_{fo}^2}{h_{TP} \; k_f} \quad \text{versus (Pr) and } (\rho_f/\rho_g).$$

This is shown graphically in Figure 4.6. A correlation coefficient of 0,914 was obtained for 52 sets of data. The equation proposed for the void fraction in the highly subcooled region then is

$$\alpha = 0{,}00649 \frac{h_{TP}.k_f}{h_{fo}^2.D} (Pr)^{0{,}351} (\rho_f/\rho_g)^{0{,}414} \qquad (4.12)$$

The data forming the basis of equation (4.12) were obtained from the void fraction curves samples of which are given in Appendix A. An example of the calculations is given in Appendix D.

Bowring (1962) showed that the subcooling at the point of departure of vapour bubbles from the heated surface could be estimated by the equation

$$\Delta t_{sub_d} = \eta \frac{\phi \rho_f}{G} \qquad (2.38)$$

The empirical factor derived for water over the pressure range 11 to 138 bar was found to depend only on the system pressure and to increase in value with increasing pressures.

The results of this study indicate, however, that in the absolute pressure range between 9 and 25 kPa, η increases with decreasing pressure. This is illustrated graphically in Figure 4.7. Levy (1967) has shown that bubble departure results from the frictional drag forces acting on the bubbles, and a possible explanation for the foregoing observation is that at the low pressures under study the void fraction increases with decreasing pressures

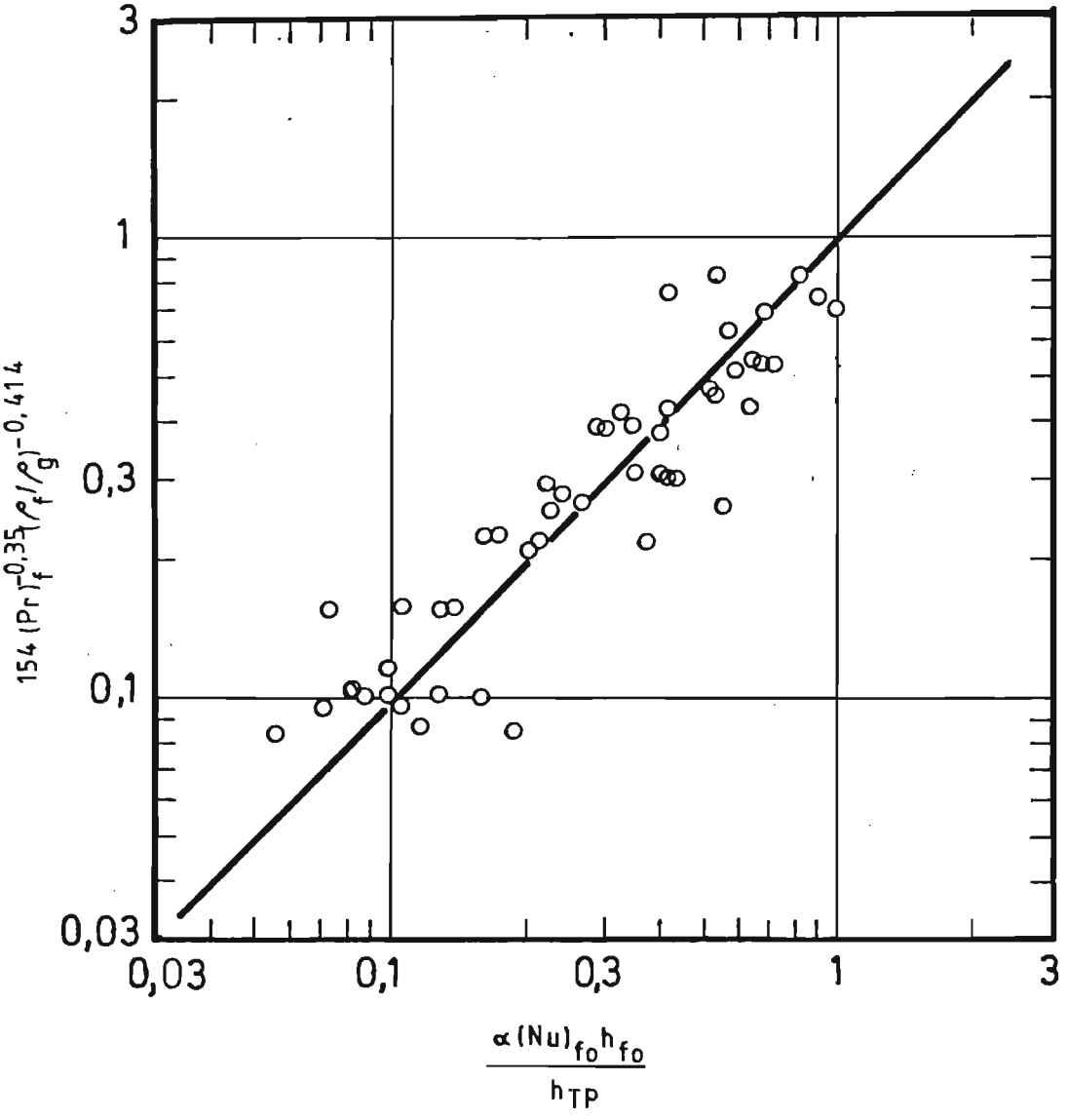

Figure 4.6. Correlation for void fraction in the highly subcooled region.

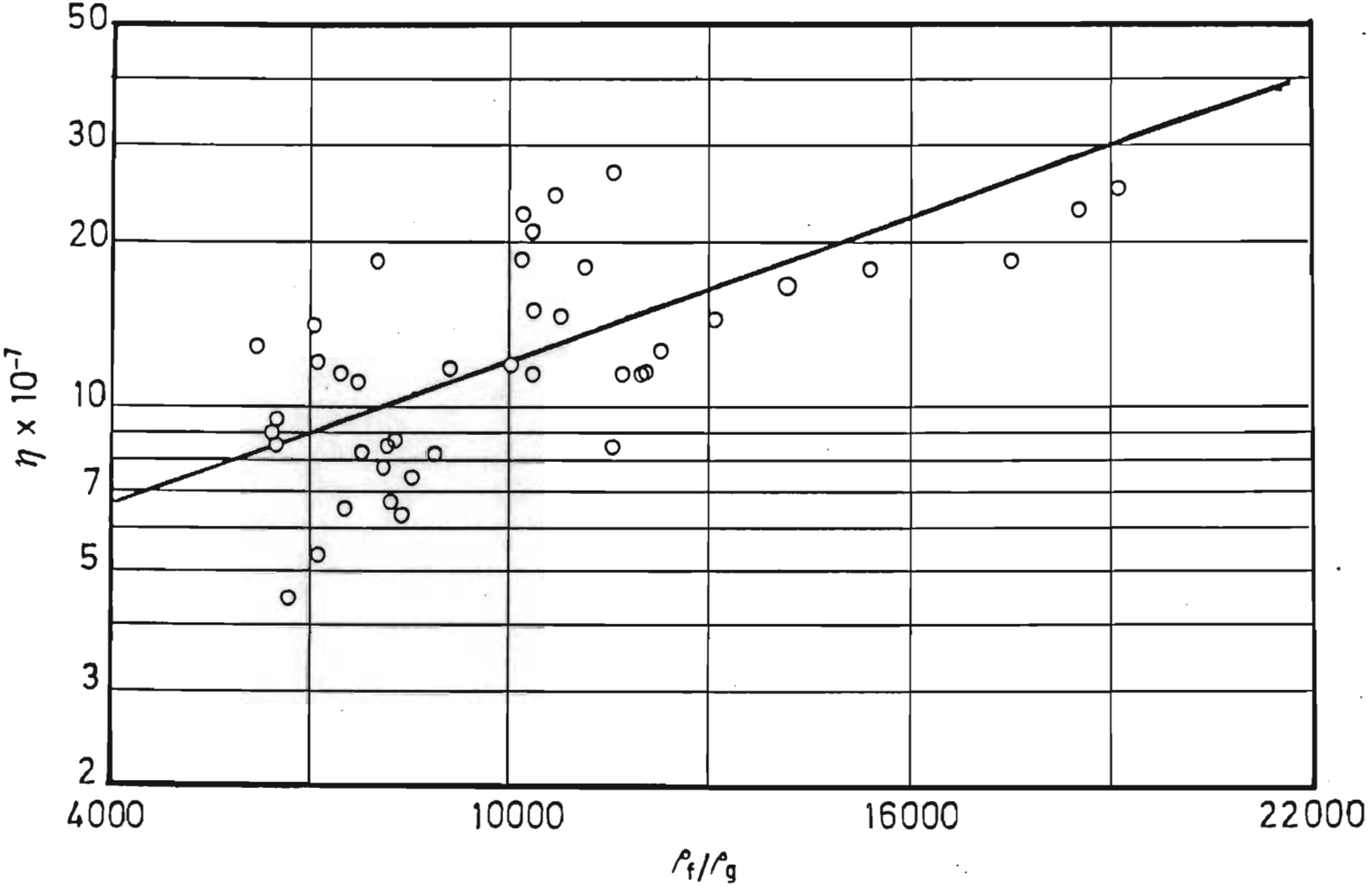

Figure 4.7. Effect of pressure on factor for subcooling at bubble departure.

so that the vapour bubbles project further away from the heat transfer surfaces. They are thus subject to a more intense frictional drag and bubble departure takes place earlier.

A regression analysis of η versus Pr also indicated that the Prandtl number has a significant influence on the subcooling at the point of bubble departure, with departure taking place at a higher subcooling the larger the Prandtl number. This again must result from the more intense frictional drag acting on the bubbles since variation in the value of the Prandtl number is caused mainly by the change in viscosity.

It was found that the value of the empirical factor for the experimental conditions of this study can be expressed by the following equation

$$\eta = 1{,}26 \times 10^{-8} (Pr)_f^{0{,}254} \exp\left[6{,}73 \times 10^{-5} (\rho_f/\rho_g)\right] \qquad (4.13)$$

with a correlation coefficient of 0,849 for 46 sets of data. This is shown graphically in Figure 4.8

4.2.6. Friction loss along tube

The measured pressure differences along the tube are made up of the gravitational, acceleration and friction losses. These losses were estimated as follows:

The boiling tube, from the exit to the level of the lowest pressure tapping, was divided into ten sections, delimitated by the position of the pressure tappings.

The gravitational loss for each section was calculated assuming a normal two phase hydrostatic pressure balance

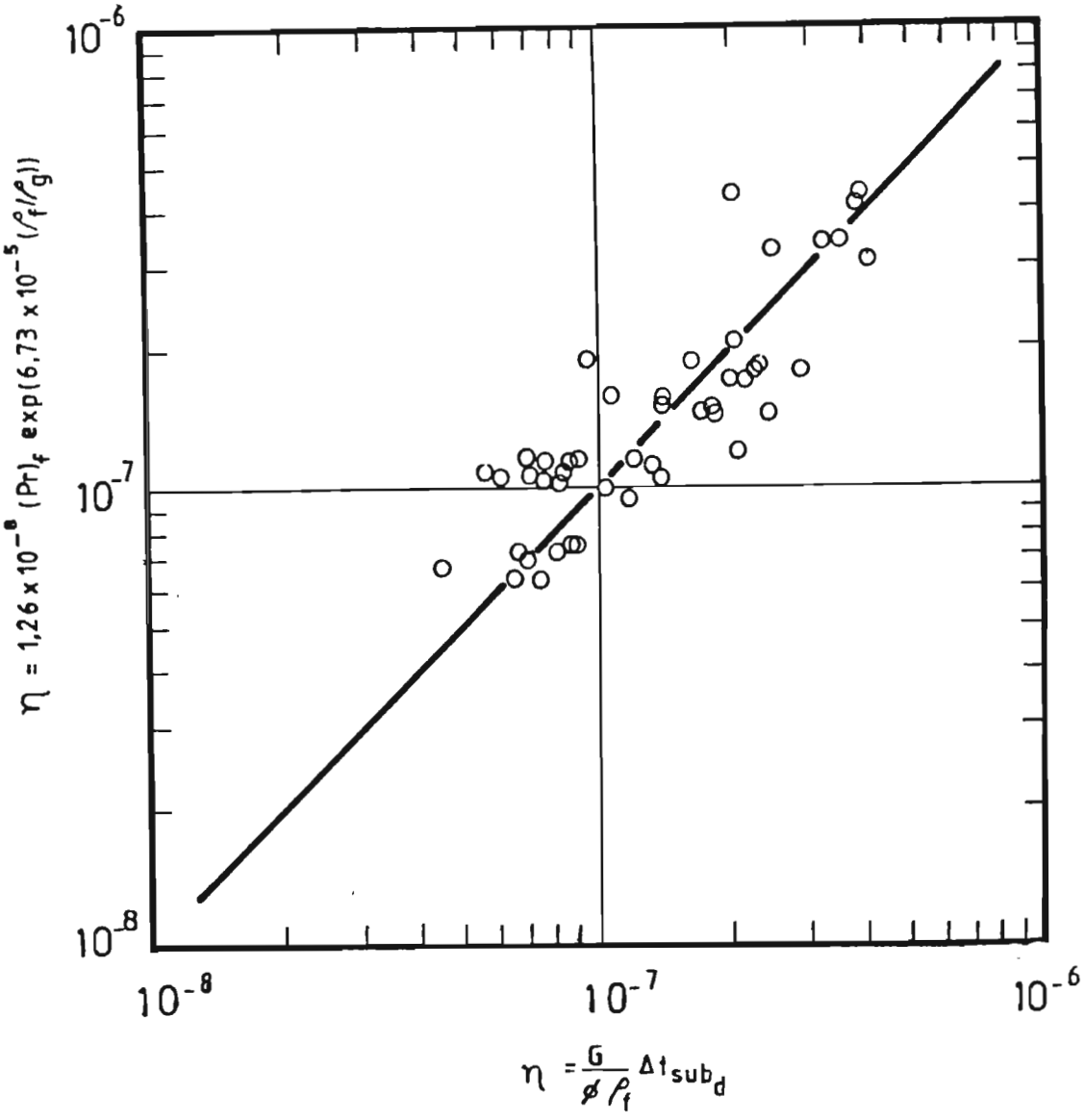

Figure 4.8. Correlation of factor η for estimation of subcooling at bubble departure.

from the equation

$$\Delta p_z = \frac{zg}{g_c}\left[\alpha\rho_g + (1-\alpha)\rho_f\right] \qquad (2.27)$$

using the average value of the experimentally determined void fraction and of the vapour and liquid density for that section. The sum of the losses for the ten sections gave the overall gravitational loss.

Similarly the acceleration loss for each section was calculated from the momentum equation of Butterworth and Hewitt (1977) which represents the difference in pressure resulting from the change in the velocity of the gas and liquid phases from level 1 to level 2.

$$\Delta p_A = \frac{G^2}{g}\left(\left[\frac{x^2}{\alpha\rho_g} + \frac{(1-x)^2}{(1-\alpha)\rho_f}\right]_2 - \left[\frac{x^2}{\alpha\rho_g} + \frac{(1-x)^2}{(1-\alpha)\rho_f}\right]_1\right) \qquad (2.28)$$

Here again the average values of the properties for that section were used, and the sum of the losses for the ten sections gave the overall acceleration loss.

The overall gravitational and acceleration loss was subtracted from the pressure difference observed between the pressure of the first measuring point and the pressure of the vapour space to give the pressure loss due to friction.

$$\Delta p_F = (p_1 - p_{\text{vapour space}}) - \sum_{i=1}^{10}\Delta p_{Ai} - \sum_{i=1}^{10}\Delta p_{zi} \qquad (4.14)$$

A sample calculation is given in Appendix D.4.

The friction loss for isothermal flow of a non-

Newtonian fluid through a straight tube with a fully developed velocity profile can be expressed by the Hagen-Poiseuille equation formulated independently by Hagen (1839) and Poiseuille (1840)

$$\Delta p_F = \frac{32\ z\ u_f\ \mu}{g\ D^2} \qquad (4.15)$$

It is customary in chemical engineering practice to define a friction factor f by the equation

$$f = \frac{\Delta p_F\ D\ g}{2\ z\ u_f^2\ \rho_f} \qquad (4.16)$$

which in terms of the pressure loss due to friction is

$$\Delta p_F = \frac{2\ f\ z\ u_f^2\ \rho_f}{g\ D} \qquad (4.17)$$

By substitution into the Hagen-Poiseuille equation the value of the friction factor for laminar flow is obtained

$$f = \frac{16}{Re} \qquad (4.18)$$

Thus under laminar conditions a plot of the friction factor calcuated from equation (4.16) versus the Reynolds number gives a straight line with an intercept of 16 and a slope of -1.

Metzner and Reed (1955) showed that pseudoplastic non-Newtonian fluids obey the conventional friction factor versus Reynolds number relationship when the flow is laminar

provided that the generalized Reynolds number is used.

$$Re = \frac{D^n u^{2-n} \rho_f}{K_f} \cdot 8. \left[\frac{n}{6n+2}\right]^n \qquad (2.19)$$

While Griffith and Wallis (1961) have shown that the relation given by equation (4.18) is valid for two phase flow in the bubble regime provided that the velocity of the liquid phase is corrected for the voidage due to the gas phase by dividing the volumetric flowrate of the liquid phase by the volumetric fraction occupied by the liquid.

$$u_f = \frac{Q_f}{A(1-\alpha)} \qquad (2.32)$$

In order to report the friction losses obtained in this study as a correlation of the friction factor against the Reynolds number, the pressure losses measured under non-isothermal flow had to be corrected for isothermal flow. The correction factor suggested by Sieder and Tate (1936) for Newtonian fluids modified for non-Newtonian fluids as described in Section 2.4.1. was used for that purpose.

$$\Delta p_{F_{noniso}} = \Delta p_{F_{iso}} \quad \frac{1}{1,1}\left[\frac{K_w 2(3n+1)}{K_b(3n-1)}\right]^{0,25} \qquad (2.23)$$

The correlation obtained between the Reynolds number and friction factor using the method described above is shown graphically in Figure 4.9. It is based on measurements done at Reynolds numbers less than 400, and has a correlation coefficient of 0,644. Transition to turbulent flow seems to take place at Reynolds numbers above 400 which is not far from the value of 1 000 observed by Hsu and Dudukovic (1980). This is shown graphically in Figure 4.10.

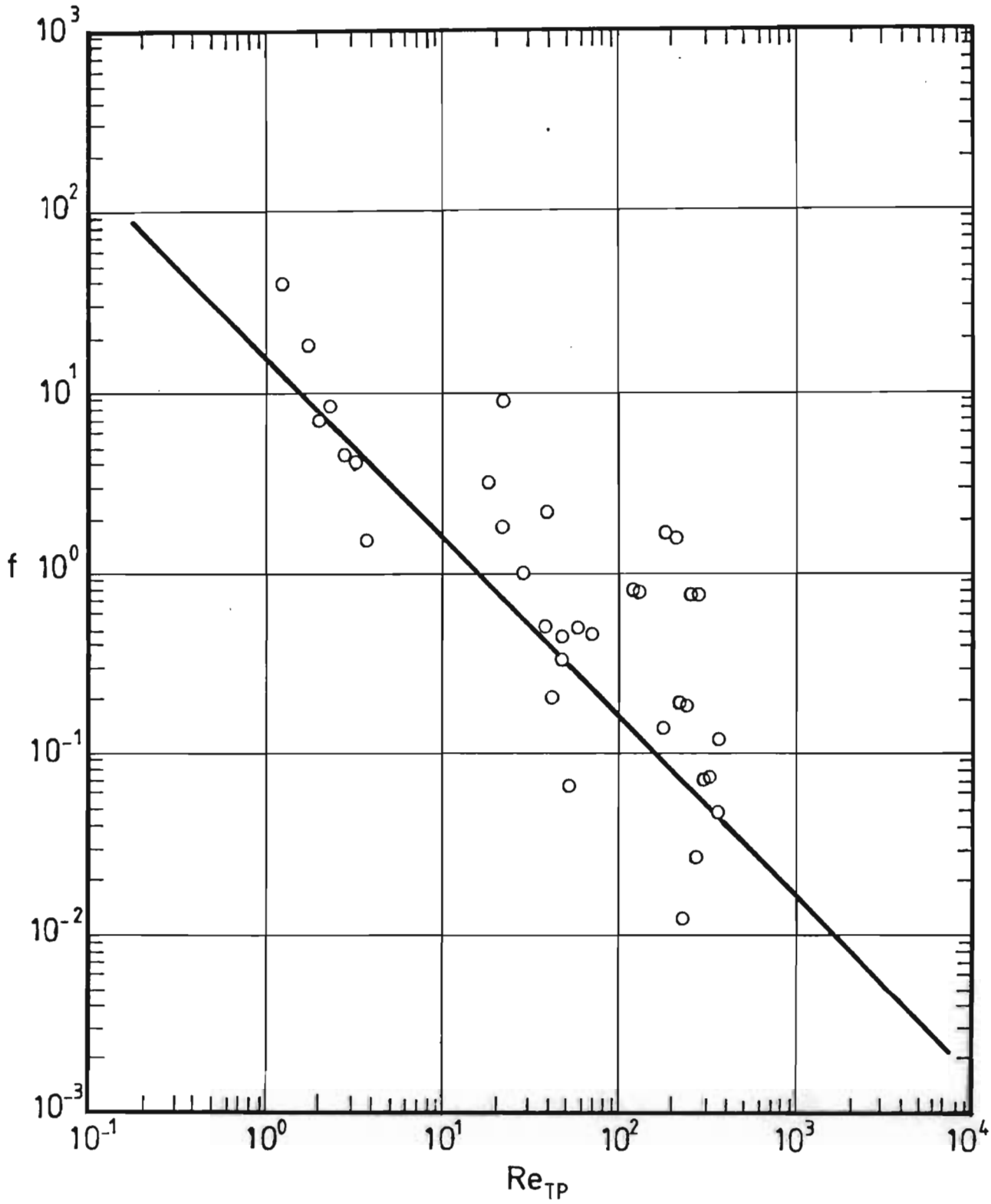

Figure 4.9. Friction factors for liquid boiling under laminar conditions.

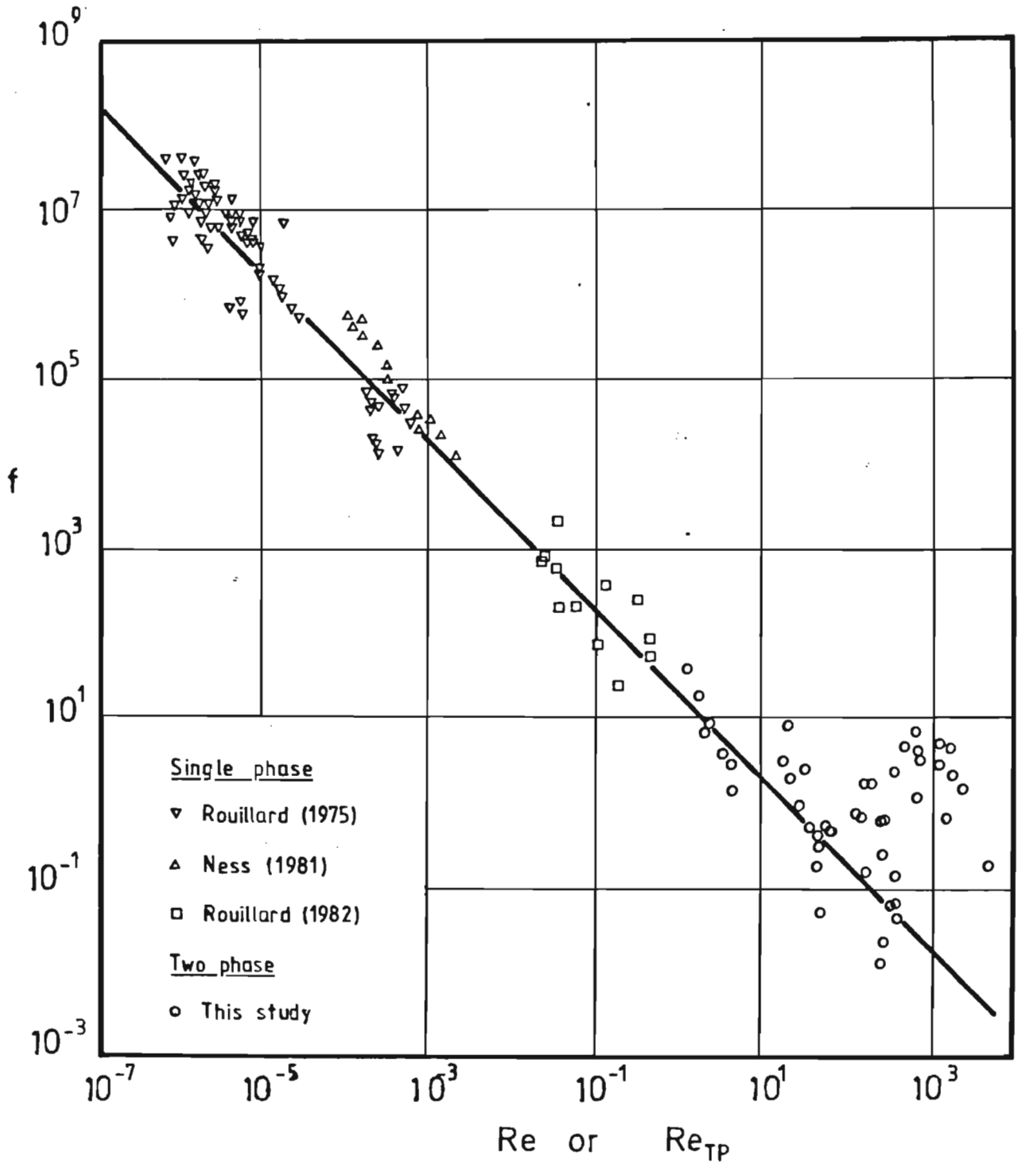

Figure 4.10. Single phase and two phase friction loss measurements on sugar products.

Also shown are single phase pressure drop measurements done on sugar products by Rouillard (1975, 1982) and Ness (1981) which illustrates the relative magnitude of the errors when doing measurements on this material.

It must be pointed out that since the pressure difference was measured between the first pressure tapping and the pressure in the vapour space, the expansion losses are included in the friction losses. However, on account of the low velocities in the tube these losses are probably negligible.

At the higher evaporation rates, fluctuations in the observed pressure and void fraction, particularly in the upper part of the tube, seemed to indicate transition from bubble flow to slug flow. The decrease in pressure drop resulting from this change in regime which had been observed by Oliver and Young Hoon (1968) and Mahalingam and Valle (1972) for pseudoplastic fluids, however, was not noticeable. This can be attributed to the inaccuracy of the pressure measurements and to the fact that the fluids used were only slightly non-Newtonian.

CHAPTER 5

COMPUTER PROGRAM FOR PAN CIRCULATION

Pan circulation is caused by the difference in hydrostatic head between a two phase mixture of massecuite and vapour flowing up the boiling tube and single phase massecuite flowing down the downtake. The rate at which this movement takes place is affected by the resistance to fluid flow resulting from the dimension and arrangement of the flow channel, by the physical properties of the liquid phase and by the amount of vapour formed. Calculation of the circulation velocity for a given pan geometry, and operating conditions and for a given fluid then entails finding the velocity at which the hydrostatic differential head equals the friction losses.

The hydrostatic head in the boiling tube is a function of the void fraction, which in turn varies with the heat transfer coefficient and friction loss along the tube. However, these parameters do not vary linearly with distance from the tube inlet. They first go through a gradual change in the highly subcooled region. The rate of change then increases starting from the point of bubble detachment. Therefore to obtain an accurate estimation of the overall void fraction, evaporation rate and friction loss it is necessary to do a stepwise calculation. The calculations must also be done iteratively until the boiling conditions assumed along the tube match the calculated values, and the friction loss in the flow channel resulting from the assumed velocity equals the hydrostatic differential head.

A program based on this principle and written in Basic for a Hewlett-Packard HP-86 computer is proposed for these calculations.

5.1. Pan circulation program

A list of the program is given in Appendix D.1. and a flow diagram in Figure 5.1. The following data inputs are required:

(a) The specifications of the pan which include the diameter of the pan and of the downtake, the number of tubes, their length, internal and external diameters and the thermal conductivity of the tube metal.

(b) The operating conditions which include the steam pressure, vacuum and height of liquid above the upper tube plate.

(c) The physical properties of the fluid including the rheological constants, surface tension, brix dry substance and purity. In the case of massecuite the dry substance and purity refer to those of the mother liquor.

As the tube outlet pressure is required to calculate the boiling parameters for the tubes, it is obtained by adding the absolute pressure in the vapour space to the hydrostatic head produced by the depth of liquid above the tube plate, the hydrostatic head being the product of depth and liquid density.

It is assumed that the liquid phase upon leaving the tubes rises towards the surface. However, the bulk of the liquid begins its descent into the downtake about halfway to the surface. Thus the temperature of the liquid in the downtake and at the inlet of the tubes corresponds to that at the mid point between the tubes outlet and the surface of the pan; that is the saturation temperature corresponding to the vacuum plus the boiling point elevation. This agrees with the temperature measurements taken in a pan by the Sugar Research Institute of Australia

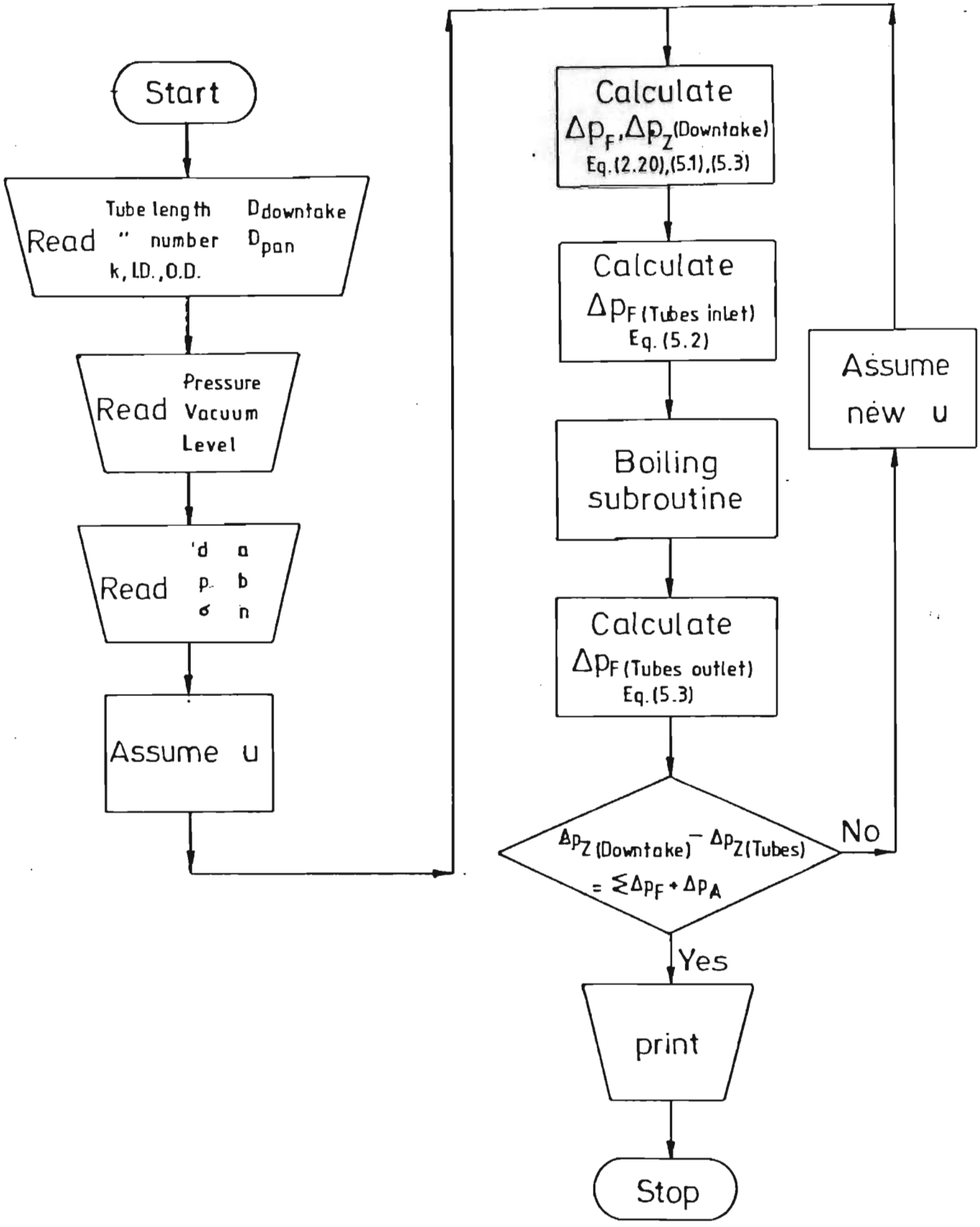

Figure 5.1. Flowchart of circulation program.

(Anon. 1963). The saturation temperature is calculated by the method of Genotelle (1980) and the boiling point elevation by the method of Batterham and Norgate (1975).

It is assumed that when the liquid phase begins its descent into the downtake the disengagement of the vapour bubbles is complete and that no bubbles are carried down into the downtake.

An arbitrary circulation velocity is assumed to initiate the iteration. It is used to calculate the friction loss in the downtake, the contraction and expansion losses at the inlet and outlet of the downtake and the contraction loss at the inlet of the tubes.

The friction loss in the downtake is calculated by the method of Metzner and Reed (1955) for friction losses in pipes for time-independent non-Newtonian fluids where

$$\Delta p_F = \frac{32zu^2\rho_f}{gDRe} \qquad (2.20)$$

in which

$$Re = \frac{D^n u^{2-n}\rho_f}{K_f} \cdot 8. \left[\frac{n}{6n+2}\right]^n \qquad (2.19)$$

The findings of Weltmann and Keller (1957) indicate that the pressure losses for non-Newtonian fluids in laminar flow through sudden contractions are very similar to those for Newtonian fluids. Therefore, the equation given by Perry and Chilton (1973) is used for calculating the entrance loss to the downtake.

$$\Delta p_F = 0{,}4 \left[1{,}25 - \left(\frac{D_{downtake}}{D_{pan}}\right)^2\right] \frac{u^2}{2g} \qquad (5.1)$$

The friction loss caused by the sudden contraction at the tube inlet is calculated from the formula

$$\Delta p_F = 0{,}5 \frac{u^2}{2g} \qquad (5.2)$$

since it is assumed that the ratio of the tube cross section to the pan cross section is infinitely small.

The expansion loss at the exit of the downtake and of the tubes is calculated from the equation given by Skelland (1967) for power law fluids

$$\Delta p_F = \frac{u_1^2 \rho_f}{g} \left(\frac{3n + 1}{2n + 1}\right)\left[\frac{n + 3}{2(5n + 3)}\left(\frac{D_1}{D_2}\right)^4 - \left(\frac{D_1}{D_2}\right)^2 + \frac{3(3n + 1)}{2(5n + 3)}\right] \qquad (5.3)$$

where the subscript 1 refers to the smaller section and 2 to the larger section.

A subroutine in the program is used to calculate the friction and acceleration losses for the boiling tubes. It also gives the tube exit velocity by means of which the expansion losses at the tube outlet can be obtained. This subroutine also calculates the void fraction in the tubes and thus the hydrostatic head.

The resistance to flow then consists of the contraction, friction and expansion losses for the tubes and downtake plus the acceleration losses in the tubes. Friction due to the movement of the fluid across the upper and lower tube plates is neglected. The driving force is the difference in hydrostatic head between the tube and downtake. If the resistance and driving force do not agree within one percent, the circulation velocity is corrected and a new iteration is done until convergence is obtained.

The calculated values produced by the program are shown in the printout in Appendix C.11. It includes details of the pressure losses, temperature, void fraction and heat transfer parameters.

5.2. Boiling subroutine

The boiling subroutine is called by the main program to calculate the void fraction, friction losses and heat transfer rate in the tubes. A list of this subroutine is given in Appendix D.2. and a flow diagram in Figure 5.2.

The basis of the subroutine is to divide the tube into a number of subdivisions. The change in the values of the pertinent variables and parameters is assumed to be linear within each subdivision. The calculation is done stepwise for each subdivision. The values assumed for the calculations are corrected by iteration until congruence is obtained.

To initiate the iteration it is assumed that a uniform temperature prevails along the tube equal to the tube inlet temperature, and that boiling does not occur. The inside tube temperature is assumed to be 3° cooler than the steam temperature.

The friction loss is calculated by the method of Metzner and Reed (1955) to account for the non-Newtonian properties of the fluid and by the method of Griffith and Wallis (1961) to account for the two phase conditions. Thus

$$\Delta p_F = \frac{32\ \rho_f\ u_f^2\ z}{g\ D\ (1 - \alpha)^2\ Re} \qquad (5.4)$$

where Re is the two phase generalized Reynolds number given

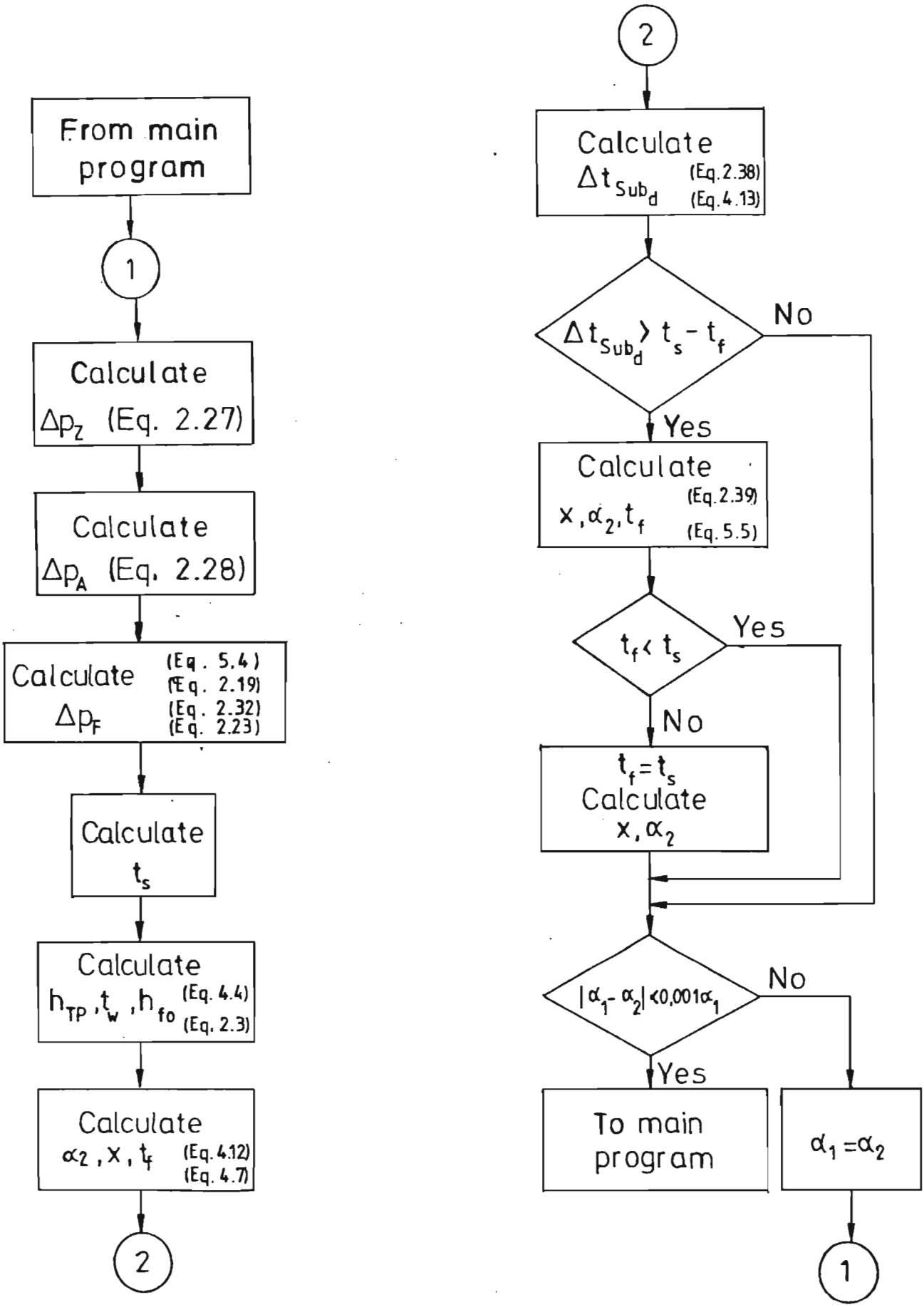

Figure 5.2. Flow chart of boiling subroutine.

by equation (2.19) with the two phase velocity calculated by equation (2.32). The isothermal friction losses calculated by equation (5.4) are converted to non-isothermal conditions by the equation

$$\Delta p_{F_{noniso}} = \Delta p_{F_{iso}} \frac{1}{1,1}\left[\frac{K_w 2(3n+1)}{K_b(3n-1)}\right]^{0,25} \qquad (2.23)$$

The gravitational loss for each section is obtained assuming a normal two phase hydrostatic pressure balance from the equation

$$\Delta p_z = \frac{zg}{g_c}\left[\alpha\rho_g + (1-\alpha)\rho_f\right] \qquad (2.27)$$

Equations (5.4), (2.32) and (2.27) apply to single phase conditions when $x = 0$.

After the first iteration the acceleration loss is calculated for the tube sections where two phase flow prevails using the momentum equation of Butterworth and Hewitt (1977).

$$\Delta p_A = \frac{G^2}{g}\left(\left[\frac{x^2}{\alpha\rho_g} + \frac{(1-x)^2}{(1-\alpha)\rho_f}\right]_2 - \left[\frac{x^2}{\alpha\rho_g} + \frac{(1-x)^2}{(1-\alpha)\rho_f}\right]_1\right) \qquad (2.28)$$

The procedure just described establishes the pressure gradient along the tube, and allows calculation of the saturation temperature by the method of Genotelle (1980) and of the boiling point elevation by the method of Batterham and Norgate (1975). This establishes the boiling temperature profile along the tube.

A nominal amount of condensate is assumed to flow down

the outside of the tube, and the local condensate film heat transfer coefficient is calculated from

$$h_c = 1,47\left[\frac{\pi D\mu_f}{4W}\right]^{1/3} \cdot \left[\frac{k_f^3 \rho_f^2 g}{\mu_f^2}\right]^{1/3} \qquad (4.1)$$

The local massecuite film heat transfer coefficient is calculated using equation (4.4) obtained in this study.

$$(Nu)_f = 4,48\ (Re_{TP})_f^{0,386}\ (\rho_f/\rho_g)^{0,202}\ (D/L)^{1/3} \qquad (4.4)$$

The values of the massecuite film resistance and condensate film resistance to heat flow plus the resistance of the tube wall allows the calculation of the overall heat transfer coefficient and local inside tube temperatures for each section.

It is also possible to calculate the actual amount of condensate formed on the steam side surface.

Calculation of the local void fraction depends on three conditions.

(a) Subcooling at bubble departure is calculated from the equation of Bowring (1962)

$$\Delta t_{sub_d} = \eta \frac{\phi \rho_f}{G} \qquad (2.38)$$

using the value of the empirical factor η obtained from this study.

$$\eta = 1,26 \times 10^{-8} (Pr)_f^{0,254} \exp\left[6,73 \times 10^{-5} (\rho_f/\rho_g)\right] \qquad (4.13)$$

If the subcooling for the section is greater than Δt_{sub_d} the local void fraction is calculated using the equation for the highly subcooled region derived in this study.

$$\alpha = 0{,}00649 \frac{h_{TP}.k_f}{h_{fo}^2.D} (Pr)^{0{,}351} (\rho_f/\rho_g)^{0{,}414} \qquad (4.12)$$

in which the single phase heat transfer coefficient, h_{fo}, is obtained from the equation of Charm and Merrill (1959) for single phase pseudoplastic fluids in straight tubes.

$$\frac{h_f D}{k_f} = 2{,}0 \left[\frac{Wc_p}{k_f z}\right]^{1/3} \left[\frac{K_b(3n+1)}{K_w 2(3n-1)}\right]^{0{,}14} \qquad (2.3)$$

The local mass vapour quality x is calculated using the equation of Nicklin et al. (1962) which accounts for the drift or relative velocity between the phases taking a value of 1,12 for the flow distribution parameter.

$$x = \frac{GC_o}{\rho_f} + 1{,}53 \left[\frac{\sigma g (\rho_f - \rho_g)}{\rho_f^2}\right]^{1/4} \Big/ G\left[\frac{1}{\alpha \rho_g} - \frac{C_o}{\rho_g} + \frac{C_o}{\rho_f}\right] \qquad (4.7)$$

(b) Starting from the section where the local subcooling is less than Δt_{sub_d} the local void fraction is calculated using the method of Levy (1967) for the low subcooling region.

$$x' = x - x_d \exp\left[\frac{x}{x_d} - 1\right] \qquad (2.39)$$

where x_d is the thermodynamic quality at the point of bubble departure

$$x_d = \frac{c_{p_f} (t_f - t_s)_d}{i_{fg}} \qquad (2.40)$$

The local massecuite temperature is calculated from the local mass vapour quality by means of a heat balance.

(c) Starting from the section where the local massecuite temperature equals the saturation temperature the local mass vapour quality is calculated from a heat balance because the thermodynamic equilibrium has then been reached.

The local void fraction for both the low subcooling and saturated boiling regions is calculated using the equation of Nicklin et al. (1962) and a flow distribution parameter of 1,12.

$$\alpha = \frac{Q_g}{C_o (Q_g + Q_f) + VA} \qquad (5.5)$$

A test for convergence is then done by comparing the void fraction calculated with the void fraction that prevailed at the start of the iteration.

If convergence is not achieved, the new values for the local void fraction are used in the equations to calculate the gravitational, acceleration and friction losses. New pressure and saturation profiles are established and the procedure for calculation of the heat transfer and local void fraction is repeated until convergence is obtained.

The accuracy of the boiling subroutine was ascertained by calculating evaporation rates based on the data given in

Appendix A.1. The calculated values are compared to the measured values in Figure 5.3. The average deviation is $\pm$ 18 percent with a maximum of 55 percent.

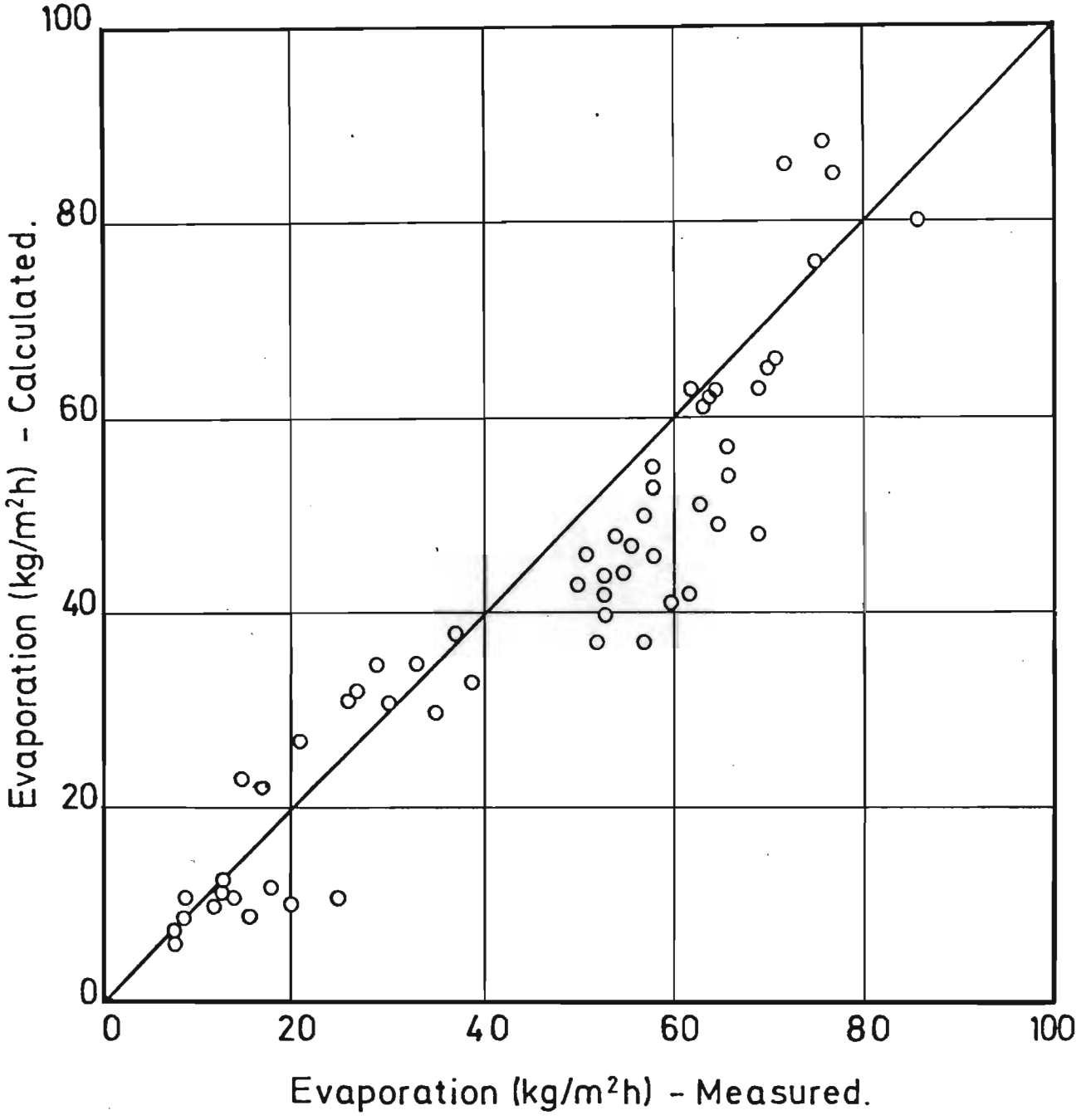

Figure 5.3. Evaporation rates calculated using computer program compared to measured values.

CHAPTER 6

APPLICATION OF PAN CIRCULATION PROGRAM

The experimental results from a full scale pilot vacuum pan designed by Tongaat-Hulett Sugar Ltd. were used to assess the computer program for pan circulation. This pan is shown in Figure 6.1. It consists of four 0,0984 m internal diameter tubes 0,6; 1,0; 1,4 and 1,8 m long connecting a common downtake and vapour space. Each tube has an individual steam jacket with its own steam inlet, incondensable gas vent and condensate drain. As the pan was intended to study the effect of tube length, head above the tubes, steam pressure and vacuum on the evaporation rate of continuous pans, the head above the upper tube plate can only reach a maximum of 1,0 metres which is the highest operational level for this type of pan.

The tests were done with A, B and C-massecuites. The influence of the different variables was determined by means of a factorial experiment. The high and low levels of the factors used are given in Table 6.1.

TABLE 6.1

Range of variables used in factorial experiment

Massecuite	Pressure (kPa abs)	Vacuum (kPa abs)	Head (m)
A	125-195	9-25	0,20-0.94
B	127-195	9-20	0,25-0,91
C	130-180	10	0,24-0,87

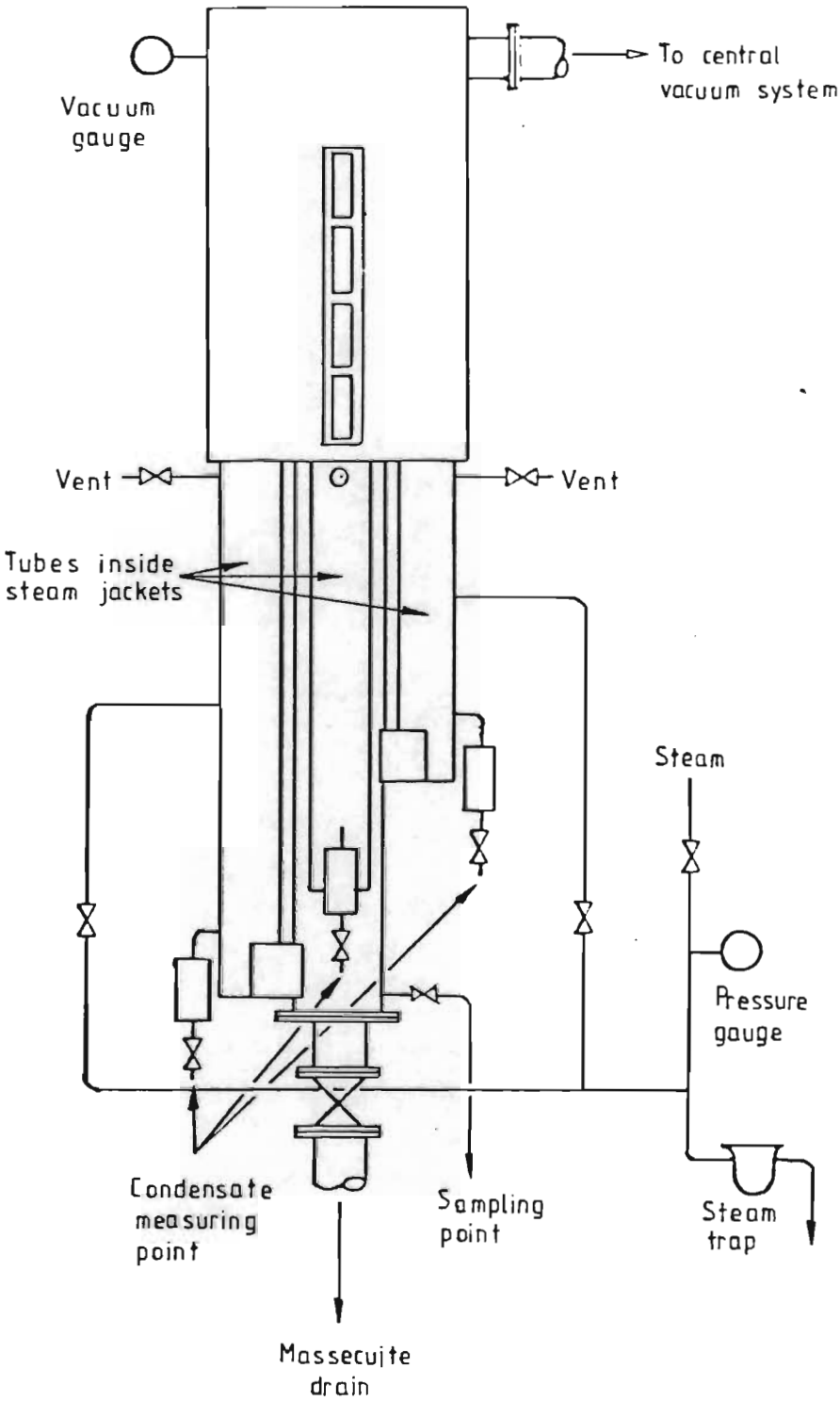

Figure 6.1. Tongaat-Hulett pilot vacuum pan.

Each run lasted for about thirty minutes, half of which was for stabilisation of the operating conditions. Collection of condensate took place during the second half. The results obtained are shown in Tables 6.2, 6.3 and 6.4.

The difficulty of obtaining reliable data when boiling a highly viscous fluid in a vertical tube is demonstrated by these results. The average deviation between the individual measurements and the mean values was 29, 18 and 11 percent for A, B and C-massecuite respectively while the maximum deviation was 92, 48 and 36 percent.

The rheological properties and surface tension of the massecuite was measured for some of the runs and these data were used to calculate the evaporation rate by means of the computer program developed in this study. The relation of the measured to the calculated values is shown in Figure 6.2. The average deviation between the measured and calculated values was 85, 16 and 14 percent respectively for A, B and C-massecuites. In the case of A-massecuite the calculated values were consistently larger than the measured evaporation rates. Therefore it appears that although the method of calculation proposed in this study is suitable for the more viscous fluids it fails to represent adequately the circulation of the less viscous material.

It is believed that the reason for this failure is that in calculating the circulation velocity it is assumed that all the energy from the hydrostatic head difference between the tubes and the downtake is used up in overcoming the friction and acceleration losses in the circulation path. However when boiling is vigorous the liquid velocity becomes so great that it is projected into the vapour disengagement space and then falls back. Part of the energy available for circulation is thus lost. In other words the circulation program overestimates the circulation velocity.

The response of the circulation program to changes in

TABLE 6.2.

Evaporation rates measured for A-massecuite

Operating conditions			Brix	Tube lengths (m)			
Steam (kPa)	Vacuum (kPa)	Head (m)		0,6	1,0	1,4	1,8
195	9	0,20	91,9 92,2 91,4	32 51 52	28 41 47	26 37 47	26 33 37
Average			91,8	45	39	37	32
195	9	0,94	88,9 89,2 92,2 91,4	53 70 35 31	41 47 30 27	46 47 28 28	38 40 25 26
Average			90,4	47	36	37	32
195	25	0,20	88,1 92,2	32 13	41 10	43 9	34 10
Average			90,2	23	25	26	22
195	25	0,94	88,2 91,8 90,5	24 39 21	12 35 13	8 37 12	10 30 8
Average			90,2	28	20	19	16
125	9	0,20	91,8 92,2 88,7	27 22 38	27 20 20	22 16 30	21 18 23
Average			90,9	29	22	23	21
125	9	0,94	89,2 91,7 92,5	33 31 30	26 31 27	27 29 23	23 - 22
Average			91,1	31	28	26	23
125	25	0,20	91,4 91,2	21 10	15 10	14 10	16 12
Average			91,6	16	13	12	14
125	25	0,94	91,6 89,9	25 10	20 6	18 4	18 4
Average			90,8	18	13	11	11

TABLE 6.3.

Evaporation rates measured for B-massecuite

Operating conditions			Brix	Tube lengths (m)			
Steam (kPa)	Vacuum (kPa)	Head (m)		0,6	1,0	1,4	1,8
195	9	0,25	92,4 91,9 90,2	17 26 27	11 22 30	15 21 35	19 22 22
Average			91,5	23	21	24	21
195	9	0,91	91,6 92,1	18 21	15 21	12 17	11 17
Average			91,9	20	18	15	14
195	20	0,25	90,8 93,6	18 19	13 18	13 16	13 13
Average			92,2	19	16	15	13
195	20	0,91	91,4 92,2	12 17	9 16	7 14	8 11
Average			91,8	15	13	11	10
127	9	0,25	93,0 91,4	19 16	14 13	11 16	12 15
Average			92,2	18	14	14	14
127	9	0,91	91,6 92,1	12 20	7 16	6 16	7 13
Average			91,9	16	12	11	10
127	20	0,25	91,1 90,9 92,5	13 6 12	8 8 11	6 8 8	7 8 7
Average			91,5	10	9	7	7
127	20	0,91	92,1 90,9 91,0	14 8 11	11 7 7	7 5 5	7 5 5
Average			91,3	11	9	6	6

TABLE 6.4.

Evaporation rates measured for C-massecuite

Operating conditions		Brix	Tube lengths (m)			
Steam (kPa)	Head (m)		0,6	1,0	1,4	1,8
180	0,24	93,5 93,9 94,0	9,5 7,9 8,8	6,5 6,0 10,3	5,5 5,4 6,5	5,5 4,9 4,5
Average		93,8	8,7	7,6	5,8	5,0
180	0,87	94,7	9,3	8,3	5,7	5,4
130	0,24	93,5 93,6	8,4 7,0	5,4 5,5	5,1 5,0	5,0 4,8
Average		93,6	7,7	5,5	5,1	4,9
130	0,87	93,5 94,5	5,5 8,6	5,5 7,3	4,1 4,3	4,1 7,4
Average		94,0	7,1	6,4	4,2	5,8

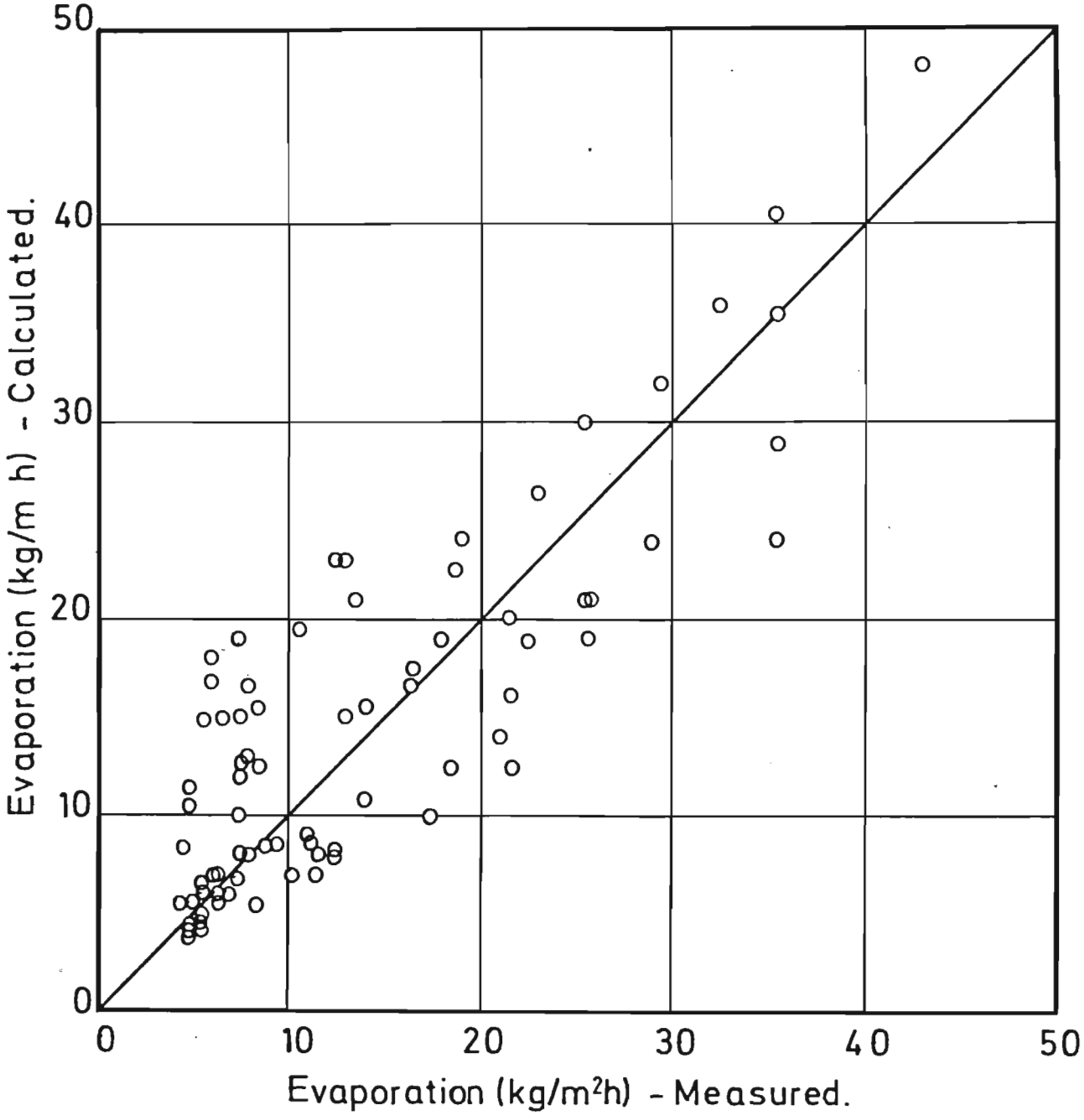

Figure 6.2. Evaporation rates measured in Tongaat-Hulett experimental pan compared to calculated values.

tube length and operating conditions was assessed by calculating the evaporation rates for the steam pressure, vacuum and heads as used in the factorial experiments for B and C-massecuites. The calculated values together with the corresponding circulation velocities, expressed as the inlet velocities to the tubes are shown in Tables 6.5. and 6.6. The physical properties assumed are shown at the top of each table.

Comparison between the figures of Table 6.5. and the average figures of Table 6.3. shows that the arbitrary assignment of an exponent of 1/3 to the dimensionless group D/L in equation (4.2) was correct since the average difference between the measured and calculated evaporation rates for tube lengths of 0,6; 1,0; 1,4 and 1,8 metres was -2,6; -5,9; -4,6 and -7,4 percent respectively.

The response of the circulation program to changes in steam pressure was also good since the average difference between measured and calculated values was -1,1 and -8,9 percent for high and low steam pressures respectively. The same applies to changes in level, the average difference being +2,0 and -12,0 percent for high and low operating levels. However, the calculated effect of changing the vacuum was the opposite of the measured effect. At high vacuum the calculated evaporation was on average low by -37,4 percent and at low vacuum it was high by 27,4 percent. This can be attributed to the dominant effect of viscosity in the heat transfer equation (Equation 4.4). An increase in vacuum results in a reduction of the saturation temperature of the massecuite, and thus an increase in viscosity.

The circulation velocities calculated for C-massecuite as shown in Table 6.6. ranged between 0,14 and 0,16 m s^{-1} which is slightly less than the maximum measured by Smith (1968) and Bosworth and Duloy (1950). However, the

TABLE 6.5.

Evaporation rates and circulation velocities calculated for B-massecuite

Properties assumed.

Dry substance massecuite	91,66
Purity massecuite	69,01
Dry substance molasses	86,06
Purity molasses	49,33
Rheological constants	
a	$1,15 \times 10^{-7}$
b	7050
n	0,712
Surface tension	0,779

Operating conditions			Tube length (m)							
Press.	Vacuum	Level	0,6		1,0		1,4		1,8	
(kPa)	(kPa)	(m)	Evap. (kg/m^2h)	Vel. (m/s)	Evap. (kg/m^2h)	Vel. (m/s)	Evap. (kg/m^2h)	Vel. (m/s)	Evap. (kg/m^2h)	Vel. (m/s)
195	9	0,25	17	0,19	14	0,19	12	0,19	10	0,19
195	9	0,91	16	0,19	13	0,20	11	0,20	10	0,20
195	20	0,25	23	0,57	19	0,59	17	0,60	15	0,61
195	20	0,91	22	0,58	18	0,60	16	0,61	15	0,61
127	9	0,25	10	0,15	8	0,16	7	0,16	7	0,16
127	9	0,91	10	0,16	8	0,16	7	0,16	6	0,16
127	20	0,25	13	0,48	11	0,49	9	0,50	8	0,50
127	20	0,91	12	0,48	10	0,50	9	0,50	8	0,50

TABLE 6.6.

Evaporation rates and circulation velocities calculated for C-massecuite

Properties assumed.

Dry substance massecuite	92.64
Purity massecuite	57,79
Dry substance molasses	88,91
Purity molasses	41,78
Rheological constants	
a	$2,11 \times 10^{-4}$
b	4447
n	0,853
Surface tension	1,670

Operating conditions		Tube length (m)							
Press.	Level	0,6		1,0		1,4		1,8	
(kPa)	(m)	Evap. (kg/m^2h)	Vel. (m/s)	Evap. (kg/m^2h)	Vel. (m/s)	Evap. (kg/m^2h)	Vel. (m/s)	Evap. (kg/m^2h)	Vel. (m/s)
180	0,24	8,2	0,16	7,8	0,16	7,6	0,16	7,3	0,16
180	0,87	7,7	0,16	7,4	0,16	7,2	0,16	7,0	0,16
130	0,24	5,9	0,15	5,7	0,14	5,5	0,14	5,3	0,14
130	0,87	5,6	0,15	5,4	0,15	5,2	0,15	5,1	0,14

viscosities used in the calculation of this table are comparatively low for a massecuite of this type.

As can be seen in Table 6.5, the circulation velocity is mainly affected by the vacuum under which boiling takes place. High vacuum results in a marked reduction of circulation velocity as a result of the increased viscosity. Long tubes produce slightly higher velocities although they have comparatively lower evaporation rates. As is to be expected reducing the steam pressure slows down the circulation.

The circulation velocity seems to increase as the tube diameter becomes larger. The calculated values are 0,15; 0,19 and 0,27 m/s for tubes of 0,0860; 0,0984 and 0,127 m respectively, under the same conditions of pressure, vacuum and depth of massecuite above the tubes, while the evaporation rate differs by less than two percent between the three sizes. The conclusions of Hugot and Jenkins (1959) that the tube diameters should be larger than those in use thus appears to be correct. However since the effect of tube diameter was not determined experimentally additonal proof is required.

CHAPTER 7

CONCLUSIONS

The main objective of this study was to produce a method for the calculation of the boiling process which takes into account the heat transfer, vapour holdup and hydraulic pressure losses. Such a method would be useful for optimizing pan design and operation. To achieve this objective it was necessary to obtain a better understanding of the mechanism of circulation and to define the variables which affect heat transfer, vapour holdup and pressure drop and assess their influence.

The major conclusions of this study are as follows:

7.1. Boiling in the lower part of the tube takes place under subcooled conditions. With high heat fluxes a change to saturated boiling occurs, but with low heat fluxes subcooling extends to the tube outlet. With a change to saturated boiling a maximum axial temperature is observed, but if only subcooled boiling occurs the change in axial temperature is not noticeable.

7.2. The boiling heat transfer coefficient, found experimentally, is well described by a correlation of the Nusselt number with the two phase Reynolds number evaluated at film conditions, the dimensionless density ratio and the ratio of the diameter to the length of the tube raised to the power of one third. (Equation 4.4). The effect of tube length on the boiling heat transfer coefficient is thus the same as that for single phase heat transfer in laminar flow. The influence of the Prandtl number was not found to be statistically significant. It is believed that this results from the dominant effect of the viscosity. As it appears in both the Reynolds and Prandtl numbers

only one of these groups can influence the Nusselt number.

Since the Prandtl number is excluded from the correlation caution must be exercised when applying the equation for boiling heat transfer derived from this study to fluids other than sugar products.

7.3. The flow distribution parameter C_o (Equation 2.42) was found to have an average value of 1,13 at the tube outlet, which is close to the findings of other workers.

7.4. The void fraction in the highly subcooled region is shown to be a function of the ratio of the two phase to single phase heat transfer coefficient, the Prandtl number and the dimensionless density ratio. (Equation 4.12).

7.5. This study shows that the subcooling at the point of bubble departure, which Bowring (1962) had indicated was a function of pressure, can be expressed as a function of the dimensionless density ratio and of the Prandtl number (Equation 4.13). The subcooling at this point was observed to increase with decreasing pressure.

7.6. Because of the difficulty of measuring the pressure and void fraction in a boiling viscous liquid, the data obtained for the estimation of the friction loss are not entirely satisfactory. The results indicate, however, that the method proposed by Griffith and Wallis (1961) (Equation 2.31) for the calculation of friction loss in bubbly flow gives a good estimate of the friction losses when boiling under laminar conditions. Transition to turbulent flow seems to occur at a Reynolds number of about 500, a value slightly lower than that of 1 000 recorded by Hsu and Dudukovic (1980) in a gas lift reactor.

7.7. A computer program is proposed for the calculation of circulation in vacuum pans as used in the sugar industry. The method suggested takes into account the heat transfer, vapour holdup and pressure losses in the boiling tubes, and equates the difference in hydrostatic head between the tubes and downtake to the pressure losses in the circulation channel in order to determine the circulation rate.

Comparison of the calculated evaporation rates obtained with this method with the values measured in a full scale pilot pan showed that good agreement is obtained for the more viscous massecuites. However, for lower viscosities the difference is appreciable.

7.8. The computer calculations indicated that for a given massecuite, the circulation rate decreases as the vacuum is increased. A slightly higher rate is produced as the length of the boiling tubes is increased but this is accompanied by a decrease in the evaporation rate.

NOMENCLATURE

A	flow area	m^2
A_c	bubble - liquid interfacial area for condensation	m^2
a	constant in eq. (B.2c)	-
B	dimensionless group in eq.(2.5)	-
B_o	constant in eq. (4.8)	-
Bl	constant in eq. (2.36)	-
b	constant in eq. (B.2c)	-
C_o	flow distribution parameter	-
C_1	parameter for rising velocity	-
C_2	parameter for effect of boiling on rising velocity	-
c_p	specific heat	$J\ kg^{-1}\ K^{-1}$
C_{sf}	constant in Rohsenow correlation eq. (2.9)	-
D	pipe diameter	m
d	dry substance	-
F	factor in Chen correlation eq.(2.11)	-
f	friction factor	-
G	mass velocity	$kg\ m^{-2}\ s^{-1}$
g	acceleration due to gravity	$m\ s^{-2}$
g_c	conversion factor	
h	heat transfer coefficient	$W\ m^{-2}\ C^{-1}$
h_c	heat transfer coefficient, convective	$W\ m^{-2}\ C^{-1}$
h_{NcB}	heat transfer coefficient for nucleate boiling	$W\ m^{-2}\ C^{-1}$
I_f	radiation intensity through liquid	-
I_g	radiation intensity through gas	-
I_{TP}	radiation intensity through two phases	-
i_f	enthalpy of saturated liquid	$J\ kg^{-1}$
i_g	enthalpy of saturated vapour	$J\ kg^{-1}$
i_{fg}	latent heat of vaporisation	$J\ kg^{-1}$
K	Armand flow distribution parameter eq.(2.41)	-
K	fluid consistency index	$kg\ s^{n-2}\ m^{-1}$
K_p	per cent crystal content	-
k	thermal conductivity of liquid	$W\ m^{-1}\ C^{-1}$

L	length	m
M	mass	kg
m	index eq.(2.50)	-
N	rotational speed	s^{-1}
n	flow behaviour index	-
P	purity	-
p	static pressure	$N\ m^{-2}$
Q	volumetric rate of flow	$m^3\ s^{-1}$
q_f	heat transferred to liquid phase	W
q_g	heat transferred to vapour phase	W
R_f	liquid holdup eq. (2.34)	-
r	radius	m
S	supression factor used in Chen correlation eq. (2.13)	-
s	% scale reading	-
T	temperature	K
t	temperature	C
t_l	inlet bulk liquid temperature	C
t_s	saturation temperature	C
t_{WONB}	wall temperature at onset of boiling	C
$t_{(z)}$	bulk liquid temperature at axial position z	C
u	velocity of flow	$m\ s^{-1}$
u_o	rate of bubble growth	$m\ s^{-1}$
V	rising velocity	$m\ s^{-1}$
v	specific volume	$m^3\ kg^{-1}$
v_{fg}	difference in specific volumes of saturated liquid and vapour	$m^3\ kg^{-1}$
W	mass rate of flow	$kg\ s^{-1}$
X	Martinelli parameter eq. (2.15)	-
x	mass vapour quality	-
z	axial coordinate	m
z_{NB}	length of tube under non boiling conditions	m

GREEK

α	void fraction	-
η	empirical factor for bubble departure eq. (2.38)	-

ρ	density	kg m^{-3}
μ	viscosity	Ns m^{-2}
ϕg or f	two phase frictional multiplier in Martinelli correlation eq. (2.29)	W m^{-2}
ϕ	heat flux	W m^{-2}
ϕ_c	convective heat flux	W m^{-2}
ϕONB	heat flux to cause boiling	W m^{-2}
σ	surface tension	N m^{-1}
τ	shear stress	N m^{-2}
ΔPA	pressure difference due to acceleration	N m^{-3}
Δp_F	pressure difference due to friction	N m^{-3}
Δp_Z	pressure difference due to static head	N m^{-3}
dp/dz	pressure gradient	N m^{-3}
du/dr	rate of shear	s^{-1}
Δt	temperature difference	C
Δt_e	effective wall superheat	C
Δt_f	temperature difference between wall and bulk liquid	C
Δt_s	superheat necessary to cause nucleation	C
Δt_{sub}	subcooling at axial position	C
$\Delta tsub_d$	subcooling at point of bubble departure	C
	superheat	C
$(\Delta t_s)_{ONB}$	superheat at onset of boiling	C

DIMENSIONLESS NUMBERS

Eo	Eotvos number eq. (2.44)
N_u	Nusselt number (h D/k)
N_f	dimensionless inverse viscosity eq. (2.49)
Pr	Prandtl number at bulk liquid temperature eq. (4.3)
Re	Reynolds number eq. (2.19)
Re_{TP}	effective two phase Reynolds number with velocity obtained from eq. (2.32)
Y	property group ($g \mu^4 / \rho\sigma^3$)

SUBSCRIPTS

b	at bulk conditions
c	condensate
d	at bubble departure
f	liquid or film conditions
fo	total flow assumed liquid
g	gas or vapour
ONB	onset of boiling
s	at saturation
TP	two phase
tt	liquid turbulent/gas turbulent
vv	liquid viscous/gas viscous
w	at wall conditions
1,2	referring to levels 1,2 etc.

REFERENCES

Adkins, B.G. (1951). Notes on the viscosity of molasses and massecuite. Proc QSSCT 13 51 - 56.

Ahmad, S.J. (1970). Axial distribution of bulk temperatures/void fraction in a heated channel with inlet subcooling J. Heat Transfer. Trans. ASME 92 595 - 609.

Allan, C.J. (1962). Some suggested revisions of pan circulation theory. Proc QSSCT 29, 89 - 94.

Allan, G.N. (1983). South African sugar factory plant installations 1983. Sugar Milling Research Institute Communication No. 133.

Anon (1963). Sugar crystallization in vacuum pans. 3 - Aspect of circulation efficiency in vacuum pans. Technical Report No. 73. Sugar Research Institute, Australia.

Anon (1964). Pan circulation tests using a radioactive isotope. Technical Report No. 77. Sugar Research Institute, Australia.

Anon (1965). Further circulation tests using a radioactive isotope. Technical Report No. 88. Sugar Research Institute, Australia.

Anon (1977). Laboratory Manual for South African Sugar factories. South African Sugar Technologists Association.

Armand, A.A. (1946). The resistance during the movement of a two phase system in horizontal pipes. Izv. Vses. Teplotek. Inst. (1) 16 - 23.

Austmeyer, K.E. (1980). Investigations on heat and mass transfer in the initial stage of vacuum pan crystallization of sucrose. PhD. Thesis. Technical University of Braunschweig.

Awang, M. and White, E.T. (1976). Effect of crystal on the viscosity of massecuites . Proc QSSCT 43 263 - 270.

Baloh, T. (1967). Some diagrams for aqueous sugar solutions. Zucker 20 608 - 679.

Bankhoff, S.G. (1960). A variable density single fluid model for two phase flow with particular reference to steam water flow. J. Heat Transfer, Trans ASME. 82 265 - 272.

Batterham, R.J. and Norgate, T.E. (1975). Boiling point elevation and superheat in impure cane sugar solutions. Int. Sug. J. 77 359 - 364.

Beardmore, R., Cousens, G., Davis, C.W., Frew, R., McAuley, A., Matthews, P. and Miller, J.R.D. (1969). Some aspects of the design of calandria vacuum pans. Cuba Azucar 4 48 - 54.

Behne, M.F. (1964). Viscosity in massecuites. Proc QSSCT 31 289 - 296.

Behne, M.F., Wright, P.G. and Day, J.C. (1971). Circulation studies on a horizontal vacuum pan. Technical Report No. 113. Sugar Research Institute, Australia.

Bosworth, C.L. (1947). J. Proc. Roy. Soc. N.S. Wales 81 156.

Bosworth, C.L. and Duloy, J.S.K. (1950). The measurement of pan circulation. Proc ISSCT 7 645 - 654.

Bowring, R.W. (1962). Physical model based on bubble detachment and calculation of steam voidage in the subcooled region of a heated channel. OECD Halden Reactor Project Report HPR - 10.

Broadfoot, R. and Wright, P.G. (1981). Design ideas for a continuous low grade pan. Proc ASSCT 23 - 29.

Brown, C.A. and Zerban, F.W. (1941). Physical and chemical methods of sugar analysis. Joh Wiley, New York.

Butterworth, D. and Hewitt, G.F. (1977). Two phase flow and heat transfer. Oxford University Press.

Charm, S.E. and Merrill, E.W. (1959). Heat transfer coefficients in straight tubes for pseudoplastic food materials in streamline flow. Food research 24 319 - 331.

Chen, J.C. (1966). Correlation for boiling heat transfer to saturated fluids in convective flow. Ind. Engng. Chem. Process Design and Development 5 322 - 329.

Cimorelli, L. and Evangelisti, R. (1967). The amplification of the capacitance method for void fraction measurement in bulk boiling conditions. Int. Jnl. Heat Mass Transfer 10 277 - 288.

Claasen, H. (1938). Evaporation and vertical tube evaporators. Schallehn and Woolbruck, Magdeburg.

Collier, J.G. (1972). Convective boiling and condensation. McGraw Hill, London.

Davidson, W.F., Hardie, P.H., Humphreys, C.G.R. Markson, A.A., Mumford, A.R. and Ravese, T. (1943). Studies of heat transmission through boiler tubing at pressures from 500 to 3300 pounds. Trans. ASME 65 553 - 591.

Davis, E.J. and Anderson, G.H. (1966). The incipience of nucleate boiling in forced convective flow. AIChe J. 12 774 - 780.

Deer, N. (1950). The history of sugar, Chapman Hall, London.

Dengler, C.E. and Addoms, J.N. (1956). Heat transfer mechanisms for vaporisation of water in a vertical tube. Chem. Eng. Progress Symp. Series 52 (18) 95 - 103.

Erlee, T.J.D. (1931). Archief. 38(2) 785 - 797.

Forster, H.K. and Zuber, N. (1955). Dynamics of vapour bubble and boiling heat transfer AIChE J. 1 531 - 535.

Forster, K.E., and Grief, R. (1959). Heat transfer to a boiling liquid - Mechanism and correlations. J. Heat Transfer Trans ASME. 81 43 - 53.

Garyazha, V.T., Artyukhov, Y.G. and Pavelko, V.I. (1974). Hydrodynamic calculations of massecuite vacuum pans. Izv. V.U.Z. Pishch. Tekhnol (5) 108 - 111.

Genotelle, J. (1980). Etude des tables relatives à la vapeur d'eau. Sucrerie Francaise. 121 357 - 367.

Graham, W.S. and Radford, D.J. (1977). Preliminary experiences with a continuous pan boiling C-massecuite. Proc ISSCT 16 3099 - 3112.

Griffith, P., Clark, J.A., and Rohsenow, W.M. (1958). Void volumes in subcooled boiling systems. Paper 58 - HT - 19. ASHME - AIChE. Heat Transfer Conference, Chicago.

Griffith, P. and Wallis, G.D. (1961). Two phase slug flow. J. Heat Transfer, Trans ASME 83 307 - 320.

Griffith, P. (1964). The prediction of low quality boiling voids. J. Heat Transfer, Trans ASME 86 327 - 333.

Hagen, G. (1839). Ann. Phys. Chem. 46 423 - 442.

Hamill, J. (1956). Vacuum pan design in relation to performance. Proc ISSCT 9 76 - 81.

Hewitt, G.F. (1978). Measurement of two phase flow parameters. Academic Press, London.

Hsu, Y.Y. (1962). On the size of range of active nucleation cavities on a heating surface. J. Heat Transfer, Trans ASME 84 207.

Hsu, Y.C. and Dudukovic, M.P. (1980). Gas holdup and liquid recirculation in gas-lift reactors. Chem. Eng. Sci. 35 135 - 141.

Hugot, E. (1950). La Sucrerie de Cannes. Dunod, Paris.

Hugot, E. and Jenkins, G.H. (1959). Circulation in vacuum pans. Proc ISSCT 10 232 - 241.

Isbin, H.S., Moy, J.E. and Cruz, A.J.R. (1957). Two phase, steam-water critical flow. 3 361 - 365.

Jenkins, G.H. (1958). Heating surface arrangement and circulation in vacuum pans. Proc QSSCT 25 199 - 200.

Jens, W.H. and Lottes, P.A. (1951). Analysis of heat transfer, burnout, pressure drop and density data for high pressure water. ANL - 4627.

Jullienne, L.M.S.A. and Munsamy, S.S. (1981). Assessment of the Gledhow and Tongaat Fives Cail-Babcock continuous pan. Proc SASTA 55 79 - 82.

Kadlec, P., Bretschneider, R. and Dandar, A. (1981). La mesure et le calcul des propriétés physico-chimiques des solutions sucrées. La Sucrerie Belge 100, 45 - 53.

Kroeger, P.G., and Zuber, N. (1968). An analysis of the effects of various parameters on the average void fractions in subcooled boiling. Int. J. Heat Mass Transfer 11 211 - 233.

Langreney, F. (1977). True continuous crystallisation. 1. Design stages. 2. Industrial application. Proc ISSCT 16 2427 - 2443.

Levy, S. (1967). Forced convection subcooled boiling-prediction of vapour volumetric fraction. Int. J. Heat Mass Transfer 10 951 - 965.

Lockhart, R.W. (1945). Isothermal pressure drop for two phase, two component, viscous-viscous flow in a tube at various angles to the horizontal. M.Sc. Thesis, University of California.

Lockhart, R.W. and Martinelli, R.C. (1949). Proposed correlation of data for isothermal two-phase, two-component flow in pipes. Chem. Eng. Prog. 45 (1) 39 - 48.

Mahalingham, R. and Valle, M.A. (1972). Momentum transfer in two-phase flow of gas-pseudoplastic liquid mixtures. Ind. Eng. Chem. Fundam. 11 (4) 470 - 477.

Marchaterre, J.F. and Petrick, M. (1956). The effect of pressure on boiling density in multiple rectangular channels. ANL - 5522.

Martinelli, R.C. and Nelson, D.B. (1948). Prediction of pressure drop during forced circulation boiling of water. Trans ASME 70 695 - 702.

McAdams, W.H. (1942). Heat transmission. McGraw Hill, New York.

McDougall, E.E. and Wallace, G.A. (1982). The Racecourse continuous vacuum pan. Proc ASSCT.

McNelly, M.J. (1953). A correlation of the rates of heat transfer to nucleate boiling liquids. I.C. Chem. Eng. Soc. J. 7 18 - 34.

Metzner, A.B. and Reed, J.C. (1955). Flow of non-Newtonian fluids - correlation of the laminar, transition and turbulent flow regions. AIChE J. 1 434 - 440.

Moles, F.D. and Shaw, J.R.G. (1972). Boiling heat transfer to subcooled liquids under conditions of forced convection. Trans Inst. Chem. Engrs. 50 76 - 84.

Mooney, M. (1931). J. Rheology 2 210.

Neduzhko, E.A. (1964). Refinement of the critical equation of heat transfer for massecuite boiling. Izvest. Vysshikh. Ucheb. Zaved. Pishchevaya Tekhol. (2) 125 - 126, 146.

Ness, J.N. (1981). Massecuite heating with finned tube heat exchangers. Proc ASSCT 55 - 60.

Nicklin, D.J., Wilkes, J.O. and Davidson, J.F. (1962). Two phase flow in vertical tubes. Trans. Instn. Chem. Engrs. 40 61 - 68.

Nielson, G.R. (1974). The 110 m^3 pan at Inkerman. Proc QSSCT 41 207 - 210.

Oliver, D.R. and Wright, S.J. (1964). Pressure drop and heat transfer in gas-liquid slug flow in horizontal tubes. Brit. Chem. Eng. 9 (9) 590 - 596.

Oliver, D.R. and Young Hoon, A. (1968). Two phase non-Newtonian flow. Part 1: Pressure drop and holdup. Trans. IChE. 46 T106 - T122.

Ostwald, W. (1926). Kollaidzschr. 38 261.

Papell, S.S. (1962). Subcooled boiling heat transfer under forced convection in a heated tube. Tech. Note D - 1583. Cleveland : NASA.

Pavelko, V.I. and Garyazha, V.T. (1975) Calculation of natural circulation in massecuite vacuum pans. Pishch. Prom. (Kiev). 21 9 - 12.

Perk, C.G.M. (1952). Coil and calandria vacuum pans. Proc SASTA 26 48 - 53.

Perry,R.H. and Chilton, C.H. ed. (1973). Chemical Engineers' Handbook. McGraw Hill Kogakusha Ltd., Tokyo.

Plato, F., Domke, J. and Harting, H. (1900) Z. Ver. dent. Zucker-Ind. 50 d 982, 1079.

Poiseuille, J.L. (1840). Compte Rendus 11, 961 and 1041.

Rohsenow, W.M. (1953). Heat transfer with evaporation. Heat transfer Symposium. University of Michigan. Summer 1952. University of Michigan Press.

Rouillard, E.E.A. (1975). Friction loss and heat transfer coefficient in finned tube heat exchangers for reheating massecuite. Proc SASTA 49, 74 - 79.

Rouillard, E.E.A. (1982). Friction losses in massecuite pipelines. Proc SASTA 56 44 - 45.

Rouillard, E.E.A.(1984) Viscosity of factory products. S.M.R.I. Technical Report No. 137 . June 12.

Rouhani, S.Z. and Axelsson, E. (1970). Calculation of void volume fraction in the subcooled and quality boiling regions. Int. J. Heat Trans. 13 383 - 393.

Schrock, V.E. and Grossman, L.M. (1959). Forced convection boiling studies, final report on forced convection vaporization project. Laurence Radiation Lab. Rep. No. TID - 14632.

Sieder, E.N. and Tate, G.E. (1936). Heat transfer and pressure drop of liquids in tubes. Ind. & Eng. Chem. 28 1429 - 1434.

Skelland, A.H.P. (1967). Non-Newtonian flow and heat transfer. John Wiley and Sons, Inc. New York.

Skyring, A. and Beale, R.F. (1967). Boiling massecuites. Proc. QSSCT 34 49 - 53.

Smith, N. (1938). Circulation in coil vacuum pans. Int. Sug. J. 40 101 - 104, 145 - 147.

Smith, W.E. (1935). Vacuum pan design and operation. Int. Sug. J. 37 20 - 22.

Spencer, G.L. and Meade, G.P. (1948). Cane sugar handbook. John Wiley, New York.

Spight, C.L. (1966). On the hydraulic characteristics of a boiling water channel with natural circulation. Tech. U. Eindhoven.

Troino, V.P. and Vaisman, M.L. (1964). Temperature and height of the point of commencement of boiling of sugar massecuites. Izvest. Vysshikh Ucheb. Zave. Pishchevaya Teknol. (2) 128 - 130, 146.

Troino, V.P. (1968). Hydrodynamics of massecuite vacuum pans. Pishch. Prom. Resp. Mazhved. Nauch. Tekh. Sb. 7 169 - 176.

Tromp, L.A. (1937). Massecuite circulation and vacuum pan design. Int. Sug. J. 39 11 - 14, 60 - 65, 89 - 102.

Van Hengel, A. (1971). Darnall pan has many new features. South African Sug. J. 52 63 - 66, 96 - 98.

Vanhook, A. and Biggins, W.F. (1952). Surface Tension of pure and impure sucrose solutions. Int. Sug. J. 54 7 - 10.

Venton, C.B. (1950). A comparative study of some new vacuum pans. Int. Sug. J. 52 63 - 66, 96 - 98.

Wallis, G.B. (1969). One dimensional two-phase flow. McGraw Hill, New York.

Webre, A.L. and Robinson, C.S. (1926). Evaporation. Chemical Catalog, New York.

Webre, A.L. (1932). Experiments of the working of the calandria pan. Proc Assoc. Cuban Sugar Technol. 124 - 140.

Webre, A.L. (1934). Circulation in vacuum pans. Trans ASME - Process Division Annual Meeting. Paper PRO-56-1.

Weltmann, R.N. and Keller, T.A. (1957). N.A.C.A. Tech. Note 3889.

Werkspoor, (1931). Tests on vacuum pan circulation. Archief. 39 11 (32) 912 - 917.

White, E.T. and Beardmore, R.H. (1962). The velocity of rise of single cylindrical air bubbles through liquids contained in vertical tubes. Chem. Eng. Sci. 17 351 - 361.

Zuber, N. and Findlay, J.A. (1965). Average volumetric concentration in two phase flow systems. J. Heat Transfer. Trans. ASME, 87 453 - 468.

APPENDIX A

EXPERIMENTAL DATA

Details of the measurements taken on the experimental pan are given here. This includes the void fraction, pressures and temperatures. Also included are the physical properties of the fluids.

TABLE A1

Experimental Data

Run No.	1			2			3			4		
Fluid	Syrup			Syrup			Syrup			Syrup		
Inlet velocity (m/s)	0,063			0,038			0,038			0,063		
Brix	72,00			72,00			72,00			72,00		
Dry substance	72,00			72,00			72,00			72,00		
Purity	100,00			100,00			100,00			100,00		
Surface tension (N/m)	0,0560			0,0670			0,0670			0,0670		
Viscosity constants												
A =	2,981E-009			1,660E-008			1,660E-008			1,660E-008		
B =	5599			4982			4982			4982		
Flow behaviour index	1,000			1,000			1,000			1,000		
Steam pressure (kPa-abs.)	100			100			115			112		
Vacuum (kPa-abs.)	13,0			13,0			24,5			24,5		
Condensate (kg/h)	30,69			34,33			25,50			26,63		
Tube length (mm)	Void	Press kPa	Temp. C	Void	Press kPa	Temp. C	Void	Press kPa	Temp. C	Void	Press kPa	Temp. C
1300	0,88	13,0	53,7	0,81	13,0	55,5	0,81	24,5	70,3	0,79	24,5	69,3
1175	0,84	13,5	54,4	0,78	13,6	56,1	0,78	25,0	70,6	0,77	24,7	69,5
1050	0,79	13,7	55,0	0,74	13,6	56,8	0,74	25,3	71,0	0,75	25,3	69,7
925	0,71	14,2	55,7	0,67	14,0	57,4	0,72	25,9	71,3	0,71	25,9	69,9
800	0,57	15,0	56,4	0,54	14,8	58,0	0,67	26,6	71,7	0,65	26,6	70,1
675	0,32	16,1	57,0	0,38	15,9	58,6	0,58	27,4	72,0	0,59	27,4	70,3
550	0,16	17,3	57,1	0,13	17,2	58,3	0,41	28,5	72,3	0,45	28,4	70,4
425	0,11	18,8	56,5	0,07	18,7	57,9	0,23	29,8	72,2	0,33	29,5	70,6
300	0,09	20,3	55,9	0,00	20,3	57,5	0,16	31,2	71,8	0,22	30,9	70,3
175	0,09	22,1	55,3	0,00	21,9	57,1	0,13	32,8	71,3	0,16	32,6	69,7
50		23,6	54,6		23,4	56,7		34,6	70,9		34,5	69,1
0			54,4			56,5			70,7			68,8

TABLE A1

Experimental Data (Continued)

Run No.	5			6			7			8		
Fluid	Molasses			Molasses			Molasses			Molasses		
Inlet velocity (m/s)	0,063			0,046			0,063			0,046		
Brix	80,65			80,65			82,30			82,35		
Dry substance	76,36			76,36			76,09			76,09		
Purity	37,01			37,01			41,24			41,24		
Surface tension (N/m)	0,1000			0,1000			0,1060			0,1060		
Viscosity constants												
A =	2,465E-006			2,465E-006			2,307E-009			2,307E-009		
B =	4700			4700			6790			6790		
Flow behaviour index	,980			,980			1,000			1,000		
Steam pressure (kPa-abs.)	132			128			129			129		
Vacuum (kPa-abs.)	12,5			12,5			24,5			25,0		
Condensate (kg/h)	23,12			23,12			20,05			22,83		
Tube length (mm)	Void	Press kPa	Temp. C	Void	Press kPa	Temp. C	Void	Press kPa	Temp. C	Void	Press kPa	Temp. C
1300	0,82	12,5	57,2	0,86	12,5	57,0	0,87	24,5	73,4	0,84	25,0	73,7
1175	0,82	13,1	57,6	0,83	13,4	57,4	0,84	25,3	73,6	0,83	25,5	73,9
1050	0,82	14,3	57,9	0,80	14,3	57,7	0,81	25,3	73,9	0,83	25,8	74,1
925	0,78	13,8	58,2	0,78	15,0	58,1	0,77	25,4	74,1	0,77	26,1	74,2
800	0,72	14,9	58,5	0,72	15,6	58,4	0,71	25,7	74,4	0,67	26,4	74,4
675	0,63	16,6	58,9	0,64	16,2	58,8	0,60	26,2	74,6	0,60	26,8	74,6
550	0,52	16,4	59,2	0,53	16,9	59,1	0,48	26,9	74,9	0,47	27,5	74,7
425	0,37	18,0	58,9	0,45	17,6	59,4	0,37	28,1	74,7	0,33	28,4	74,8
300	0,26	19,2	58,1	0,32	18,5	59,0	0,24	29,6	74,3	0,21	29,8	74,3
175	0,14	21,3	57,3	0,15	19,7	58,3	0,15	31,7	73,9	0,11	31,7	73,9
50		22,9	56,5		21,3	57,7		34,3	73,5		33,9	73,4
0			56,2			57,4			73,4			73,2

TABLE A1

Experimental Data (Continued)

Run No.	9			10			11			12		
Fluid	C-seed			C-seed			C-seed			C-seed		
Inlet velocity (m/s)	0,079			0,063			0,046			0,079		
Brix	84,70			84,70			84,70			84,70		
Dry substance	85,96			85,96			85,96			85,96		
Purity	72,38			72,38			72,38			72,38		
Surface tension (N/m)	0,4160			0,4160			0,4160			0,4160		
Viscosity constants												
A =	2,189E-005			2,189E-005			2,189E-005			2,189E-005		
B =	4364			4364			4364			4364		
Flow behaviour index	0,980			0,980			0,980			0,980		
Steam pressure (kPa-abs.)	140			140			140			140		
Vacuum (kPa-abs.)	12,0			12,0			12,0			20,5		
Condensate (kg/h)	5,09			7,42			10,03			8,09		
Tube length (mm)	Void	Press kPa	Temp. C	Void	Press kPa	Temp. C	Void	Press kPa	Temp. C	Void	Press kPa	Temp. C
1300	0,57	12,0	58,4	0,66	12,0	58,6	0,83	12,0	58,7	0,41	20,5	68,7
1175	0,56	13,4	59,2	0,57	13,4	59,0	0,63	13,0	59,2	0,34	21,3	68,7
1050	0,56	13,9	59,0	0,47	14,5	59,4	0,44	13,2	57,7	0,28	21,6	68,6
925	0,39	15,9	58,9	0,39	16,1	59,1	0,34	14,6	60,2	0,25	23,1	68,5
800	0,33	17,3	58,7	0,32	17,5	58,8	0,26	15,7	60,2	0,19	24,5	68,4
675	0,30	18,7	58,5	0,25	19,0	58,6	0,22	17,0	59,8	0,15	26,1	68,5
550	0,27	20,1	58,3	0,21	20,6	58,3	0,21	18,6	59,3	0,13	28,0	68,6
425	0,21	21,5	58,2	0,18	22,3	58,0	0,20	20,4	58,8	0,02	29,9	68,7
300	0,14	22,8	58,0	0,14	24,0	57,8	0,15	22,4	58,3	0,10	31,8	68,8
175	0,12	24,2	57,8	0,08	25,7	57,5	0,10	24,6	57,8	0,06	33,6	68,9
50		25,2	57,7		27,5	57,2		26,5	57,4		35,5	69,0
0			57,6			57,1			57,2			69,0

TABLE A1

Experimental Data (Continued)

Run No.	13			14			15			16		
Fluid	C-seed			C-seed			C-seed			C-seed		
Inlet velocity (m/s)	0,063			0,079			0,063			0,046		
Brix	84,70			86,80			86,80			86,80		
Dry substance	85,96			87,02			87,02			87,02		
Purity	72,38			67,29			67,29			67,29		
Surface tension (N/m)	0,4160			0,4160			0,4160			0,4160		
Viscosity constants												
A =	2,189E-005			2,189E-005			2,189E-005			2,189E-005		
B =	4364			4364			4364			4364		
Flow behaviour index	0,980			0,980			0,980			0,980		
Steam pressure (kPa-abs.)	150			156			157			158		
Vacuum (kPa-abs.)	20,0			20,0			20,0			20,0		
Condensate (kg/h)	4,86			5,15			5,49			6,45		
Tube length (mm)	Void	Press kPa	Temp. C	Void	Press kPa	Temp. C	Void	Press kPa	Temp. C	Void	Press kPa	Temp. C
1300	0,47	20,0	70,0	0,48	20,0	68,4	0,61	20,0	70,0	0,56	20,0	69,3
1175	0,46	20,8	70,0	0,48	21,3	69,0	0,60	21,1	70,0	0,56	21,0	69,5
1050	0,45	21,0	70,0	0,48	21,7	69,0	0,59	21,5	70,0	0,56	21,4	69,4
925	0,42	22,5	69,8	0,45	23,3	69,9	0,55	23,0	69,9	0,53	22,9	69,4
800	0,37	23,9	69,8	0,36	24,4	68,7	0,48	24,0	69,9	0,46	24,0	69,3
675	0,29	25,5	69,9	0,29	25,4	68,7	0,36	25,1	69,8	0,37	25,2	69,3
550	0,25	27,2	70,0	0,24	26,6	68,8	0,33	26,3	69,8	0,30	26,4	69,2
425	0,19	28,9	70,1	0,21	27,8	68,9	0,26	27,5	69,8	0,22	27,6	69,2
300	0,14	30,4	70,1	0,17	29,2	69,0	0,16	28,8	69,7	0,14	28,9	69,1
175	0,11	31,7	70,1	0,12	30,7	69,0	0,12	30,1	69,7	0,11	30,3	69,1
50		33,5	70,3		31,9	69,0		31,7	69,6		32,1	69,0
0			70,4			69,0			69,6			69,0

TABLE A1

Experimental Data (Continued)

Run No.	17			18			19			20		
Fluid	C-seed			C-seed			C-seed			C-seed		
Inlet velocity (m/s)	0,079			0,079			0,063			0,046		
Brix	86,80			82,30			82,30			82,30		
Dry substance	87,02			84,51			84,51			84,51		
Purity	67,29			67,29			67,29			67,29		
Surface tension (N/m)	0,4160			0,3290			0,3290			0,3290		
Viscosity constants												
A =	2,189E-005			3,909E-004			3,909E-004			3,909E-004		
B =	4364			3557			3557			3557		
Flow behaviour index	0,980			0,935			0,935			0,935		
Steam pressure (kPa-abs.)	168			164			164			173		
Vacuum (kPa-abs.)	28,0			26,5			26,5			26,5		
Condensate (kg/h)	3,42			3,67			3,32			3,41		
Tube length (mm)	Void	Press kPa	Temp. C	Void	Press kPa	Temp. C	Void	Press kPa	Temp. C	Void	Press kPa	Temp. C
1300	0,32	28,0	68,8	0,43	26,5	5,0	0,43	26,5	71,2	0,36	26,5	70,0
1175	0,32	29,2	68,8	0,40	28,1	70,6	0,40	28,1	69,5	0,36	28,1	68,9
1050	0,32	30,6	68,9	0,36	29,4	70,6	0,36	29,4	70,0	0,36	29,4	68,8
925	0,30	32,2	69,1	0,35	30,5	70,7	0,34	30,4	70,0	0,34	30,4	69,0
800	0,27	33,9	69,2	0,31	31,4	70,8	0,28	31,4	70,0	0,28	31,3	69,0
675	0,22	35,6	69,3	0,21	32,4	70,9	0,23	32,5	70,0	0,23	32,4	69,0
550	0,16	37,3	69,4	0,20	33,6	70,9	0,20	33,8	70,0	0,19	33,7	69,0
425	0,14	38,9	69,4	0,16	35,3	71,0	0,17	35,7	70,0	0,16	35,6	69,1
300	0,14	40,3	69,5	0,13	37,5	71,0	0,11	38,1	70,0	0,10	38,2	69,1
175	0,14	41,5	69,5	0,09	40,4	71,1	0,07	41,4	70,0	0,05	41,7	69,1
50		42,8	69,5		45,2	71,2		46,4	70,0		47,8	69,1
0			69,0			71,2			70,0			69,1

TABLE A1

Experimental Data (Continued)

Run No.	21			22			23		
Fluid	Molasses			Molasses			Molasses		
Inlet velocity (m/s)	0,079			0,063			0,046		
Brix	79,90			79,90			79,90		
Dry substance	74,25			74,25			74,25		
Purity	41,24			41,24			41,24		
Surface tension (N/m)	0,0949			0,0949			0,0949		
Viscosity constants									
A =	1,052E-011			1,052E-011			1,052E-011		
B =	8279			8279			8279		
Flow behaviour index	,932			,932			,932		
Steam pressure (kPa-abs.)	115			114			113		
Vacuum (kPa-abs.)	11,5			12,0			12,0		
Condensate (kg/h)	26,59			25,96			27,45		
Tube length (mm)	Void	Press kPa	Temp. C	Void	Press kPa	Temp. C	Void	Press kPa	Temp. C
1300	0,88	11,5	54,3	0,88	12,0	54,4	0,83	12,0	54,3
1175	0,88	12,1	54,5	0,88	12,7	54,8	0,93	12,6	54,6
1050	0,88	12,4	54,7	0,88	12,7	55,1	0,93	13,0	54,6
925	0,86	12,9	55,0	0,86	13,4	55,4	0,80	13,6	55,2
800	0,82	13,5	55,2	0,76	14,0	55,8	0,73	14,2	55,4
675	0,64	14,2	55,4	0,71	14,8	56,1	0,66	14,9	55,7
550	0,45	15,2	55,6	0,49	15,7	56,1	0,51	15,8	56,0
425	0,27	16,4	55,2	0,34	16,9	55,8	0,37	16,8	55,7
300	0,15	17,9	54,8	0,17	18,3	55,4	0,27	18,0	55,3
175	0,09	19,6	54,4	0,11	19,9	55,0	0,09	19,3	54,9
50		19,5	54,1		19,3	54,7		21,0	54,5
0			53,9			54,5			54,3

TABLE A1

Experimental Data (Continued)

Run No.	24			25			26		
Fluid	Molasses			Molasses			Molasses		
Inlet velocity (m/s)	0,079			0,063			0,046		
Brix	79,90			79,90			79,90		
Dry substance	74,25			74,25			74,25		
Purity	41,24			41,24			41,24		
Surface tension (N/m)	0,0949			0,0949			0,0949		
Viscosity constants									
A =	1,052E-011			1,052E-011			1,052E-011		
B =	8279			8279			8279		
Flow behaviour index	,932			,932			,932		
Steam pressure (kPa-abs.)	123			123			123		
Vacuum (kPa-abs.)	21,0			21,0			21,0		
Condensate (kg/h)	21,53			23,23			23,89		
Tube length (mm)	Void	Press kPa	Temp. C	Void	Press kPa	Temp. C	Void	Press kPa	Temp. C
1300	0,84	21,0	69,7	0,83	21,0	69,7	0,80	21,0	69,2
1175	0,84	21,6	69,9	0,80	22,0	69,9	0,78	22,0	69,4
1050	0,84	21,9	70,0	0,77	22,4	70,0	0,76	22,4	69,6
925	0,82	22,3	70,2	0,75	22,7	70,2	0,73	22,7	69,8
800	0,71	22,7	70,4	0,69	23,1	70,4	0,64	23,1	70,0
675	0,59	23,3	70,5	0,57	23,7	70,6	0,56	23,6	70,1
550	0,45	24,0	70,7	0,44	24,3	70,7	0,43	24,3	70,3
425	0,33	24,9	70,5	0,30	25,2	70,7	0,26	25,2	70,1
300	0,23	26,1	70,3	0,13	26,5	70,3	0,13	26,5	69,8
175	0,15	27,7	70,0	0,03	28,3	70,0	0,09	28,3	69,5
50		29,0	69,8		30,9	69,6		30,5	69,3
0			69,7			69,4			69,1

TABLE A1

Experimental Data (Continued)

Run No.	27			28			29		
Fluid	Molasses			Molasses			Molasses		
Inlet velocity (m/s)	0,079			0,063			0,046		
Brix	79,90			79,90			79,90		
Dry substance	74,25			74,25			74,25		
Purity	41,24			41,24			41,24		
Surface tension (N/m)	0,0949			0,0949			0,0949		
Viscosity constants									
A =	1,052E-011			1,052E-011			1,052E-011		
B =	8279			8279			8279		
Flow behaviour index	,932			,932			,932		
Steam pressure (kPa-abs.)	130			132			136		
Vacuum (kPa-abs.)	27,5			27,5			27,5		
Condensate (kg/h)	20,39			21,07			21,10		
Tube length (mm)	Void	Press kPa	Temp. C	Void	Press kPa	Temp. C	Void	Press kPa	Temp. C
1300	0,87	27,5	76,3	0,82	27,5	76,2	0,83	27,5	76,2
1175	0,82	28,1	76,5	0,78	28,2	76,4	0,83	28,3	76,4
1050	0,78	28,5	76,7	0,75	28,5	76,5	0,83	28,8	76,5
925	0,75	29,1	76,8	0,72	29,2	76,7	0,81	29,2	76,7
800	0,66	29,7	77,0	0,60	30,0	76,8	0,71	29,6	76,8
675	0,49	30,5	77,2	0,52	33,0	77,0	0,58	30,1	77,0
550	0,38	31,4	77,3	0,35	31,7	77,1	0,45	30,6	77,1
425	0,23	32,6	77,0	0,27	32,5	77,1	0,30	31,4	77,2
300	0,13	34,0	76,8	0,18	33,0	76,8	0,19	32,5	76,8
175	0,05	35,7	76,6	0,08	35,3	76,6	0,14	33,9	76,4
50		37,4	76,4		36,7	76,4		34,9	76,0
0			76,3			76,3			75,8

TABLE A1

Experimental Data (Continued)

Run No.	30			31			32			33		
Fluid	Syrup			Syrup			Syrup			Syrup		
Inlet velocity (m/s)	0,079			0,063			0,046			0,079		
Brix	71,40			71,40			71,40			71,40		
Dry substance	71,40			71,40			71,40			71,40		
Purity	100,00			100,00			100,00			100,00		
Surface tension (N/m)	0,0711			0,0711			0,0711			0,0711		
Viscosity constants												
A =	2,294E-009			2,294E-009			2,294E-009			2,294E-009		
B =	5642			5642			5642			5642		
Flow behaviour index	1,000			1,000			1,000			1,000		
Steam pressure (kPa-abs.)	100			100			100			108		
Vacuum (kPa-abs.)	12,5			13,0			12,5			21,0		
Condensate (kg/h)	29,94			30,23			28,90			28,09		
Tube length (mm)	Void	Press kPa	Temp. C	Void	Press kPa	Temp. C	Void	Press kPa	Temp. C	Void	Press kPa	Temp. C
1300	0,91	12,5	54,2	0,76	13,0	54,5	0,78	12,5	53,1	0,82	21,0	65,1
1175	0,83	12,9	54,5	0,74	13,3	54,9	0,75	12,9	53,7	0,81	21,3	65,5
1050	0,76	13,4	54,8	0,72	13,6	55,3	0,72	13,3	54,2	0,80	21,6	66,0
925	0,71	14,1	55,1	0,70	14,2	55,7	0,67	13,8	54,8	0,76	22,2	66,4
800	0,52	15,1	55,4	0,58	15,0	56,1	0,56	14,6	55,4	0,66	23,1	66,8
675	0,29	16,2	55,7	0,51	16,0	56,5	0,39	15,6	55,9	0,45	24,2	67,2
550	0,17	17,6	55,2	0,25	17,3	56,7	0,19	16,8	56,5	0,27	25,5	67,0
425	0,14	19,1	54,7	0,15	18,8	56,0	0,10	18,3	56,5	0,17	27,0	66,6
300	0,08	20,8	54,2	0,13	20,7	55,3	0,08	20,0	55,6	0,13	28,7	66,2
175	0,08	22,6	53,7	0,10	22,7	54,6	0,08	21,9	54,7	0,12	30,4	65,8
50		25,3	53,1		24,5	53,8		23,9	53,8		32,5	65,4
0			52,9			53,6			53,4			65,2

TABLE A1

Experimental Data (Continued)

Run No.	34			35			36			37		
Fluid	Syrup			Syrup			Syrup			Syrup		
Inlet velocity (m/s)	0,063			0,046			0,079			0,063		
Brix	71,40			71,40			71,40			71,40		
Dry substance	71,40			71,40			71,40			71,40		
Purity	100,00			100,00			100,00			100,00		
Surface tension (N/m)	0,0711			0,0711			0,0711			0,0711		
Viscosity constants												
A =	2,294E-009			2,294E-009			2,294E-009			2,294E-009		
B =	5642			5642			5642			5642		
Flow behaviour index	1,000			1,000			1,000			1,000		
Steam pressure (kPa-abs.)	100			110			122			121		
Vacuum (kPa-abs.)	21,0			21,0			27,0			27,0		
Condensate (kg/h)	27,74			28,45			25,67			25,40		
Tube length (mm)	Void	Press kPa	Temp. C	Void	Press kPa	Temp. C	Void	Press kPa	Temp. C	Void	Press kPa	Temp. C
1300	0,82	21,0	64,9	0,82	21,0	64,6	0,80	27,0	71,1	0,82	27,0	71,0
1175	0,82	21,3	65,3	0,79	21,4	65,0	0,80	27,5	71,4	0,79	27,3	71,2
1050	0,82	21,8	65,6	0,76	21,8	65,4	0,79	28,0	71,7	0,77	27,8	71,5
925	0,80	22,4	66,0	0,71	22,4	65,7	0,78	28,7	71,9	0,74	28,4	71,7
800	0,72	23,2	66,4	0,67	23,1	66,1	0,66	29,5	72,2	0,66	29,2	71,9
675	0,52	24,2	66,7	0,56	24,0	66,4	0,52	30,4	72,4	0,53	30,3	72,2
550	0,31	25,4	67,1	0,34	25,2	66,8	0,36	31,5	72,7	0,34	31,4	72,4
425	0,18	26,8	66,8	0,18	26,5	67,1	0,21	32,8	72,5	0,23	32,6	72,6
300	0,13	28,4	66,4	0,08	28,1	66,5	0,16	34,2	72,1	0,15	33,9	72,2
175	0,10	30,2	65,9	0,08	29,8	65,8	0,12	35,9	71,7	0,13	35,3	71,6
50		32,2	65,5		32,0	65,1		37,4	71,4		36,1	71,0
0			65,3			64,9			71,2			70,7

TABLE A1

Experimental Data (Continued)

Run No.	38			39			40			41		
Fluid	Syrup			C-seed			C-seed			C-seed		
Inlet velocity (m/s)	0,046			0,046			0,071			0,096		
Brix	71,40			87,20			87,20			87,20		
Dry substance	71,40			84,08			84,08			84,08		
Purity	100,00			55,76			55,76			55,76		
Surface tension (N/m)	0,0711			0,2220			0,2220			0,2220		
Viscosity constants												
A =	2,294E-009			9,991E-011			9,991E-011			9,991E-011		
B =	5642			8023			8023			8023		
Flow behaviour index	1,000			0,904			0,904			0,904		
Steam pressure (kPa-abs.)	125			148			145			147		
Vacuum (kPa-abs.)	27,0			9,4			9,4			9,4		
Condensate (kg/h)	25,87			14,02			15,83			13,29		
Tube length (mm)	Void	Press kPa	Temp. C	Void	Press kPa	Temp. C	Void	Press kPa	Temp. C	Void	Press kPa	Temp. C
1300	0,76	27,0	71,0	0,79	9,4	53,7	0,86	9,4	52,2	0,85	9,4	52,8
1175	0,76	27,5	71,3	0,67	10,3	53,9	0,73	9,7	52,7	0,70	10,0	53,5
1050	0,76	27,9	71,5	0,55	11,8	54,1	0,60	10,3	53,3	0,56	10,8	54,2
925	0,72	28,5	71,8	0,26	13,6	54,3	0,38	11,4	53,8	0,33	11,9	54,1
800	0,65	29,3	72,0	0,16	15,7	54,4	0,22	12,7	53,7	0,22	13,4	53,7
675	0,55	30,2	72,3	0,13	17,8	54,0	0,16	14,2	53,4	0,15	15,0	53,4
550	0,38	31,3	72,6	0,12	19,8	53,7	0,14	16,0	53,0	0,11	16,8	53,0
425	0,20	32,6	72,8	0,10	21,7	53,4	0,12	17,9	52,7	0,08	18,7	52,7
300	0,14	33,9	72,4	0,05	23,1	53,0	0,07	19,8	52,4	0,05	20,5	52,3
175	0,09	35,4	72,0	0,03	24,0	52,7	0,05	21,9	52,0	0,04	22,2	51,9
50		37,5	71,6		26,9	52,3		22,5	51,7		24,9	51,6
0			71,4			52,2			51,6			51,4

TABLE A1

Experimental Data (Continued)

Run No.	42			43			44			45		
Fluid	C-seed			C-seed			C-seed			C-seed		
Inlet velocity (m/s)	0,121			0,046			0,071			0,096		
Brix	87,20			87,20			87,20			87,20		
Dry substance	84,08			84,08			84,08			84,08		
Purity	55,76			55,76			55,76			55,76		
Surface tension (N/m)	0,2220			0,2220			0,2220			0,2220		
Viscosity constants												
A =	9,991E-011			9,991E-011			9,991E-011			9,991E-011		
B =	8023			8023			8023			8023		
Flow behaviour index	0,904			0,904			0,904			0,904		
Steam pressure (kPa-abs.)	148			159			157			152		
Vacuum (kPa-abs.)	9,4			22,5			26,0			16,0		
Condensate (kg/h)	14,54			6,89			6,24			11,94		
Tube length (mm)	Void	Press kPa	Temp. C	Void	Press kPa	Temp. C	Void	Press kPa	Temp. C	Void	Press kPa	Temp. C
1300	0,81	9,4	52,3	0,29	22,5	73,5	0,20	26,0	76,9	0,81	16,0	64,2
1175	0,66	9,7	53,2	0,21	25,2	73,7	0,15	27,4	77,0	0,56	17,4	64,4
1050	0,52	10,4	54,0	0,14	25,7	73,6	0,10	28,7	76,9	0,32	18,3	64,6
925	0,34	11,6	53,9	0,10	26,7	73,5	0,07	30,2	76,8	0,21	19,5	64,8
800	0,24	13,0	53,7	0,08	32,6	73,5	0,07	31,8	76,9	0,17	20,9	64,7
675	0,19	14,7	53,5	0,08	30,4	73,4	0,06	33,6	76,9	0,11	22,5	64,6
550	0,15	16,6	53,3	0,08	31,8	73,5	0,06	35,5	76,9	0,08	24,1	64,4
425	0,12	18,5	53,0	0,07	34,5	73,5	0,05	37,4	76,9	0,07	25,9	64,3
300	0,08	20,3	52,8	0,05	37,1	73,5	0,05	39,4	76,9	0,05	27,7	64,2
175	0,06	22,0	52,6	0,04	37,9	73,5	0,04	41,4	76,9	0,04	29,6	64,1
50		24,7	52,4		38,9	73,5		43,7	76,9		30,8	64,0
0			52,3			73,5			76,9			63,9

TABLE A1

Experimental Data (Continued)

Run No.	46			47			48			49		
Fluid	C-seed			C-seed			C-seed			C-seed		
Inlet velocity (m/s)	0,046			0,071			0,096			0,121		
Brix	87,20			87,20			87,20			87,20		
Dry substance	80,82			80,82			80,82			80,82		
Purity	60,06			60,06			60,06			60,06		
Surface tension (N/m)	0,1880			0,1880			0,1880			0,1880		
Viscosity constants												
A =	9,991E-011			9,991E-011			9,991E-011			9,991E-011		
B =	8023			8023			8023			8023		
Flow behaviour index	0,904			0,904			0,904			0,904		
Steam pressure (kPa-abs.)	158			154			152			153		
Vacuum (kPa-abs.)	17,3			17,0			17,0			17,0		
Condensate (kg/h)	8,24			10,77			10,49			11,59		
Tube length (mm)	Void	Press kPa	Temp. C	Void	Press kPa	Temp. C	Void	Press kPa	Temp. C	Void	Press kPa	Temp. C
1300	0,85	17,3	64,5	0,81	17,0	64,4	0,81	17,0	64,7	0,72	17,0	64,9
1175	0,59	18,3	64,7	0,65	17,9	64,7	0,67	18,1	64,9	0,61	18,6	65,2
1050	0,34	19,3	64,9	0,49	18,9	64,9	0,53	19,2	65,1	0,49	19,9	65,5
925	0,16	20,6	65,1	0,33	19,9	65,2	0,36	20,3	65,3	0,34	21,0	65,9
800	0,07	22,2	65,1	0,22	21,1	65,5	0,29	21,5	65,5	0,22	22,1	65,7
675	0,04	24,0	65,0	0,14	22,3	65,7	0,17	22,8	65,4	0,14	23,2	65,4
550	0,05	25,9	64,8	0,08	23,7	66,0	0,10	24,3	65,2	0,07	24,4	65,2
425	0,03	28,1	64,7	0,04	25,2	66,3	0,07	25,9	65,0	0,04	25,8	64,9
300	0,02	30,3	64,5	0,04	27,0	66,1	0,04	27,6	64,8	0,04	27,6	64,6
175	0,02	32,7	64,4	0,02	28,9	65,9	0,03	29,6	64,6	0,04	29,9	64,3
50		35,7	64,2		30,6	65,7		29,8	64,3		32,7	64,0
0			64,1			65,6			64,3			63,9

TABLE A1

Experimental Data (Continued)

Run No.	50			51			52			53		
Fluid	Molasses			Molasses			Molasses			Molasses		
Inlet velocity (m/s)	0,046			0,071			0,096			0,121		
Brix	81,00			81,00			81,00			81,00		
Dry substance	75,40			75,40			75,40			75,40		
Purity	38,75			38,75			38,75			38,75		
Surface tension (N/m)	0,1120			0,1120			0,1120			0,1120		
Viscosity constants												
A =	1,052E-011			1,052E-011			1,052E-011			1,052E-011		
B =	8279			8279			8279			8279		
Flow behaviour index	,932			,932			,932			,932		
Steam pressure (kPa-abs.)	114			114			114			114		
Vacuum (kPa-abs.)	15,0			15,0			15,0			15,0		
Condensate (kg/h)	24,85			22,25			22,83			25,14		
Tube length (mm)	Void	Press kPa	Temp. C	Void	Press kPa	Temp. C	Void	Press kPa	Temp. C	Void	Press kPa	Temp. C
1300	0,86	15,0	60,6	0,85	15,0	61,4	0,86	15,0	61,6	0,83	15,0	61,6
1175	0,83	15,4	60,8	0,85	15,9	61,9	0,85	15,2	61,9	0,83	16,0	61,9
1050	0,80	15,7	61,0	0,85	16,4	62,0	0,83	15,4	62,2	0,83	16,9	62,1
925	0,77	16,0	61,3	0,79	16,8	62,2	0,81	15,9	62,4	0,74	17,7	62,4
800	0,72	16,3	61,5	0,74	17,1	62,5	0,72	16,7	62,7	0,60	18,5	62,6
675	0,72	16,8	61,8	0,63	17,6	62,8	0,55	17,3	63,0	0,42	19,3	62,8
550	0,62	17,3	62,0	0,49	18,2	62,7	0,39	18,8	63,3	0,27	20,1	62,6
425	0,40	18,0	62,2	0,28	19,1	62,4	0,23	20,1	63,0	0,18	21,1	62,3
300	0,24	18,8	61,8	0,17	20,3	62,2	0,14	21,5	62,6	0,14	22,3	62,1
175	0,18	19,8	61,3	0,15	21,9	61,9	0,13	23,0	62,2	0,11	23,7	61,9
50		21,7	60,9		23,8	61,7		24,7	61,8		25,0	61,6
0			60,7			61,6			61,6			61,5

TABLE A1

Experimental Data (Continued)

Run No.	54			55			56			57		
Fluid	Molasses			Molasses			Molasses			Molasses		
Inlet velocity (m/s)	0,046			0,071			0,096			0,121		
Brix	81,00			81,00			81,00			81,00		
Dry substance	74,94			74,94			74,94			74,94		
Purity	38,71			38,71			38,71			38,71		
Surface tension (N/m)	0,1050			0,1050			0,1050			0,1050		
Viscosity constants												
A =	1,052E-011			1,052E-011			1,052E-011			1,052E-011		
B =	8279			8279			8279			8279		
Flow behaviour index	,932			,932			,932			,932		
Steam pressure (kPa-abs.)	121			121			122			122		
Vacuum (kPa-abs.)	22,0			22,0			22,0			22,0		
Condensate (kg/h)	20,81			21,10			21,96			21,19		
Tube length (mm)	Void	Press kPa	Temp. C	Void	Press kPa	Temp. C	Void	Press kPa	Temp. C	Void	Press kPa	Temp. C
1300	0,81	22,0	69,6	0,83	22,0	70,0	0,82	22,0	69,6	0,82	22,0	70,0
1175	0,80	22,2	69,6	0,80	22,3	70,2	0,79	22,2	69,8	0,78	22,1	70,3
1050	0,80	22,3	69,8	0,77	22,5	70,4	0,76	22,4	70,0	0,74	22,4	70,6
925	0,79	22,7	70,0	0,76	22,8	70,6	0,72	22,8	70,5	0,68	22,9	70,3
800	0,70	23,2	70,2	0,66	23,2	70,8	0,62	23,3	70,6	0,55	23,7	69,5
675	0,62	23,8	70,4	0,59	23,7	71,1	0,47	24,0	70,8	0,38	24,6	69,2
550	0,51	24,7	70,8	0,43	24,5	71,1	0,35	24,8	70,7	0,27	25,8	68,9
425	0,35	25,7	70,9	0,31	25,4	70,8	0,20	25,8	70,6	0,18	27,2	68,9
300	0,22	26,9	70,8	0,19	26,6	70,4	0,16	27,0	70,2	0,11	28,6	68,8
175	0,15	28,4	70,5	0,13	28,0	70,1	0,08	28,3	69,9	0,07	30,3	68,7
50		30,2	69,9		29,5	69,8		30,1	69,6		32,0	68,6
0			69,6			69,5			69,2			68,6

APPENDIX B

Methods and equations used for physical properties of fluids and vapour

B.1. Density

The brix of the liquids used was measured using a refractometer as is the normal practice in the sugar industry (Laboratory Manual for South African Sugar Factories, 1977). The density was calculated using the following correlation developed from brix - specific gravity tables given by Spencer and Meade (1948) and density tables given by Perry and Chilton (1973).

$$\rho_f = 938,8 + 6,298 \text{ brix} - 0,8365 \text{ t} \qquad \text{(B.1)}$$

where t is the temperature

Since the brix increases along the tube because of evaporation a correction is necessary. It is done using the equation

$$\text{brix}_2 = \text{brix}_1 / (1 - x)$$

where x is the mass vapour quality.

B.2. Dry substance and purity

The dry substance was determined by vacuum oven using the standard procedure (Anon 1977). The purity was based on chemical sucrose analysis.

B.3. Rheological properties

The rheological properties were obtained using a

Brookfield HBT rotating cylinder viscometer with a cylindrical spindle which is shown in Figure B.1. Torque and speed were measured starting from the highest speed, and using all speeds that gave a reading on the instrument's scale. Where the rheological properties were time dependent, the readings were made only after the indicator had settled to a constant value on the instrument scale.

The shear rate was calculated from the equation

$$\frac{du}{dr} = \frac{5{,}75 \times 10^{-3} s}{200 \pi r^2 L} \qquad \text{(B.2a)}$$

where s = % scale reading
r = spindle radius
L = spindle length

The shear stress at the surface of the rotating cylinder was obtained by

$$\tau = \frac{4 \pi N}{n} \qquad \text{(B.2b)}$$

where N = rotational speed
n = flow behaviour index given by slope of log-log plot of torque versus speed

The consistency was obtained as the intercept from a plot of the shear rate versus the shear stress on logarithmic coordinates.

The determinations were repeated at different temperatures and expressed by the equation

$$K = a.e^{b/T} \qquad \text{(B.2c)}$$

where K = consistency

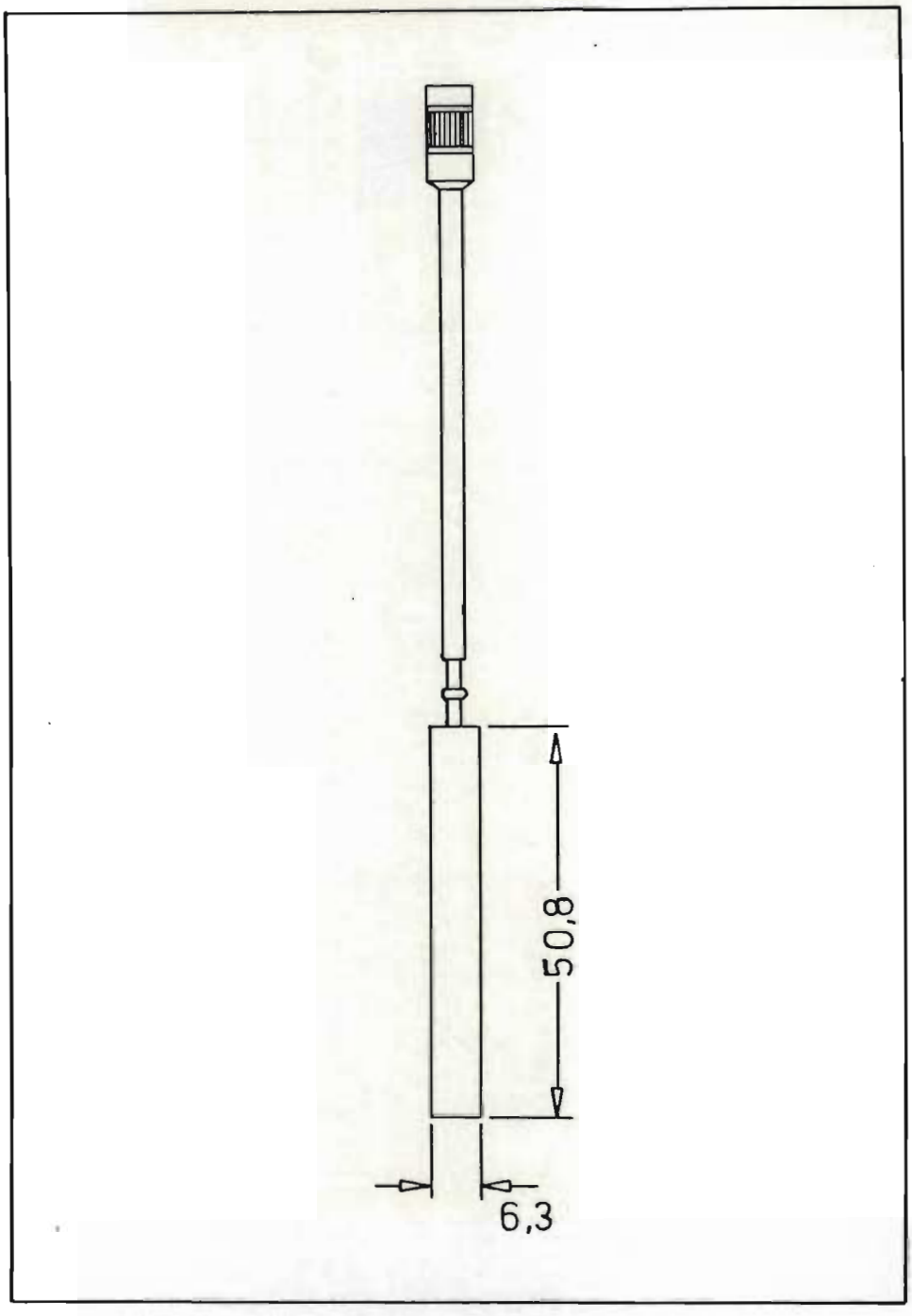

Figure B.1. Cylindrical spindle used for measuring rheological properties

a and b = constants

T = temperature, °K.

B.4. Boiling point elevation

The boiling temperature was calculated using the method of Batterham and Norgate (1975).

$$t = t_s + At_o + B + C \qquad (B.3)$$

where $A = 0{,}3604 - 2{,}5681 \times 10^{-2} d + 6{,}8488 \times 10^{-4} d^2 - 8{,}0158 \times 10^{-6} d^3 + 3{,}5601 \times 10^{-8} d^4$ (B.4)

$$B = 50{,}84 - 3{,}516\, d + 9{,}122 \times 10^{-2} d^2 - 1{,}0492 \times 10^{-3} d^3 + 4{,}611 \times 10^{-6} d^4 \qquad (B.5)$$

$$C = -0{,}272 - 2{,}27 \times 10^{-2} P + 2{,}542 \times 10^{-4} P^2 + 5{,}311 \times 10^{-4}.d.(100 - P) \qquad (B.6)$$

where d is the dry substance and P is the purity.

B.5. Surface tension

The surface tension was measured by the ring method of Du Nouy as described in Brown and Zerban (1941). The surface tension was calculated from the equation

$$\sigma = \frac{Mg}{2L} \qquad (B.7)$$

where M is the mass equalising the pull on the ring and L the mean circumference of the ring

B.6. Specific heat

The specific heat of the fluid was calculated using the equation of Janovskii and Archangelskii (1928)

as reported by Kadlec et al. (1981).

$$\left.\begin{aligned} a &= 41868 - d(0{,}0297 - 4{,}6 \times 10^{-5}p) \\ b &= 7{,}5 \times 10^{-5}d \\ cp &= a + bt \end{aligned}\right\} \quad (B.8)$$

where d = dry substance
p = purity
t = temperature °C

B.7. Thermal conductivity

This property of the fluid was calculated using the following equations

$$k = Ad + B$$

where

d = dry substance
$A = t(5{,}466 \times 10^{-8}\ t - 1{,}176 \times 10^{-5}) - 0.003024$
$B = t(0.001976 - 7.847 \times 10^{-6}t) + 0.563$
t = temperature °C

These equations are based on the data of Bosworth (1947).

B.8. Physical properties of steam and vapour

The physical properties of steam and vapour were calculated using the equations proposed by Genotelle (1980).

B.8.1. Specific volume of vapour

The specific volume of vapour was calculated from the temperature and pressure observed at each measuring level. The vapour saturation temperature was first obtained by trial and error using the relations.

$$A = 12{,}7 + \left[\frac{374 - t_s}{339{,}6}\right] 2{,}174 \quad (B.9)$$

and

$$t_s = \frac{99,63 + 273\ Ln(p)/A}{1 - Ln(p)/A} \qquad (B.10)$$

where ts is the saturation temperature and p the pressure.

The specific volume at the saturation temperature was obtained from

$$v_s = \left[4,622 - \left(\frac{T_s}{536,8}\right)^{5,835}\right] \frac{t_s}{10p} \qquad (B.11)$$

However, because superheated vapour is present in the tube as a result of the boiling point elevation, the specific volume must be corrected for the superheat and is obtained from

$$v = v_s \left[1 + \left(\frac{T - T_s}{T_s}\right) \left(1,03 + \frac{p}{0,743}\right)\right] \qquad (B.12)$$

where T and Ts are the vapour and saturation temperatures respectively, °K.

B.8.2. Enthalpy of vapour

The enthalpy per unit mass of vapour at any point along the tube was obtained in the following manner:

The enthalpy of the dry saturated vapour was calculated from the equation

$$i_g = 658,4 + 0,5903\ t_s - 27932/(455 - t_s) \times 4186.8 \qquad (B.13)$$

The specific heat of the vapour caused by the superheat was

$$cp_g = \left(\frac{1}{1 + \frac{1}{12,2p}} \left[0,485 + (p+6) \frac{0,88}{\Delta t+90} \right] \right) 4186.8 \qquad (B.14)$$

and the enthalpy of condensate

$$i_f = \left[0,9984 + 0,2425 \, (p/t_s) \right] \times 4186.8 \qquad (B.15)$$

The change in enthalpy during condensation was obtained by combining equations (B.13), (B.14) and (B.15)

$$i_{fg} = \left[i_f + cp \, (t-t_s) - i_g \right] \qquad (B.16)$$

B.8.3. Enthalpy of condensation of steam

The enthalpy of condensation of steam was calculated from

$$t_s = (1168,4 + 228,42 \ln(p/100))/(11,727 - \ln(p/100)) \qquad (B.17)$$

$$i_{fg} = 600,54 - 0,6093 \, t_s - 9,576 \cdot 10^{-3} p \qquad (B.18)$$

APPENDIX C

Computer Program for Calculation of Circulation

```
10 ! ....THIS PROGRAM CALCULATES THE CIRCULATION IN A VACUUM
20 ! ....PAN GIVEN PAN SPECIFICATIONS, OPERATING CONDITIONS AND
30 ! ....PHYSICAL PROPERTES OF MASSECUITE
40 OPTION BASE 0
50 DIM A0(14),A1(14),C(14),D(14),I3(14),P(14),PA(14),PE(14),PF(1
4),T(14),T0(14),V(14),V0(14),X0(14),X1(14),D0(14),T1(14),T2(14),
C0(14)
60 DIM R5(14),P3(14),HF(14),U0(14),Q(14),QS(14),DT(14),HFS(14),U
1(14),A02(14),T3(14),HSP(14)
70 ! ******SYSTEM GEOMETRY******
80 ! ......NUMBER OF TUBES......
90 NTUBE=4
100 ! ......TUBE LENGTH (M)......
110 L=.6
120 ! ......INT. TUBE DIAM. (M)......
130 D0=.0984
140 ! ......EXT. TUBE DIAM. (M)......
150 D3=.1016
160 ! ......THERMAL CONDUCTIVITY TUBE (W/M.C)......
170 K3=45
180 ! ......PAN DIAMETER (M)......
190 DPAN=.9144
200 ! ......DOWNTAKE DIAMETER (M)......
210 DDOWN=.3048
220 ! ******FLUID PROPERIES******
230 ! ......DRY SUBSTANCE MOTHER LIQUOR......
240 D1=86.06
250 ! ......PURITY MOTHER LIQUOR......
260 P0=49.33
270 ! ......DRY SUBSTANCE MASSECUITE......
280 B1=91.66
290 ! ......RHEOLOGICAL CONSTANTS MASSECUITE......
300 A=.000000115
310 B=7050
320 N=.712
330 ! ......SURFACE TENSION......
340 S=.779
350 ! *****OPERATING CONDITIONS*****
360 ! ......STEAM PRESSURE (KPA)......
370 P2=130
380 ! ......PRESSURE IN VAPOUR SPACE......
390 PVAP=20
400 ! ......LEVEL ABOVE UPPER TUBE SHEET (M)......
410 HEAD=.25
420 ! ......NUMBER OF TUBE SUBDIVISIONS REQUIRED......
430 N0=10
440 ! ******CALCULATE STEAM CONDITIONS******
450 GOSUB 4320
460 ! ******SATURATION TEMPERATURE AT SURFACE******
470 T=65
```

```
480 A1=12.7+((374+T)/339.6)^2.174
490 T1(1)=(99.63+273*LOG (PVAP/100)/A1)/(1-LOG (PVAP/100)/A1)
600 IF ABS (T1(1)-T)<.01 THEN 620
610 T=T1(1) @ GOTO 480
620 D2=D1 @ GOSUB 4230
630 T(1)=T1(1)+A2*T1(1)+B0+C0
640 BPE=T(1)-T1(1)
650 ! ******HYDROSTATIC HEAD******
660 D(1)=938.8375+6.298*B1-.8365*T(1)
670 PHYDRO=D(1)*HEAD*.00980665
680 P(N0+1)=PVAP+PHYDRO
690 ! *******CLEAR ARRAYS*******
700 FOR I=1 TO N0
710 C0(I)=.00000001
720 NEXT I
730 FOR I=1 TO N0+1
740 A0(I),A1(I),X0(I),X1(I),V0(I)=0
750 T3(I)=T(1)
760 NEXT I
770 C(N0+1)=1.E-15
780 ! ******MAX. TEMP. PER SUBDIVISION******
790 FOR I=2 TO N0+1
800 T(I)=T(1)
810 NEXT I
820 ! ******ASSUME INNER TUBE TEMPERATURE******
830 FOR I=1 TO N0+1
840 I3(I)=T3-3
850 NEXT I
860 ! ******ASSUME TUBE INLET VELOCITY******
870 V=.005
880 ITER=0
890 A0=PI *D0^2/4
900 V0=V*A0 @ COUN=0
910 G=V*D(1) @ W=G*A0
920 ! ******ENTRANCE LOSS DOWNTAKE******
930 A0D=PI /4*DDOWN^2
940 V0D=V0*NTUBE
950 VD=V0D/A0D
960 IDLOSS=.4*(1.25-(DDOWN/DPAN)^2)*.00980665*VD^2*D(1)/(2*9.793
)
970 ! ******FRICTION LOSS DOWNTAKE******
980 K=A*EXP (B/(T(1)+273.15))
990 R5=DDOWN^N*VD^(2-N)*D(1)*8*(N/(6*N+2))^N/K
1000 DOHEAD=L*D(1)*.00980665
1010 FDLOSS=32*L*VD^2*D(1)*.00980665/(DDOWN*R5*9.793)
1020 ! ******EXIT LOSS DOWNTAKE******
1030 AFAC=V0D^2*D(1)*.00980665/9.793*(3*N+1)/(2*N+1)
1040 EDLOSS=AFAC*((N+3)/(2*(5*N+3))*(DDOWN/DPAN)^4-(DDOWN/DPAN)^
2+3*(3*N+1)/(2*(5*N+3)))
1050 ! ******ENTRANCE LOSS TUBE******
1060 ITLOSS=.5*V^2*D(1)*.00980665/(2*9.793)
1070 GOSUB 2510
1090 REM *****TUBE EXIT LOSSES*****
1100 VOUT=Q4/(A0*(1-A0(N0+1)))
1110 AFAC=VOUT^2*D(N0+1)*.00980665/9.793*(3*N+1)/(2*N+1)
1120 ETLOSS=AFAC*((N+3)/(2*(5*N+3))*(A0*NTUBE/(DPAN^2*PI /4))^2-
A0*NTUBE/(DPAN^2*PI /4)+3*(3*N+1)/(2*(5*N+3)))
```

```
1130 O,ATLOSS,FTLOSS=0
1140 FOR I=1 TO N0
1150 O=O+PE(I)
1160 ATLOSS=ATLOSS+PA(I)
1170 FTLOSS=FTLOSS+PF(I)
1180 NEXT I
1190 FORCE=DOHEAD+O
1200 RESIST=IDLOSS+FDLOSS+EDLOSS+ITLOSS+FTLOSS+ATLOSS+ETLOSS
1210 ITER=ITER+1
1220 IF ITER=5 THEN 1260
1230 IF ABS (FORCE-RESIST)<.01*FORCE THEN 1260
1240 PRINT "FORCE=";FORCE;"RESISTANCE=";RESIST
1250 V=V*FORCE/RESIST @ GOTO 900
1260 PRINTER IS 701,132
1270 PRINT
1280 PRINT "OPERATING CONDITIONS" @ PRINT
1290 PRINT USING 1295 ; B1
1295 IMAGE "BRIX",37X,DD.DD
1300 PRINT USING 1305 ; P0
1305 IMAGE "PURITY",35X,DD.DD
1310 PRINT USING 1315 ; S
1315 IMAGE "SURFACE TENSION (N/m)",21X,Z.4D
1320 PRINT USING 1325 ; P2
1325 IMAGE "STEAM PRESSURE (kPa)",20X,3D.D
1340 PRINT USING 1345 ; PVAP
1345 IMAGE "VAPOUR PRESSURE (kPa)",20X,2D.D
1350 PRINT USING 1355 ; HEAD
1355 IMAGE "HEAD (m)",34X,Z.DD
1360 PRINT USING 1365 ; D0
1365 IMAGE "TUBE DIAMETER (m)",25X,Z.4D
1380 PRINT USING 1385 ; L
1385 IMAGE "TUBE LENGTH (m)",27X,Z.DD
1390 PRINT USING 1395 ; V0/A0
1395 IMAGE "TUBE INLET VELOCITY (m/s)",17X,Z.3D
1400 PRINT USING 1405 ; C(1)*3600
1405 IMAGE "CONDENSATE (l/h)",25X,DZ.3D
1410 EVAP=C(1)*3600/(PI *D0*L)
1420 PRINT USING 1425 ; EVAP
1425 IMAGE "EVAPORATION (kg/m^2.h)",19X,DZ.3D
1430 PRINT USING 1435 ; BPE
1435 IMAGE "BOILING POINT ELEVATION (C)",14X,DZ.DD
1437 PRINT
1440 PRINT "CONDITIONS ALONG BOILING TUBE"
1450 PRINT USING 1460
1460 IMAGE 8("------------")
1470 PRINT "     TUBE          VOID       PRESSURE        TEMP.     SP.
 VOLUME     QUALITY      DENSITY   CONSISTENCY"
1480 PRINT " LENGTH (mm)  FRACTION        (kPa)          (C)       (m
^3/kg)                  (kg/m^3)"
1490 PRINT USING 1460
1500 FOR I=N0+1 TO 1 STEP -1
1520 K1=A*EXP (B/(T(I)+273.15))
1530 PRINT USING 1540 ; L/N0*(I-1)*1000,A0(I),P(I),T(I),V(I),X0(
I),D(I),K1
1540 IMAGE 4X,4D,7X,Z.4D,3(7X,DD.2D),5X,D.2DE,4X,4D.D,6X,4D.D
1550 NEXT I
1560 PRINT USING 1460
1570 PRINT
```

```
1580 PRINT "PRESSURE DROPS (kPa)"
1590 PRINT "-------------------------------------------------------"
1600 PRINT "  EL          ACC        FRIC.     TOTAL      RE. NUM"
1610 PRINT "-------------------------------------------------------"
1620 O,O0,O1,O2,O3=0
1630 FOR I=N0 TO 1 STEP -1
1640 PRINT USING 1650 ; PE(I),PA(I),PF(I),PE(I)+PA(I)+PF(I),R5(I
+1)
1650 IMAGE 4(DZ.3D,4X),D.DDE
1660 O=O+PE(I)
1670 O0=O0+PA(I)
1680 O1=O1+PF(I)
1690 O2=O2+PE(I)+PA(I)+PF(I)
1700 O3=O3+R5(I+1)
1710 NEXT I
1720 PRINT "-------------------------------------------------------"
1730 PRINT USING 1650 ; O,O0,O1,O2,O3/N0
1740 PRINT "-------------------------------------------------------"
1745 PRINT
1750 PRINT USING 1755 ; IDLOSS
1755 IMAGE "ENTRANCE LOSS DOWNTAKE",21X,Z.5D
1760 PRINT USING 1765 ; FDLOSS
1765 IMAGE "FRICTION LOSS DOWNTAKE",21X,Z.5D
1767 PRINT USING 1768 ; EDLOSS
1768 IMAGE "DOWNTAKE EXIT LOSS",25X,Z.5D
1770 PRINT USING 1775 ; ITLOSS
1775 IMAGE "ENTRANCE LOSS TUBE",25X,Z.5D
1780 PRINT USING 1785 ; FTLOSS
1785 IMAGE "FRICTION LOSS TUBE",24X,DZ.5D
1790 PRINT USING 1795 ; ATLOSS
1795 IMAGE "ACCELERATION LOSS TUBE",21X,Z.5D
1800 PRINT USING 1805 ; ETLOSS
1805 IMAGE "TUBE EXIT LOSS",29X,Z.5D
1810 PRINT @ PRINT @ PRINT @ PRINT @ PRINT @ PRINT
1820 PRINT @ PRINT @ PRINT
1830 PRINT "TEMPERATURES (C)"
1840 PRINT USING 1845
1845 IMAGE "-------------------------------------------------------
-------------------"
1850 PRINT "TUBE            SATURATED       SUPERHEATED         AVERA
GE       INSIDE TUBE"
1860 PRINT "LENGTH (mm)     VAPOUR            VAPOUR            LIQUI
D          SURFACE"
1870 PRINT USING 1845
1880 O,O0,O1,O2=0
1890 FOR I=N0+1 TO 1 STEP -1
1900 FLUX=U0(I)*(T3-T(I))
1910 PRINT USING 1920 ; L/N0*(I-1)*1000,T1(1),T2(I),T(I),I3(I)
1920 IMAGE 4D,4(11X,3D.D)
1930 O=O+T1(I)
1940 O0=O0+T2(I)
1950 O1=O1+T(I)
1960 IF I=1 THEN 1980
1970 O2=O2+I3(I)
1980 NEXT I
1990 PRINT USING 1845
2000 PRINT USING 2010 ; O/(N0+1),O0/(N0+1),O1/(N0+1),O2/N0
2010 IMAGE 4X,4(11X,3D.D)
```

```
2020 PRINT USING 1845
2030 PRINT USING 2035 ; T3
2035 IMAGE "STEAM TEMP.=",10X,3D.DD,"(C)"
2040 PRINT @ PRINT "VOID FRACTION PARAMETERS"
2050 PRINT "-----------------------------------------"
2060 PRINT "QG/VOID*A        (QG+QF)/A        RIS. VEL."
2070 PRINT "-----------------------------------------"
2080 FOR I=N0+1 TO 1 STEP -1
2090 Q3=V0*X0(I)*D(1)*V(I)
2100 Q4=V0*(1-X0(I))*D(1)/D(I)
2110 IF A0(I)=0 THEN 2130
2120 Q5=Q3/(A0(I)*A0) @ GOTO 2140
2130 Q5=0
2140 Q6=(Q3+Q4)/A0
2150 F1=1.53*(S*9.793*(D(I)-1/V(I))/D(I)^2)^.25
2160 PRINT USING 2170 ; Q5,Q6,F1
2170 IMAGE 2(2DZ.3D,9X),Z.4D
2180 NEXT I
2190 PRINT "-----------------------------------------"
2200 PRINT @ PRINT "HEAT TRANSFER PARAMETERS"
2210 PRINT "-----------------------------------------------------
---------------------"
2220 PRINT "TOTAL HEAT       SENSIBLE HEAT    FILM HTC          OVER
AL HTC        PRANDTL"
2230 PRINT "TRANSFERRED      TRANSFERRED      (W/m^2.C)         (W/m
^2.C)         NUMBER"
2240 PRINT "-----------------------------------------------------
---------------------"
2250 Q,Q0,Q1,Q2,Q3,Q4=0
2260 FOR I=N0 TO 1 STEP -1
2270 PRINT USING 2280 ; Q(I),QS(I),HF(I),U0(I),P3(I)
2280 IMAGE 4(5D.DD,8X),6D.DD
2290 Q=Q+Q(I)
2300 Q0=Q0+QS(I)
2310 Q1=Q1+HF(I)
2320 Q2=Q2+U0(I)
2330 Q3=Q3+P3(I)
2340 NEXT I
2350 PRINT "-----------------------------------------------------
---------------------"
2360 PRINT USING 2280 ; Q,Q0,Q1/N0,Q2/N0,Q3/N0
2370 PRINT "-----------------------------------------------------
---------------------"
2380 PRINT @ PRINT @ PRINT @ PRINT
2390 PRINT @ PRINT @ PRINT
2400 END
4100 ! ******SPECIFIC HEAT SUBROUTINE******
4110 A9=4.1868-D2*(.0297-.0000000046*P0)
4120 B9=.000075*D2
4130 C9=(A9+B9*T)*1000 @ RETURN
4140 ! ******THERMAL CONDUCTIVITY SUBROUTINE******
4150 A9=T1*(.00000005466*T1-.00001176)-.003024
4160 B9=T1*(-(.000007847*T1)+.001976)+.563
4170 K2=A9*D2+B9 @ RETURN
4180 ! ******CONDENSATE FILM HTC SUBROUTINE******
4190 A1=.5627+.0015*T
4200 U=.0013303-.000023714*T+.00000019127*T^2-5.8796E-10*T^3
```

```
4210 D6=1004.5-.1958*T-.002659*T^2 @ RETURN
4220 ! ******BOILING POINT ELEVATION SUBROUTINE******
4230 A2=.3604-.025681*D2+.00068488*D2^2-.0000080158*D2^3+.000000
035601*D2^4
4240 B0=50.84-3.516*D2+.09122*D2^2-.0010492*D2^3+.00000461l*D2^4

4250 C0=-.272-.0227*P0+.0002542*P0^2+.0005311*D2*(100-P0) @ RETU
RN
4260 ! ******VAPOUR & CONDENSATE ENTHALPY SUBROUTINE******
4270 H1=658.4+.5903*T1-27932/(455-T1)
4280 C0=1/(1+1/(12.2*P9))*(.485+(P9+6)*(.88/(T-T1+90)))
4290 H2=H1+C0*(T2-T1)
4300 H3=.9984*T1+.2425*P9 @ RETURN
4310 ! ******STEAM PROPERTIES SUBROUTINE******
4320 P9=P2/100
4330 T3=(1168.4+228.42*LOG (P9))/(11.727-LOG (P9))
4340 R=600.54-.6093*T3-.9576*P9 @ RETURN
```

Subroutine for Boiling Process

```
2410 ! ******BOILING SUBROUTINE******
2420 FOR I=2 TO N0+1
2430 PRINT I;"A02(I)";A02(I)
2440 A0(I)=A02(I)
2450 A1(I-1)=(A0(I-1)+A0(I))/2
2460 NEXT I
2470 FOR I=1 TO N0+1
2480 IF T2(I)>T(I) THEN 2500
2490 T(I)=T2(I)
2500 NEXT I
2510 ! ******AVG. TEMP. PER SUBDIVISION******
2520 FOR I=1 TO N0
2530 T0(I)=(T(I)+T(I+1))/2
2540 NEXT I
2550 ! ******FLUID DENSITY******
2560 FOR I=2 TO N0+1
2570 B2=B1/(1-X0(I))
2580 D(I)=938.8375+6.298*B2-.8365*T(I)
2590 NEXT I
2600 ! ******AVG FLUID DENSITY******
2610 FOR I=1 TO N0
2620 D0(I)=(D(I)+D(I+1))/2
2630 NEXT I
2640 FOR I=N0 TO 1 STEP -1
2650 C(I)=C0(I)+C(I+1)
2660 NEXT I
2670 ! ******ELEVATION LOSS******
2680 FOR I=1 TO N0
2690 IF V0(I) AND A1(I)>0 THEN 2720
2700 PE(I)=D0(I)*L/N0*.00980665
2710 GOTO 2730
2720 PE(I)=(A1(I)/V0(I)+D0(I)*(1-A1(I)))*L/N0*.00980665
2730 NEXT I
2740 !. ******ACCELERATION LOSS******
2750 FOR I=2 TO N0+1
2760 IF A0(I)>0 THEN 2780
2770 PA(I)=0 @ GOTO 2790
2780 PA(I)=G^2/D(I)*(X0(I)^2*D(1)*V(I)/A0(I)+((1-X0(I))/(1-A0(I)
))^2-1)*.00980665/9.793
2790 NEXT I
2800 PA(1)=0
2810 FOR I=2 TO N0+1
2820 PA(I-1)=PA(I)-PA(I-1)
2830 NEXT I
2840 ! ******FRICTION LOSS******
2850 FOR I=1 TO N0
2860 K0=A*EXP (B/((I3(I)+I3(1+1))/2+273.15))
2870 Q4=V0*(1-X1(I))*D(1)/D0(I)
2880 K1=A*EXP (B/(T0(I)+273.15))
2890 R5=D0^N*(Q4/(A0*(1-A1(I))))^(2-N)*D0(I)*8*(N/(6*N+2))^N/K1
2900 IF R5>1000 THEN 2930
2910 FRIC=16/R5
2920 GOTO 2940
```

```
2930 FRIC=3.81+.125*R5^.32
2940 PF(I)=L/N0*(04/(A0*(1-A1(I))))^2*D0(I)*2/(9.793*D0*1.1)*(K0
*2*(3*N-1)/(K1*(3*N+1)))^.25*9.80665/1000*FRIC
2950 NEXT I
2960 REM *****TOTAL PRESSURE*****
2970 FOR I=N0 TO 1 STEP -1
2980 P(I)=P(I+1)+PE(I)+PA(I)+PF(I)
2990 NEXT I
3000 ! ******SATURATION TEMPERATURES*****************************
*****
3010 T=T(1)
3020 FOR I=1 TO N0+1
3030 A1=12.7+((374-T)/339.6)^2.174
3040 T1(I)=(99.63+273*LOG (P(I)/100)/A1)/(1-LOG (P(I)/100)/A1)
3050 IF ABS (T1(I)-T)<.01 THEN 3070
3060 T=T1(I) @ GOTO 3030
3070 NEXT I
3080 ! ******BOILING POINT ELEVATION, SATURATION TEMPERATURES &
SPECIFIC VOLUME*********************
3090 FOR I=1 TO N0+1
3100 D2=D1/(1-X0(I)) @ GOSUB 4230
3110 T2(I)=T1(I)+A2*T1(I)+B0+C0
3120 T0=T1(I)+273.15
3130 V1=(4.662-(T0/536.8)^5.835)*T0/(P(I)*1000/100)
3140 T2=T2(I)+273.15
3150 V(I)=V1*(1+(T2-T0)/T0*(1.03+P(I)/100/74.3))
3160 NEXT I
3170 ! ******AVG. SPECIFIC VOLUME OF VAPOUR******
3180 FOR I=1 TO N0
3190 V0(I)=(V(I+1)+V(I))/2
3200 NEXT I
3210 TAG,00=0
3220 ! ******HTC IN BOILING SECTION******
3230 FOR I=1 TO N0+1
3240 D2=D1/(1-X1(I))
3250 GOSUB 4110
3260 T1=(T(I)+I3(I))/2
3270 GOSUB 4150
3280 K1=A*EXP (B/(T1+273.15))
3290 04=V0*(1-X0(I))*D(1)/D(I)
3300 R5(I)=D0^N*(04/(A0*(1-A0(I))))^(2-N)*D(I)*8*(N/(6*N+2))^N/K
1
3310 HF(I)=4.48*K2/D0*R5(I)^.386*(D(I)*V(I))^.202
3320 RES1=1/HF(I)
3330 RES2=D0*(D3-D0)/(K3*(D3+D0))
3340 I4=(I3(I)+T3)/2
3350 T=I4 @ GOSUB 4190
3360 U1(I)=1.47*(PI *U*D3/(4*C(I)))^(1/3)*(A1^3*D6^2*9.793/U^2)^
(1/3)
3370 RES3=D0/(D3*U1(I))
3380 U0(I)=1/(RES1+RES2+RES3)
3390 I3(I)=T3-(RES2+RES3)/(RES1+RES2+RES3)*(T3-T(I))
3400 NEXT I
3410 FOR I=1 TO N0
3420 D2=D1/(1-X1(I)) @ T=T(I)
3430 GOSUB 4110 @ GOSUB 4150
3440 K0=A*EXP (B/(I3(I)+273.15))
```

```
3450 K1=A*EXP (B/(T(I)+273.15))
3460 HSP(I)=2*K2/D0*(V0*D(1)*C9/(K2*L*I/N0))^(1/3)*(K1*(3*N+1)/(
K0*2*(3*N-1)))^.14
3470 NEXT I
3480 A02(1),X0(1),HTOT,SUP=0
3490 FOR I=1 TO N0
3500 D2=D1/(1-X1(I)) @ T=(T(I)+I3(I))/2
3510 GOSUB 4110 @ GOSUB 4150
3520 K1=A*EXP (B/(T+273.15))
3530 HTOT=HTOT+HF(I)
3540 HAV=HTOT/I
3550 Q3=V0*X1(I)*D(1)*V0(I)
3560 Q4=V0*(1-X1(I))*D(1)/D0(I)
3570 Q6=(Q3+Q4)/A0
3580 P3(I)=C9*K1/(8*K2)*(Q6/D0)^(N-1)*((6*N+2)/N)^N
3590 BF=154*(P3(I)^(-.351))*((D(I)*V(I))^(-.414))
3600 A02(I+1)=HAV*K2/(BF*D0*HSP(I)^2)
3610 F1=1.53*(S*9.793*(D(I)-1/V(I))/D(I)^2)^.25
3620 FAC1=1.12*A02(I+1)*V0*D(1)/D(I)+F1*A0*A02(I+1)
3630 FAC2=(1-1.12*A02(I+1))*V0*D(1)*V(I+1)+1.12*A02(I+1)*V0*D(1)
/D(I+1)
3640 X0(I+1)=FAC1/FAC2
3650 ETA=.0000000126*P3(I)^.254*EXP (.000673*(D(I)*V(I)))
3660 DTB=ETA*HF(I)*(I3(I)-T(I))/V0
3670 P9=P(I+1)/100 @ T1=T1(1+1)/100 @ T=T(I+1) @ T2=T2(I+1) @ GO
SUB 4270
3680 IF T2(I)-T(1)>DTB THEN 3800
3690 SUP=SUP+1
3700 IF SUP>1 THEN 3720
3710 XD=C9*(T(I)-T2(I))/((H2-H3)*4186.8) @ XZ=X0(I+1)
3720 IF SUP=1 THEN 3800
3730 XA=C9*(T(I)-T2(I))/((H2-H3)*4186.8)
3740 XB=XA-XD*EXP (XA/XD-1)
3750 X0(I+1)=XZ+XB
3760 Q3=V0*X0(I+1)*D(1)*V(I+1)
3770 Q4=V0*(1-X0(I+1))*D(1)/D(I+1)
3780 Q6=(Q3+Q4)/A0
3790 A02(I+1)=Q3/(A0*(1.12*Q6+F1))
3800 U0=(U0(I)+U0(I+1))/2
3810 TD=(T3-T(I)+T3-T(I+1))/2
3820 Q(I)=U0*TD*L/N0*D0*PI
3830 D2=D1/(1-X0(I)) @ T=T(I) @ GOSUB 4110
3840 HIN=W*(1-X0(I))*C9*(T(I)-20)
3850 HOUT=Q(I)+HIN-(X0(I+1)-X0(I))*(W*(H2-H3)*4186.8)
3860 QS(I)=HOUT-HIN
3870 D2=D1/(1-X0(I+1)) @ T=T(I+1) @ GOSUB 4110
3880 T(I+1)=HOUT/(W*(1-X0(I+1))*C9)+20
3890 IF T(I+1)<= T2(I+1) THEN 4000
3900 QS(I)=0
3910 T(I+1)=T2(I+1)
3920 HOUT=W*(1-X0(I+1))*C9*(T(I+1)-20)
3930 QUAL=(Q(I)+HIN-HOUT)/(W*(H2-H3)*4186.8)
3940 QUAL=QUAL+X0(I)
3950 X0(I+1)=QUAL
3960 Q3=V0*X0(I+1)*D(1)*V(I+1)
3970 Q4=V0*(1-X0(I+1))*D(1)/D(I+1)
```

```
3980 Q6=(Q3+Q4)/A0
3990 A02(I+1)=Q3/(A0*(1.12*Q6+F1))
4000 C0(I)=Q(I)/(R*4186.8)
4010 X1(I)=(X0(I)+X0(I+1))/2
4020 Q0=Q0+Q(I)
4030 NEXT I
4040 COUN=COUN+1
4050 IF COUN=5 THEN 4090
4060 FOR I=2 TO N0+1
4070 IF ABS (A02(I)-A0(I))>.001*A02(I) THEN 2410
4080 NEXT I
4090 RETURN
```

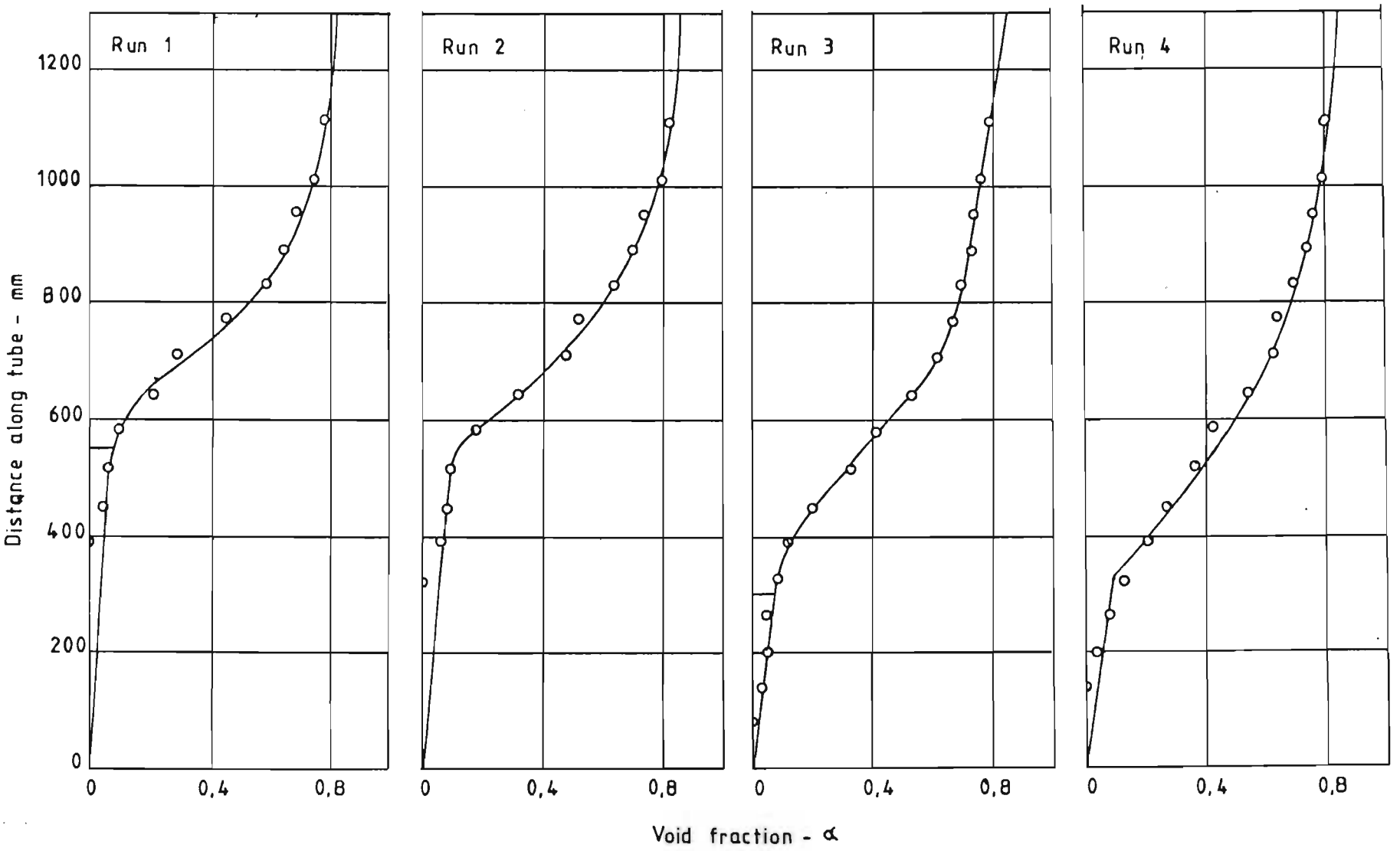

Best fit of Void Fraction Profile Measured by Gamma Ray Absorption.

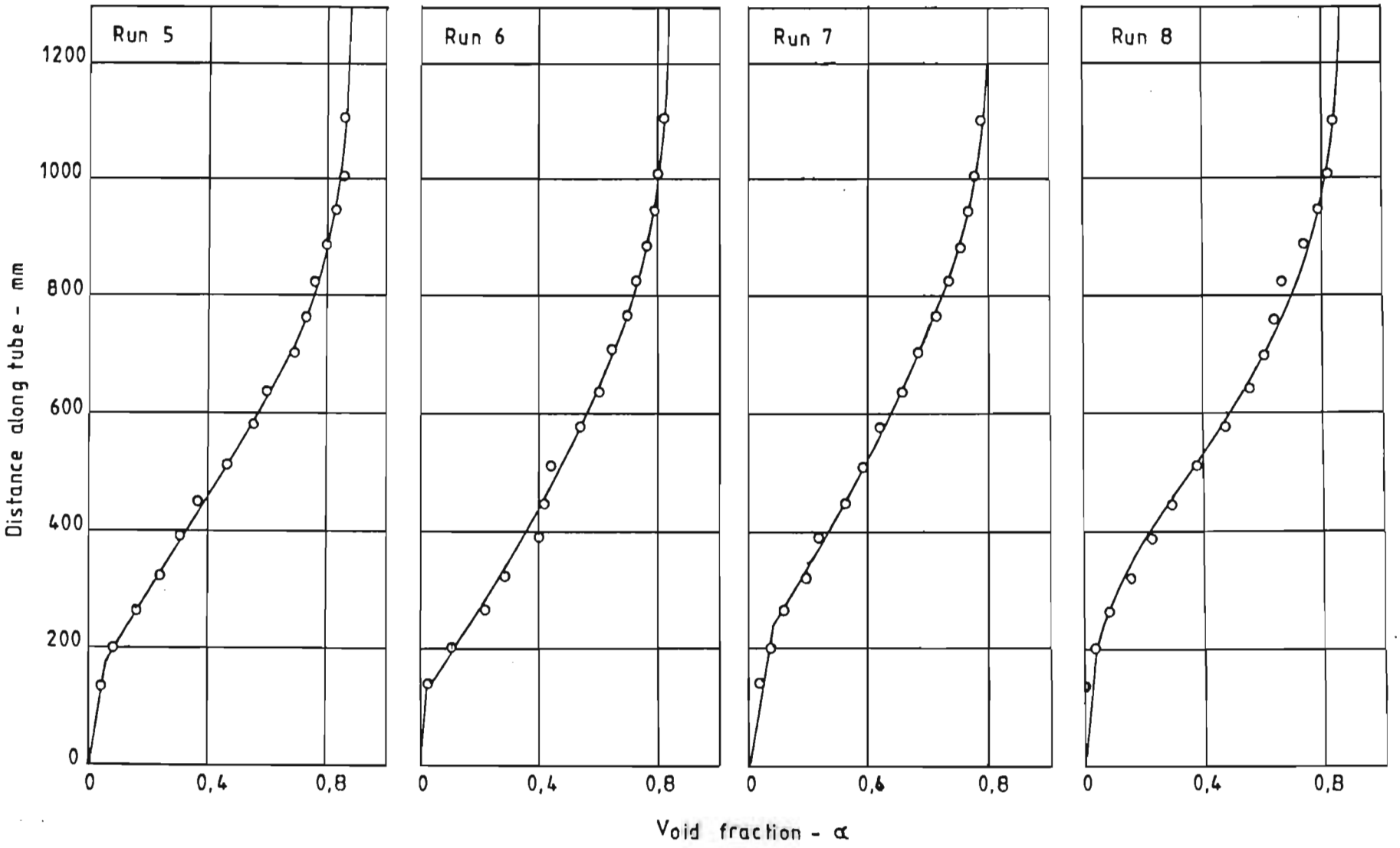

Best Fit of Void Faaction Measured by Gamma Ray Absorption.

Printed Results of Circulation Program

OPERATING CONDITIONS

BRIX	91.66
PURITY	49.33
SURFACE TENSION (N/m)	0.7790
STEAM PRESSURE (kPa)	130.0
VAPOUR PRESSURE (kPa)	20.0
HEAD (m)	0.25
TUBE DIAMETER (m)	0.0984
TUBE LENGTH (m)	0.60
TUBE INLET VELOCITY (m/s)	0.491
CONDENSATE (l/h)	1.922
EVAPORATION (kg/m^2.h)	10.362
BOILING POINT ELEVATION (C)	13.71

CONDITIONS ALONG BOILING TUBE

TUBE LENGTH (mm)	VOID FRACTION	PRESSURE (kPa)	TEMP. (C)	SP. VOLUME (m^3/kg)	QUALITY	DENSITY (kg/m^3)	CONSISTENCY
600	0.0701	23.56	76.02	6.85	1.50E-005	1452.5	67.5
540	0.0628	25.79	76.01	6.29	1.45E-005	1452.5	67.6
480	0.0560	28.03	76.00	5.82	1.38E-005	1452.6	67.6
420	0.0496	30.26	75.99	5.42	1.31E-005	1452.6	67.6
360	0.0433	32.49	75.98	5.07	1.21E-005	1452.6	67.7
300	0.0372	34.72	75.97	4.76	1.10E-005	1452.6	67.7
240	0.0312	36.95	75.96	4.49	9.70E-006	1452.6	67.7
180	0.0251	39.18	75.96	4.25	8.17E-006	1452.6	67.8
120	0.0186	41.41	75.95	4.04	6.35E-006	1452.6	67.8
60	0.0129	43.63	75.94	3.84	4.58E-006	1452.6	67.8
0	0.0000	45.87	75.94	3.67	0.00E+000	1452.6	67.8

PRESSURE DROPS (kPa)

EL	ACC	FRIC.	TOTAL	RE. NUM
0.798	0.006	1.429	2.233	7.25E+000
0.804	0.006	1.423	2.233	7.14E+000
0.810	0.005	1.417	2.232	7.07E+000
0.815	0.005	1.411	2.231	7.00E+000
0.820	0.005	1.405	2.230	6.94E+000
0.825	0.005	1.399	2.230	6.88E+000
0.831	0.005	1.394	2.229	6.82E+000
0.836	0.005	1.388	2.229	6.76E+000
0.841	0.004	1.382	2.228	6.71E+000
0.849	0.009	1.373	2.232	6.65E+000
8.229	0.055	14.021	22.305	6.92E+000

ENTRANCE LOSS DOWNTAKE	0.01390
FRICTION LOSS DOWNTAKE	1.89739
DOWNTAKE EXIT LOSS	0.00026
ENTRANCE LOSS TUBE	0.00700
FRICTION LOSS TUBE	14.02086
ACCELERATION LOSS TUBE	0.05493

TEMPERATURES (C)

TUBE LENGTH (mm)	SATURATED VAPOUR	SUPERHEATED VAPOUR	AVERAGE LIQUID	INSIDE TUBE SURFACE
600	63.6	77.5	76.0	106.9
540	65.7	79.6	76.0	106.7
480	67.5	81.6	76.0	106.7
420	69.3	83.5	76.0	106.7
360	70.9	85.2	76.0	106.7
300	72.5	86.9	76.0	106.6
240	74.0	88.5	76.0	106.6
180	75.4	90.0	76.0	106.6
120	76.7	91.4	75.9	106.6
60	78.0	92.7	75.9	106.6
0	79.2	94.0	75.9	106.6
	72.1	86.4	76.0	106.7

STEAM TEMP.= 107.14(C)

VOID FRACTION PARAMETERS

QG/VOID*A	(QG+QF)/A	RIS. VEL.
1.044	0.565	0.4119
1.035	0.556	0.4119
1.026	0.549	0.4119
1.019	0.542	0.4119
1.011	0.535	0.4119
1.004	0.529	0.4119
0.997	0.522	0.4119
0.990	0.516	0.4119
0.983	0.510	0.4119
0.976	0.504	0.4119
0.000	0.491	0.4119

HEAT TRANSFER PARAMETERS

TOTAL HEAT TRANSFERRED	SENSIBLE HEAT TRANSFERRED	FILM HTC (W/m^2.C)	OVERAL HTC (W/m^2.C)	PRANDTL NUMBER
129.33	122.49	223.76	220.78	75302.42
126.22	117.14	219.38	216.22	75689.79
123.76	112.47	215.43	212.17	76034.01
121.56	108.00	211.81	208.51	76353.15
119.56	103.57	208.46	205.14	76656.36
117.71	99.00	205.35	202.02	76950.34
115.99	94.03	202.42	199.10	77241.52
114.37	88.12	199.64	196.32	77538.18
112.85	87.33	197.07	193.77	77824.77
111.25	44.91	193.96	190.70	65133.40
1192.61	977.06	207.73	204.47	75472.40

APPENDIX D

Sample calculations (Run No. 51)

D.1. Flow distribution parameter at tube outlet

(1) Heat input from steam

Condensate rate	= 0,00618 kg/s
Pressure	= 114 kPa
Enthalpy of condensation	
From Appendix B.8	= $2,246.10^6$ J/kg
Heat input	= 13884 J/s

(2) Heat released by flashing of liquid phase.

Assume mass vapour quality	
at tube outlet	= 0,00743
Tube inlet conditions	
Volumetric flow rate	= 0,000576 m^3/s
Density	= 1397 kg/m^3
Dry substance	= 75,40
Purity	= 38,75
Temperature	= 61,6°C
Tube outlet conditions	
Temperature	= 61,4°C
From Appendix B	
Specific heat	= 2295,8

Heat released = 1397 x 2295,8 x 0,000576(1 - 0,00743) x (61.6 - 61.4)
= 367 J/s

(3) Mass vapour quality (x)

Heat available for evaporation = 13884 + 367
= 14251 J/s

Vacuum = 15 kPa

Enthalpy of evaporation
From Appendix B.8 $= 2{,}384.10^6$ J/kg

Mass flow rate of vapour $= \frac{14251}{2{,}384.10^6} = 0{,}00598$ kg/s

Mass flow rate of liquid =
$0{,}000576 \times 1397 = 0{,}8043$ kg/s

Mass vapour quality $= \frac{0{,}00598}{0{,}8043} = 0{,}00743$

(4) Flow distribution parameter (C_o)

Specific volume of vapour
From Appendix B.8. $= 10{,}27\ m^3/kg$
Volumetric rate of flow of
vapour (Q_g). From eq.(4.5)
$= 0{,}000576$ c $0{,}00743 \times 1397/10.27 = 0{,}0582\ m^3/s$
Volumetric rate of flow of
liquid (Q_f). From eq. (4.6)
$= 0{,}000576(1 - 0{,}00743) \times 1397/1397 = 0{,}000572\ m^3/s$
Void fraction (α) $= 0{,}85$

$\frac{Q_g}{\alpha A} = \frac{0{,}0582}{0{,}85} \cdot \frac{4}{\pi \times 0{,}1016^2} = 8{,}45$ m/s

$\frac{Q_g + Q_f}{A} = (0{,}0582 + 0{,}000572) \cdot \frac{4}{\pi \times 0{,}1016^2} = 7{,}25$ m/s

Rising velocity (V) (From Eq. 2.46) $= 0{,}256$ m/s

From eq. (2.42)
$C_o = (8{,}45 - 0{,}256)/7{,}25 = 1{,}13$

D.2. Local mass vapour quality

The data obtained from measurements along the tube were as shown below

Distance from inlet (m)	Void fraction	Pressure (kPa)	Axial temp. (C)
1,300	0,85	15,0	61,4
1,175	0,85	15,9	61,9
1,050	0,85	16,4	62,0
0,925	0,79	16,8	62,2
0,800	0,74	17,1	62,5
0,675	0,63	17,6	62,8
0,550	0,49	18,2	62,7
0,425	0,28	19,1	62,4
0,300	0,17	20,3	62,2
0,175	0,15	21,9	61,9
0,050		23,8	61.7
0,000			61,6

At 675 mm from tube inlet

Pressure = 17,6 kPa

Specific volume of vapour

From Appendix B.8. = 8,84 m^3/kg

Dry substance = 75,4

Purity = 38,75

Saturation temperature

From Appendix B.4 = 64,4°C

Mass vapour quality. From eq. (4.7)

$$x = \frac{\frac{0,000576 \times 1397 \times 4 \times 1,12}{\pi \times 0,1016^2 \times 1397} + 0,256}{\frac{0,000576 \times 1397 \times 4}{\pi \times 0,1016^2}\left[\frac{8,84}{0,63} - 8,80 \times 1,12 + \frac{1,12}{1397}\right]}$$

$$= 0,00082$$

D.3. Void fraction in highly subcooled region

From void fraction profile curve:

Estimated point of bubble departure = 0,37 m from inlet

Void fraction = 0,06

Single phase heat transfer coefficient (Eq. 2.3) = 275,5 $w/m^2.°C$

Thermal conductivity (Appendix B.7) = 0,3873 $w/m.°C$

Estimated two phase heat transfer coefficient = 525 $w/m^2-°C$

$$\text{Factor} \quad \frac{\alpha.D.h_{fo}^2}{h_{TP}\, k_f}$$

$$= \frac{0,06 \times 0,1016 \times 275.5^2}{525 \times 0,3873}$$

$$= 2,28$$

D.4. Friction loss along tube

The data required for the calculation of the gravtational and acceleration losses are given in the following table. The void fraction was measured. The specific volume of the vapour was calculated as described in Appendix B.8. The quality was calculated as described in Appendix D.2. The density of the liquid phase was calculated as described in Appendix B.1.

Conditions along boiling tube.

Distance from inlet (m)	Void fraction		Mass vapour Quality X 10-4		Specific volume of vapour (m^3/kg)		Density of liquid (kg/m^3)	
	Max.	Avg.	Max.	Avg.	Max.	Avg.	Max.	Avg.
1.300	0.85		74.3		10.3		1401	
		0.85		74.1		10.0		1401
1.175	0.85		73.8		9.7		1401	
		0.85		74.0		9.6		1401
1.050	0.85		74.2		9.5		1401	
		0.82		49.0		9.4		1401
0.925	0.79		24.0		9.3		1400	
		0.77		19.0		9.2		1400
0.800	0.74		14.4		9.1		1398	
		0.69		11.0		8.9		1398
0.675	0.63		8.2		8.8		1397	
		0.56		5.1		8.7		1397
0.550	0.49		3.3		8.6		1397	
		0.39		2.2		8.4		1397
0.425	0.28		1.0		8.2		1397	
		0.23		0.6		8.0		1397
0.300	0.17		0.2		7.7		1397	
		0.16		0.2		7.5		1397
0.175	0.15		0.1		7.2		1397	
		0.12		0.1		6.9		1397
0.050	0.09		0.0		6.4		1397	

The gravitional loss was calculated from eq. (2.27)

For example for bottom section.

$$\Delta p_z = (0{,}12/6.7 + (1 - 0{,}12) \times 1397) \times (0{,}175 - 0{,}050) \times 0{,}00981$$
$$= 1{,}506 \text{ kPa}$$

The acceleration loss was calculated from eq. (2.28)

For the bottom section

$$\Delta Pa = \left[\frac{0,000576 \times 1397 \times 4}{\pi \times 0,1016^2}\right]^2 \left[\frac{0,0011^2 \times 7,0}{0,15} + \frac{(1-0,0011)^2}{(1-0,15)\times 1397}\right] \times \frac{0,00981}{9,793}$$

$= 0,0088$ kPa

The gravitational and acceleration losses for the ten sections along the tube was as follows for Run 51.

Section No.	Gravitational loss	Acceleration loss
1	0,258	0,000
2	0,258	0,000
3	0,309	0,154
4	0,395	0,057
5	0,531	0,054
6	0,753	0,024
7	1,044	0,014
8	1,318	0,003
9	1,438	0,001
10	1,506	0,009
Total	7,810	0,316

Pressure difference between first pressure tapping and vapour space = 24,039 - 15,000 = 9,039 kPa

Friction loss then is

$$\Delta P_f = 9,039 - 7,810 - 0,316$$
$$= 0,913 \text{ kPa}$$

APPENDIX E

Dimensionless Analysis for Heat Transfer to a Fluid Boiling under Laminar Conditions.

For subcooled heat transfer in pipes under conditions of forced convection in laminar flow the variables

$$D,\ u_{TP},\ \mu_f,\ \rho_f,\ c_p,\ k_f,\ \rho_g,\ L \text{ and } h_{TP}$$

will be used as a starting point for dimensional analysis. If mass, length, time, heat and temperature are chosen as the fundamental dimensions and since there are nine variables, then a minimum of four dimensionless groups may be expected from the analysis. The basic equation relating the variables is

$$h_{TP} = f\ (D^a \mu_{TP}^b \rho_f^c \mu_f^d c_p^e k_f^f \rho_g^g L^h) \qquad (E.1)$$

The corresponding dimensional equation is

$$H/\Theta L^2 T = (L)^a (L/\Theta)^b (M/L^3)^c (M/\Theta L)^d (H/MT)^e (H/\Theta LT)^f (M/L^3)^g (L)^h \qquad (E.2)$$

Applying the conditions of dimensional homogeneity, there results the following set of equations:

$$\begin{aligned} &M: && c + d - e + g = 0 \\ &L: && a + B - 3c - d - f - 3g + h = -2 \\ &\Theta: && -b - d - f = -1 \\ &H: && e + f = 1 \\ &T: && -e - f = -1 \end{aligned} \qquad (E.2)$$

Since two of these equations are identical then five dimensionless groups should be expected from the analysis. Choosing the variables u_{TP}, c_p, ρ_g, L and h_{TP} as those which will appear in only one group each, then D, ρ_f, μ_f and k will be the repeating variables. Solving equations (E.2) for a, c, d and f equations (E.3) are obtained:

$$\begin{aligned} a &= b - h - 1 \\ c &= b - g \\ d &= e - b \\ f &= 1 - e \end{aligned} \qquad \text{(E.3)}$$

Substituting into equation (E.1) and rearranging we obtain

$$\frac{h_{TP}D}{k_f} = f\left\{\left[\frac{Du_{TP}\rho_f}{\mu_f}\right]^b \left[\frac{C_p\mu_f}{k_f}\right]^c \left[\frac{\rho_f}{\rho_g}\right]^d \left[\frac{L}{D}\right]^h\right\} \qquad \text{(E.4)}$$

Whilst equation (E.4) is essentially identical to that for single phase heat transfer, it is argued that it takes into consideration all the variables which are likely to have a significant influence on heat transfer to a fluid boiling under laminar conditions. Thus equation (E.4) forms the basis for the correlation of the heat transfer data obtained in this study.